ISSN (Print): 0256-6524
ISSN (Online): 0976-2418

www.isae.in

Journal of Agricultural Engineering

VOL. 57, No. 3, July-September 2020

INDIAN SOCIETY OF AGRICULTURAL ENGINEERS

Publication Enquiries

The Journal of Agricultural Engineering, a publication of the Indian Society of Agricultural Engineers, is published in four issues per year. This journal is not responsible for statements and opinions expressed by the authors of papers published in it. Reprints may be made from this publication on the condition that full credit is given to the author(s) and the Journal of Agricultural Engineering.

All communications regarding the publication or submission of manuscripts should be addressed to The Chief Editor, Journal of Agricultural Engineering at the address given below or at the email address mentioned above.

Subscription Rate

Annual subscription Rs. 2000/- or US $400 ($ 50 extra for air mail dispatch)

Per copy Rs. 600/- or US $ 150 ($ 25 extra for air mail dispatch)

Payment are to be made by crossed cheque/ draft including bank charges in favour of "Indian Society of Agricultural Engineers", payable at New Delhi, India, and directly sent to the Society Headquarters at the address given below. Online payment gateway details are available on the website of the Society.

Indian Society of Agricultural Engineers

G-4, National Societies Block, National Agricultural Science Centre Complex,
Dev Prakash Shastri Marg, Pusa Campus, New Delhi – 110012, India
Tel / Fax: 091-11-25849003
E-mail: isae1960@gmail.com
Web: www.isae.in

Designed & Printed at New United Process, A-26, Naraina Indl. Area, Ph-II, New Delhi-110028 Phone : 9811426024

http://www.isae.in / journal_jae.aspx

Journal of Agricultural Engineering

Vol. 57 (3): July-September, 2020

Design and Performance Evaluation of Self-propelled Intra-Canopy Boom Spraying System

Bhabani Shankar Dash[1*], Arun Kumar[2], Rajesh U. Modi[3] and Sharad Kumar Namdev[4]

[1]M. Tech. student, [2]Professor, Department of Farm Machinery and Power Engineering, College of Technology, G. B. Pant University of Agriculture and Technology, Uttarakhand- 263145, India. [3]Scientist, Division of Agricultural Engineering, ICAR-Indian Institute of Sugarcane Research, Lucknow-226002, India. [4]Research Scholar, Farm Machinery and Power Engineering, Vaugh Institute of Agricultural Engineering and Technology, Sam Higginbottom University of Agriculture, Technology and Sciences (Prayagraj), Uttar Pradesh (India)-211007. *Corresponding author email address: dash.bhabani2009@gmail.com

Article Info

Manuscript received:
July, 2019
Revised manuscript accepted:
June, 2020

***Keywords*:** Boom spraying system, droplet size, intra-canopy spraying, spray nozzle, swivel body

ABSTRACT

A self-propelled intra-canopy boom spraying system was designed for spraying chemicals in small height row crops. The performance of the spraying system was evaluated both under laboratory and field conditions to assess the efficacy and minimize the loss of spray liquid. Flat fan and hollow cone nozzles were tested to determine the boom volumetric distribution, swath and spray angle at different combinations of pressure and height. The flat fan nozzle gave better volumetric distribution at 2.5 $kgf.cm^{-2}$, while the hollow cone nozzle gave at 2.0 $kgf.cm^{-2}$ pressure corresponding to 300 mm nozzle height. The spraying system was tested on soybean crop at forwarding speeds of 1.5, 2.0 and 2.5 $km.h^{-1}$. With an increase in forwarding speed, the mean percentage of coverage decreased significantly (30.30 - 15.37 % for top and 20.01- 4.12 % for bottom part of the leaves), and the mean droplet density varied significantly (277.35 - 243.40 $no.cm^{-2}$ for top and 262.87 - 78.44 $no.cm^{-2}$ for the bottom part of the leaves) at 5 % level of significance. A good percentage of leaf area coverage (30.30 % and 20.01 % for top and bottom of the plant) was obtained at low forward speed (1.5 $km.h^{-1}$) while compromising more spray volume and less field capacity as compared to higher forward travel speeds. The effect of forwarding travel speed, position of tags and nozzle types were significant ($p<0.05$) for mean droplet size, number median diameter, percentage coverage of leaf area and droplet density. The field capacity of the spraying system ranged between 0.22 and 0.36 $ha.h^{-1}$ with an increase in forward travel speed from 1.50 $km.h^{-1}$ to 2.50 $km.h^{-1}$ at an average swath of 1.8 m.

India produces a large quantity of pulses and vegetables as they constitute a significant proportion of daily diet of its' population, and it also ensures crop and livelihood security of the farmer. The total production of pulses in India was more than 25.23 Mt from an area of 29.99 Mha during the year 2017-18 (Anon., 2020a). Vegetable production in India during the year 2018-19 was above 187.47 Mt in an area of about 10.44 Mha (Anon., 2020a). Plant protection is an essential operation among the basic practices of crop production. Data show that diseases, insects and weeds put together cause 31 - 41 % damages to the crops produced worldwide (Anon., 2016a). Various plant protection measures are followed throughout India; among them, the chemical method is most widely used. Presently, India is the fourth-largest producer of pesticides after the USA, Japan and China. Pests and diseases destroy 15-25 % of the food produced by Indian farmers every year (Anon., 2016). Therefore, plant protection becomes a vital operation to be taken into consideration.

The average size of operational farm landholding in India declined from 1.15 ha to 1.08 ha between the year 2010-11 and 2015-16. The small and marginal holdings taken together (less than 2.0 ha) constitutes 86.08 % of the total holdings during the year 2015-16 as against 85.01 % during the year 2010-11 (Anon., 2019a). Small-sized lands pose operational difficulties in operating tractor-drawn sprayer. Acute labour shortage, along with increasing labour wages, made manual spraying costly. Thus, farm mechanization in spraying can be a better option for effective farm operations. Farm mechanisation level in India is about 40 %, and about 34 % of pulse cultivation is mechanised. Intercultural and plant protection operations account for 20 % mechanisation in pulses, and are relatively low as compared to major cereal crops such as rice (30 % mechanized) and wheat (50 % mechanized) (Mehta *et al.*, 2019). A low level of mechanisation in plant protection operations can be attributed to the small landholdings and poor economic conditions of farmers.

There is a vast array of sprayers available for the farmers in the Indian market. Sprayers like knapsack type (both manual and power operated), hand compression sprayers, motorised knapsack mist blower-cum-duster, tractor mounted sprayers, self-propelled lightweight boom sprayer, self-propelled high clearance sprayer, etc. are available in India (Anon., 2020b). Leading manufacturers like ASPEE, Honda and Kisankraft, along with local manufacturers, have flooded the market with excellent and cheap sprayers. However, most of the commercial sprayers spray the solution from the top of the canopy leading to improper distribution of chemicals on the crop foliage. Leaves and canopy that are exposed receive most of the substances, while those parts which lie beneath receive less or no chemicals. Such improper spray distribution reduces the effectiveness of spray, and leads to higher chemical concentration in certain parts of the plants. The insects or pests that remain inside or underneath the canopy cover are thus not directly affected by the spray. It is challenging to achieve under-leaf coverage with regular spraying equipment as the leaves intercept and block the flow of chemicals inside the canopy. Rear-mounted sprayers also block the visibility and accessibility of the operators.

Narang *et al.* (2013) reported that an air-assistance sprayer gave significant droplet deposition at the underside of the cotton plant leaves as compared to almost negligible by conventional sprayers. They also developed a front-mounted power tiller-operated air assistance intra-canopy sprayer and obtained about 18.0 % of coverage on the front and backside of the leaves of pigeon pea crop. Patel *et al.*(2016) evaluated an electrostatic sprayer for cotton crop in Punjab, India. The area covered by droplets of the electrostatic sprayer was 44.55 % at the top, 55.26 % at the middle, and 68.68 % at the bottom leaves of the canopy. The droplet density and bio-efficiency were also higher as compared to other sprayers like tractor-operated gun-type sprayer, lever-operated knapsack sprayer and power-operated knapsack sprayer. Dhaliwal (2018) worked on an engine-operated walk-type drop-down sprayer for cotton crop. Area covered by droplets on the underside and upper side of plant leaves at 1.0, 1.3 and 1.7 m height varied between 0.91-9.79 %, 0.28-11.19 % and 0.22-10.17 %, respectively. It was concluded that with an increase in forward speed, leaf area coverage and droplet density reduced significantly. Above studies thus showed significant results in obtaining higher leaf area coverage, droplet density, etc. in crops using alternative means as air assistance, electrostatic charging and drop-down arrangement. Modi *et al.*, (2020) expressed the need for an improved boom floatation and nozzle design to enhance the input-use efficiency of pesticides.

Less coverage at the bottom of the plant leaf allows insects/pests to flourish and cause plant damage,which ultimatelyleads to yield loss. A cost-effective way of performing under leaf and intra-canopy spraying for row crops isthus needed for Indian farming conditions. Therefore, the necessity of a self-propelled spraying system with the ability to spray chemicals both from the top as well as the bottom of the plant in row crops was felt. Thus, a study was undertaken to design a self-propelled boom spraying system for intra-canopy spraying and evaluate its performance in row crops (soybean). It will cover more plant canopy area in an efficient way.

MATERIALS AND METHODS

Achieving intra-canopy and under-leaf spraying using conventional sprayers by spraying from the top of the plant canopy is difficult since spray gets intercepted by the leaves and little amount of chemical penetrates the canopy. It is possible through an air-assisted sprayer, electrostatic sprayer, or any mechanism that sprays the chemical from the bottom of the plant. Electrostatic sprayers are expensive and need technical knowledge to operate. Air assistance sprayer needs a separate blower unit, which reduces the manoeuvrability of the whole spraying system due to its additional weight along with adding an extra cost. Alternate mechanism was, therefore, preferred to improve the boom section while considering intra-canopy and under-leaf spraying in row crop.

Self-propelled Boom Spraying System

The mechanism used here had arrangements for placing nozzles in-between the rows at a low height (minimum 100 mm). Hose-drops were selected to carry the chemical to a suitable nozzle arrangement to discharge chemical at the bottom of the plant.The designed spray boom had four even-flat fan nozzles mounted on the top (facing ground) to cover four rows at a time. Hollow-cone nozzles were placed in between the rows at one-third of canopy height from the bottom (facing up at 45°) with the help of hose-drops and swivel bodies. The boom section was designed such that the hose-drops would pass in between the rows, and the nozzles would spray chemicals in both lateral directions along the forward path. A pressure gauge and a flow control valve were provided to set the working pressure and control the liquid supply, respectively. The boom section was attached to a self-propelled unit with a 5-kW diesel engine. The engine power was transmitted to a piston pump fitted adjacent to the engine through a V-belt drive. Power was conveyed to the front wheels from the same shaft through V-belt and chain drive. The whole unit was a front-mounted walk-behind type self-propelled boom spraying system. Development and fabrication were carried out at the Research Laboratory, Department of Farm and Power Engineering, GBPUA&T, Pantnagar, Uttarakhand, India.

Boom and frame section

The boom frame and body were fabricated to support the boom section as well as allow free movement of the boom to fit the desired height of the crops within a range of 450 to 800 mm above the ground. A dry boom was used as a span to attach the nozzles and provide support to the hose line to carry the spray solution. A dry boom section (Fig. 1a) was made by welding two MS angles (25×25×3 mm) length of 1800 mm to form a rigid hollow bar. The frame had a T-section (MS angle of 350×35×3 and MS flat of 300×35×3 mm) and L-section (250×200×35×3 mm) as shown in Fig. 1 (b) and 1 (c), respectively. The T-section was fixed to the body by welding for support of the boom. Holes were drilled on its surface for attaching the other parts of the frame with a bolted joint. The L-section was connected to the T-section with bolt and nut. The L-section had holes drilled on it to attach the spray bar to it. The L section was adjustable by 350 mm to change the boom height. The nozzle spacing could be changed from 200 mm to 600 mm. The sectional view of the boom is shown in Fig. 2.

Selection of nozzles

Nozzle selection is essential to increase the effectiveness of spray and reduce spray losses. The correct nozzle tip size depends on the required application rate (l), ground speed (km.h^{-1}), and effective spray width of each nozzle (W_i). Flat-fan nozzles were chosen for uniform coverage across the entire width of the spray pattern, and hollow cone for better penetration of droplets (Anon., 2019b).

Conventional knapsack sprayers require 400-600 l.ha^{-1} of spray solution, and high-volume sprayers spray more than 400 l.ha^{-1} of chemical (Singh, 2011). Therefore, considering 500 l.ha^{-1} quantity of spray and different forward speeds of walk-behind type sprayers (1.5, 2.0 and 2.5 km.h^{-1}), discharge of an individual nozzle (Q, l.min^{-1}) was determined by the following expression (Dash, 2016):

$$Q = \frac{V\,S\,W_i}{600} \qquad \ldots(1)$$

Where,

V = Total discharge, l.ha^{-1},

S = Forward speed, km.h^{-1}, and

W_i = Row spacing divided by the number of nozzles per row for directed spraying, m.

Nozzle tips (TP8001E and TXA8001VK) discharging the required amount of spray (0.21-0.35 l.min^{-1}) were selected for the study. The TP8001E wasa category of even flat spray nozzle tip providing uniform distribution throughout the spray pattern. The nozzle tip material was brass with 80^0 angle nozzle tips, and a pressure range of 1.40 kgf.cm^{-2} to 4.22 kgf.cm^{-2}. TXA8001VK wasa hollow cone spray tip with a pressure range of 2.1 kgf.cm^{-2} to 8.7 kgf.cm^{-2} (Anon., 2020c). After the selection of the nozzles, their actual discharge (l.min^{-1}) was measured in the laboratory at different operating pressures. The average discharge obtained from the nozzles in 1.0 min time was taken into consideration, and the total flow requirement (F, l.min^{-1}) calculated as:

$$F = \frac{S_w \times A \times S}{600} \qquad \ldots(2)$$

Where,

S_w = Swath, m,

A = Recommended application rate, l.ha^{-1}, and

S = Operating speed, km.h^{-1}.

The swath was kept at 1800 mm, taking into consideration four rows with 450 mm width each for soybean crop. The total flow requirement for three

(a) Dry boom section

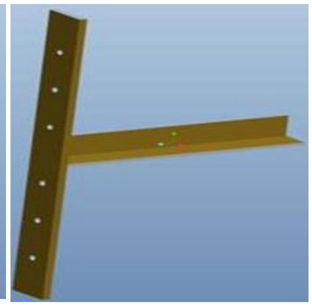

(b) T section

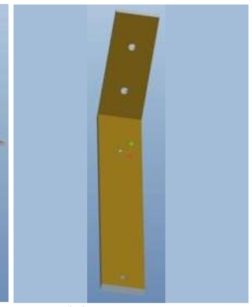

(c) L section

(d) Swivel body

(e) Hose drop

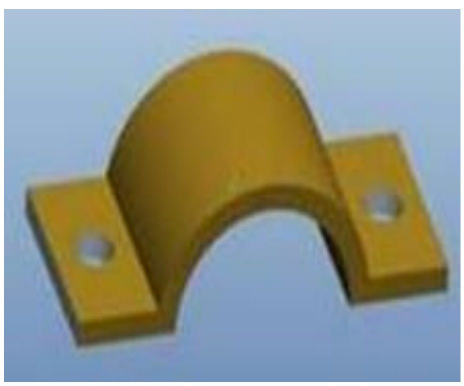

(f) Clamp

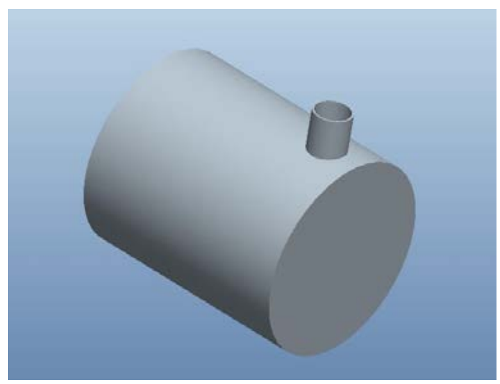

(g) Tank

Fig. 1: Various components of spraying system

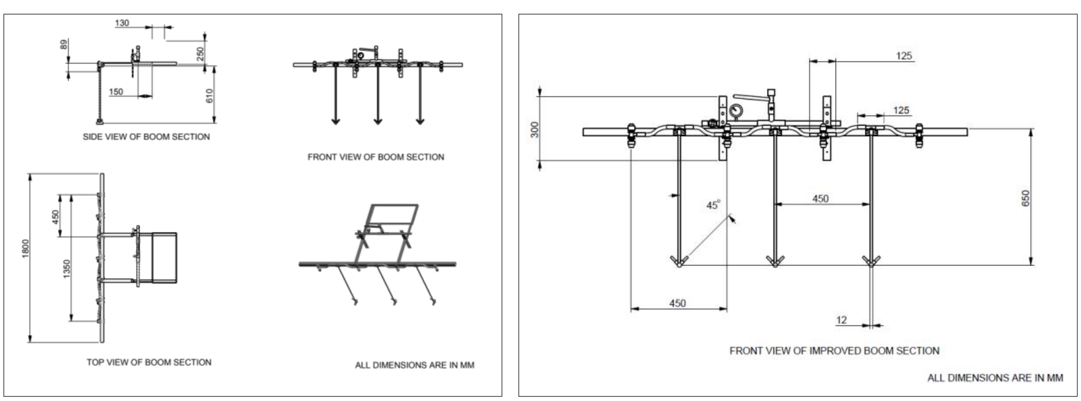

Fig. 2: Sectional views of boom

forward speeds of 1.5, 2.0 and 2.5 $km.h^{-1}$ keeping the application rate (500 $l.ha^{-1}$) fixed was found to be 2.5, 3.33, and 4.17 $l.min^{-1}$, respectively.

Selection of flow pump

A pump that can fulfil the total flow requirement of the boom (4.17 $l.min^{-1}$ for spray) and still generate 10 % extra flowfor agitation (8.34 $l.min^{-1}$) was selected for the study. A reciprocating type three-cylinder piston pump (USHA make, SPRAYMAX 22B) was chosen to produce enough flow for both application rates and tank agitation requirements. The rotational speed was 500-1000 rpm with a suction capacity of 18-22 $l.min^{-1}$ at a pressure range of 10-40 $kgf.cm^{-2}$.

The pump was tested under laboratory conditions to ensure its proper working and delivering the required flow. The discharge of the pump was calculated by running the pump and collecting the discharged water in a bucket for 1.0 min. The experiment was repeated three times. The flow obtained from the piston pump was measured atdifferent throttle positions (corresponding to forward speeds of 1.5, 2.0 and 2.5 $km.h^{-1}$) as per the markings on the hand throttle position of the engine. The respective average discharge obtained at three throttle positions was 13.0, 18.2 and 24.4 $l.min^{-1}$, which satisfied the total flow requirement of the spraying system.

Selection of swivel body, hose drop and clamp

Swivel bodies (Fig. 1d) had nozzle holding arrangements that could rotate in 360^0, and was suitable for spraying in-between row crops. TeeJet's swivel (QJ 8600) nylon bodied (8.0 mm inner diameter) were selected for the boom section to perform intra-canopy spraying. Two hollow cone nozzles were mounted on each swivel body at 45^0 with horizontal for spraying liquid uniformly in opposite directions from the bottom of the canopy. Stainless steel hose-drops, 610 mm long and 12 mm in outer diameter (Fig. 1e), were selected according to the size of the swivel body. They were attached to the horizontal boom section using clamps. Clamps (Fig. 1f) were made using MS sheet (53×2 mm) moulded to hold the hose-drops. An arrangement was made to move the hose-drops vertically (100-400 mm upward) as well as horizontally (200-600 mm) to fit the crop conditions.

Design of spray tank

The design considerations of a sprayer tank include storage capacity that can provide 15 - 20 minutes of continuous spraying, and the actual tank capacity is kept 5-15 % higher than the theoretical capacity to ensure that there is always enough liquid for adequate agitation (Varshney *et al*., 2004; Sharma and Mukesh, 2013).

The tank capacity (Q_t, l) was calculated as:

$$Q_t = D_b \times t \qquad \ldots(3)$$

Where,

D_b = Total discharge rate of all nozzles, $l.min^{-1}$, and

t = Duration of use, min.

The tank capacity was found to be 83.4 l, considering the nozzle discharge rate of 4.17 $l.min^{-1}$, which can spray for a duration of 20 min. With an additional 10 % extra flow for agitation, the final tank capacity was found to be 91.74 l (say 92 l).

A cylindrical tank (Fig. 1g) of 500 mm diameter and 600 mm long made of G.I. sheet (18 gauge) was attached to the unit at the front of the frame. The liquid overflow of the pump was bypassed/recirculated to the tank to assist the stirring of the ingredients. The storage tank of 118 litre capacity was sufficient to spray 0.24 ha in one fill.

Laboratory Evaluation of Nozzles

The uniformity of spray distribution across the boom, or within the spray swath, is essential to achieve maximum chemical effectiveness with minimal cost and reduction in non-target contamination. The uniformity of the nozzlespray was determined using a patternator at the Department of Farm Machinery and Power Engineering, Punjab Agricultural University, Ludhiana, India. A patternator of size 2000×2000 mm made of acrylic sheet with inner dimensions of 2000×30×100 mm for each channel (63 rectangular channels) was used for testing, as shown in Fig. 3. The spray channels were inclined at angle of 9-10^0 with horizontal. The nozzles were mounted at the centre of a metallic frame perpendicular to the patternator channels. The height of the nozzle assembly was also adjustable up to 2000 mm. The nozzles were connected to a constant water supply through a piston pump, and a pressure gauge was mounted to check the pressure. The nozzles were tested at different pressures (2.0, 2.5 and 3.0 $kg.cm^{-2}$) and heights (300, 400 and 500 mm) to check uniformity of distributions and their swaths. Collecting tubes were provided to collect the water from the channels during spraying. The nozzle was given a preliminary run until a constant flow rate was achieved from the patternator, and the readings were subsequently taken (ISI, 1977).

The procedure was replicated thrice. The treatment with the least coefficient of variation (C.V.) was considered as best for field evaluation.

Field Performance Evaluation

Field evaluation of the designed spraying system was carried out at the Breeders Seed Production Centre, GBPUA&T, Pantnagar. Agronomical conditions of the crop (crop height, canopy spread and row spacing) and the functional requirements were considered for the evaluation of the nozzle spray. Before operating in the field, the spraying system was calibrated according to the ISI standards (ISI, 1985) under laboratory conditions to ensure proper working of the components. A preliminary test was conducted on standing cowpea crop (Pant Lobia III, 45 DAS, 400 mm row-to-row spacing, 500 mm plant height). During the preliminary test, the spraying system was found to be working satisfactorily.

The self-propelled spraying system was further tested on soybean crop (Variety: PS 1225) at Crop Research Centre, GBPUA&T, Pantnagar (Fig. 4). At the crop age of 48 days, the average crop height was 350 mm with row-to-row spacing of 450 mm. Three plants along a row were selected at an interval of 3 m for each treatment. Six collector tags (WSPs, 75 × 25 mm) were fixed to each selected plant (Hofmann and Hewitt, 2005). The machine was checked, and an initial run (3.0 m) was given before spraying over the allotted plants. The spray liquid used was pure water with a dye solution (methylene dye @5g.l^{-1}). Dye was used for evaluating the spray deposit on the plant leaves by attaching water-sensitive paper (WSP) on them (Singh *et al.*, 2019). The spraying system was run at three forward speeds (1.5, 2.0 and 2.5 km.h^{-1}) at maintained operating pressure of 2.5 kgf.cm^{-2} (245.16 kPa) based on the laboratory study. The tags were collected after spraying, and subsequently dried. Spray deposition analysis was done at Plant Protection Laboratory, Agricultural Mechanization Division, CIAE, Bhopal, using an image analysis software (LEICA QWin).

Analysis of sample tags

Various researchers used different software for analysing the sample tags as per their requirement (Zhu

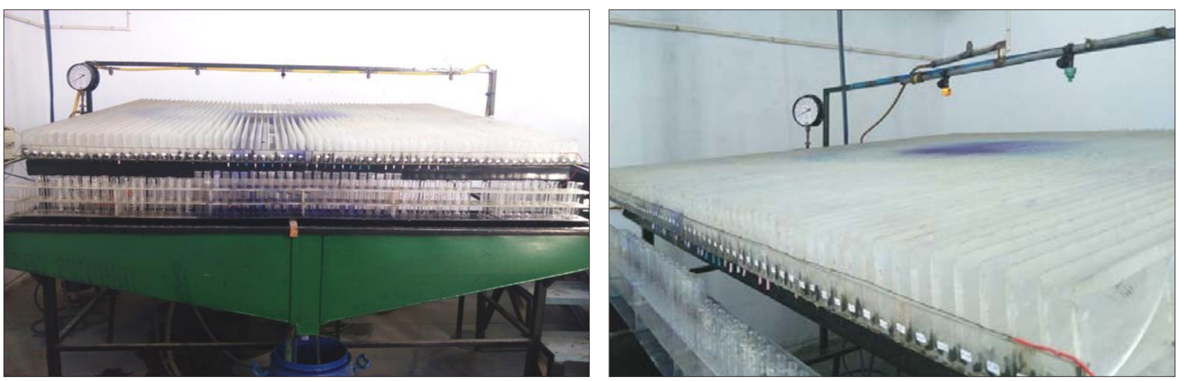

Fig. 3: Nozzles attached at the centre of the adjustable frame over the patternator

Fig. 4: Field performance evaluation of self-propelled boom spraying system in soybean crop

et al., 2011; Mishra *et al*., 2014). The tags collected from the field test were analysed using "LEICA QWin (QWin Plus) image analysis software" (Narang *et al*., 2013). It was a swift and sophisticated application capable of addressing and solving the most intricate image analysis tasks functioning in the Microsoft Windows operating environment. The WSP tags were scanned at 600 dpi and exported as BMP image files, followed by their analyses, as shown in Fig. 5. The mean droplet size, number median diameter (NMD), leaf area coverage, and droplet densities were measured using the software and exported in an Excel file.

NMD was calculated for finding the median (M) of a grouped data by using the statistical formula:

$$M = L_m + \left[\frac{\frac{n}{2} - F}{f_m}\right] i \qquad \ldots(4)$$

Where,

n = Total frequency,

F = Cumulative frequency before the class median,

f_m = Frequency of the class median,

i = Class width, and

L_m = Lower boundary of the class median.

Droplet density (D, droplet.cm^{-2}) was calculated from the obtained data using the following formula:

$$D = \frac{D_n}{A_f} \qquad \ldots(5)$$

Where,

D_n = Number of droplets in the frame, and

A_f = Frame area, cm^2.

The area covered by the droplets on WSP was calculated by dividing the total drop area by that of WSP. The percentage area covered by the droplets was calculated by dividing the total droplet area to that of frame area multiplied by 100.

Leaf area coverage (L_c, %) was determined by

$$L_c = \frac{A_d}{A_f} \times 100 \qquad \ldots(6)$$

Where,

A_d = Total area of droplets in the frame, cm^2, and

A_f = Total frame area, cm^2.

The relative standard deviation (RSD, %) values of the four parameters were calculated to compare the data from the mean values by using the following equation:

$$RSD = \frac{S}{|X|} \times 100 \qquad \ldots(7)$$

Where,

S = Sample standard deviation, and

|X| = Mode of the sample mean.

Measurement of other field parameters

The forward speed of the spraying system was increased/decreased using a throttle setting, whereas power was engaged/disengaged from engine to transmission through a lever. Forward speed was measured for 20 m long marked run (using ranging rods) at a constant throttle position, and the time taken to cover the distance was recorded using a stopwatch (precision: 0.01 s). Thus, a forward speed was calculated, and the

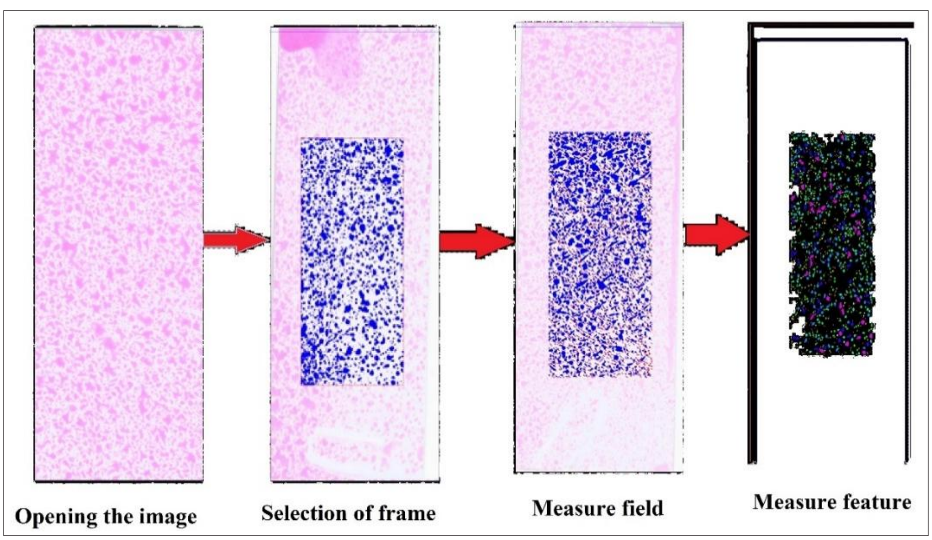

Fig. 5: Steps followed in LEICA QW in software for analysis of tags

throttle position was accordingly marked for forward speed of 1.5, 2.0 and 2.5 km.h^{-1}.

The plant dimensions (row spacing, plant height and canopy width) were measured manually using a meter tape (3.0 m) having least count of 1.0 mm. The canopy spread was the lateral distance measured between two outermost vertical axes touching to the extreme leaf tips using the metre tape. The measurements were taken at several locations (10 random places) in the field, and their average was considered.

Design of Experiment

The experimental field layout was 12 × 36 m (432 m^2), having 18 number of plots of size 20 m^2. The length of each run was 10 m with an additional head land of 1.5 m on two parallel sides for making a run.

Field experiments were laid in a randomized block design (RBD), and data obtained from the field were analysed to determine the effect of independent parameters (forward speed S1 (1.5 km.h^{-1}), S2 (2.0 km.h^{-1}), and S3 (2.5 km.h^{-1}); location of tag L1 (top of plant leaves) and L2 (bottom of plant leaves) individually and their interactions. The dependent variables were mean droplet size (μ), number median diameter (μ), leaf area coverage (%), and droplet density (droplet.cm^{-2}). Tags were attached after a distance of 3.0 m from the headland and at intervals of 3.0 m. Among the six tags collected, three tags with good and clear marks on them were taken for the analysis, and a similar process was followed for both tag locations. The experiment was replicated thrice, and the data obtained from the field were statistically analysed using analysis of variance (ANOVA) at 5 % level of significance with SAS 9.3.

RESULTS AND DISCUSSION

The technical specifications of the spraying system are presented in Table 1. It was field-tested in a soybean (PS 1225) field at three different operating speeds (1.5, 2.0 and 2.5 km.h^{-1}) at constant (2.5 kgf.cm^{-2}) operating pressure and boom height (300 mm). Performance

Table 1. Technical specifications of intra-canopy boom spraying system

Sl. No.	Item/Particulars	Specifications
1.	Name of the machine	Intra canopy boom spraying system
2.	Type	Walk-behind type
3.	Power source	Self-propelled
4.	Engine	
	Type	Diesel, 4-stroke engine
	Power, kW	5.0
	Transmission	V-belt and chain drive
5.	Maximum forward speed of travel, km.h^{-1}	2.8
6.	No. of nozzles	10
7.	Types of nozzles	Hollow cone and flat fan
8.	Nozzle spacing range, mm	200- 600
9.	Operating pressure of nozzles, kgf.cm^{-2}	
	Flat fan	1.40 to 4.50
	Hollow cone	1.50 to 4.50
10.	Length of hose pipe, mm	610
11.	Tank capacity, l	118
12.	Pump type	Piston pump (three cylinder)
13.	Pressure rating, kgf.cm^{-2}	10-40
14.	Pump discharge, l.min^{-1}	13-24.4
15.	Boom height range, mm	750-1000
16.	Front drive wheel (two) diameter, mm	350
17.	Rear guide wheel diameter, mm	350
18.	Ground clearance, mm	450
19.	Overall dimensions, mm	2050 ×1800×1500
20.	Net weight, kg	180

results of the spraying system are discussed in this section.

Crop Parameters

Soybean (*Glycine max*) grown in parts of the plains and *tarai* region of Uttarakhand has a maturity period of 120-125 days. The PS1225 variety is a medium height plant (>500 mm) and resistant to diseases like yellow mosaic virus (YMV), bacterial pustule (BP), and moderately resistant to Rhizoctonia aerial blight. The variety had white flowers, semi-erect growth habit with pointed ovate leaf shape (Anon., 2016).

At 48 days after sowing (DAS), the plant height, canopy spread, and row-to-row spacing were observed as 350, 340 and 450 mm, respectively. It was in the growing (pre-flowering) stage, and the height and canopy width were expected to grow more. Plant height for PS 1225 variety was observed at 735 mm (Singh *et al*., 2015). Negi (2018) marked that the plant height (PS1225) after 40 and 80 DAS was 299 and 501 mm, respectively. Respective values for canopy spread were 424 mm and 527 mm. The package of practices includeda wide range of chemical treatments, including keeping crop free from weeds till 45 DAS. For controlling diseases (Rust, YMV, BP, etc.), the spray includes quick spray after symptoms are visible to the second spray after few days (10-20 days) of the first spray (Anon., 2018).

Laboratory Evaluation of Nozzle and Pump

The nozzles selected for the boom spraying system were Even Flat Spray Tip (TP8001E) and Hollow Cone Tip (TXA8001VK) of TeeJet Technologies (USA). The best volumetric distribution in terms of CV for flat fan nozzle was at the pressure of 2.5 kgf.cm^{-2} and 300 mm nozzle height (18.5 %); while that of the hollow cone nozzle was at 2.0 kgf.cm^{-2} pressure and at 300 mm nozzle height (34.16 %), Table 2. The lower CV values ensure higher uniformity throughout the spray pattern and *vice-a-versa*. With an increase in pressure from 2.0 kgf.cm^{-2} to 3.0 kgf.cm^{-2}, the discharge of the flat fan nozzle increased from 0.29 l.min^{-1} to 0.36 l.min^{-1}.

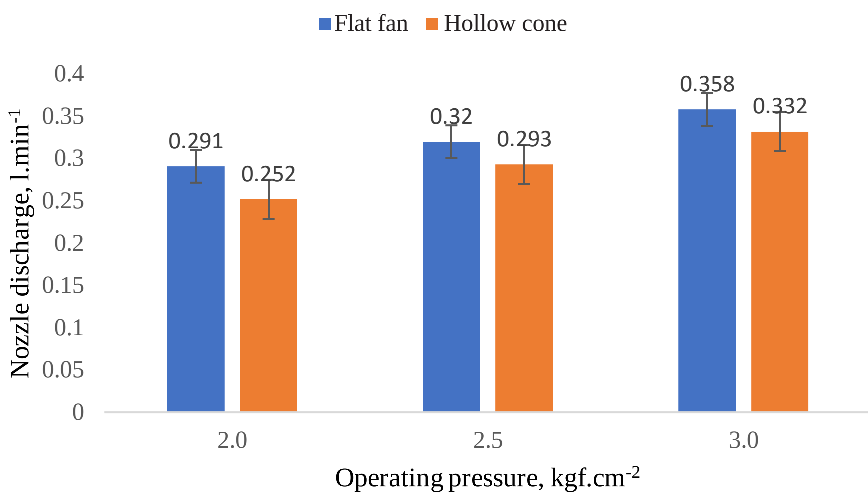

Fig. 6: Effect of operating pressure on nozzle discharge rate

Table 2. Swath and C.V. of hollow cone and flat fan nozzles at different operating pressures and pressure

Nozzle type	Operating pressure, kg.cm^{-2}	Swath width at different height, mm (C.V., %) Nozzle height, mm		
		300	400	500
Hollow cone	2.00	250 (34.16)	275 (42.60)	275 (40.85)
	2.50	275 (44.27)	280 (44.87)	280 (43.87)
	3.00	275 (39.15)	300 (38.33)	300 (45.33)
Flat fan	2.00	300 (27.65)	400 (29.93)	400 (27.19)
	2.50	350 (18.5)	425 (22.8)	425 (34.54)
	3.00	350 (34.52)	425 (26.47)	475 (27.20)

At this pressure range, the discharge rate of the hollow cone nozzle also improved from 0.25 $l.min^{-1}$ to 0.33 $l.min^{-1}$. The average discharge rate of the hollow cone nozzle was lower than the flat fan nozzle by 13.40 %, 8.43 % and 7.26 % at the three operating pressures.

The discharge obtained from the positive displacement pump varied between 13.0 $l.min^{-1}$ to 24.4 $l.min^{-1}$ at the three throttle positions for forward speedrange of 1.5-2.5 $km.h^{-1}$ during field operations.

Field Performance

The results obtained from the laboratory (swath, pressure and nozzle height) tests were considered while running the machine in the field (Fig. 4). The swath obtained from the nozzles were simulated as plant canopy widths (340 mm), and the corresponding boom heights (300 mm) and the operating pressure (2.5 $kgf.cm^{-2}$) were fixed for the study. The actual field capacity of the boom sprayer varied between 0.22 $ha.h^{-1}$ to 0.36 $ha.h^{-1}$ (at 80 % field efficiency) with forward speed increasing from 1.5 $km.h^{-1}$ to 2.5 $km.h^{-1}$ with an average swath of 1800 mm. The results on the effect of operating speed on spray characteristics are discussed below.

Mean droplet size

The effect of forward travel speeds and location of tags on the mean droplet size is shown in Fig. 7 and corresponding ANOVA in Table 3. At forward travel speed of 1.5 $km.h^{-1}$ and a top location, the mean droplet size was found to be higher (263.8 μ) due to more exposed canopy area and lower speed resulting in higher spray deposition. All combinations, except the combination of S1L1, were statistically at par for mean droplet size. The individual effect of forward travel speed and location of the tag was found to be significant ($p<0.05$). The droplet sizes varied between 49-800 μ at all forward travel speeds. However, bottom leaves received droplets with relatively smaller size (194.96 μ) as compared to top leaves. It might be due to the presence of a hollow cone nozzle at the bottom side, which produces finer droplets compared to flat fan nozzles.

Number median diameter (NMD)

Figure 8 and Table 4 illustrates the effect of forward speed and location of tags on the NMD of the spray droplets. The NMD of droplets at 1.5 $km.h^{-1}$ (S1L1) forward speed was significantly ($p<0.05$) higher (234.9 μ) from the other combinations. The effect of forward travel speed, location of the tag, and their interactions were non-significant ($p>0.05$). It might be due to the constant operating pressure of the nozzles ensuring less variation among the NMD's.

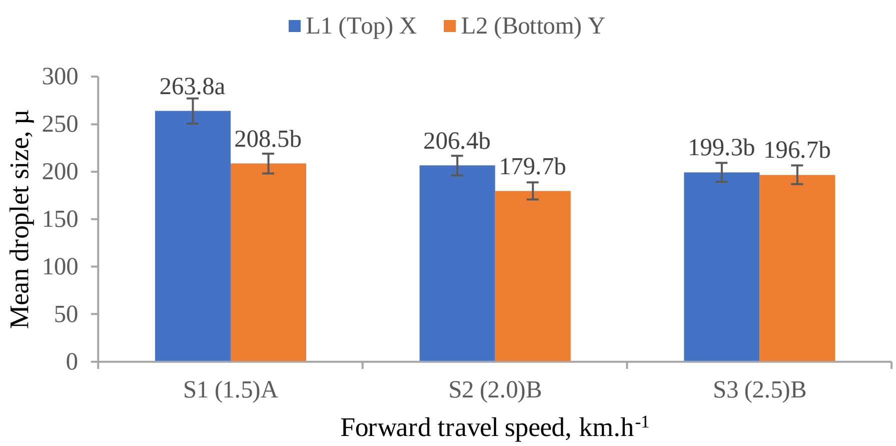

(Mean values and independent parameters with same letters are not significantly different, $p>0.05$)

Fig. 7: Effect of forward speed on mean droplet size

Table 3. ANOVA table on the effect of operating speed and location on mean droplet size

Source	DF	Type III SS	Mean Square	F value	p value
Speed	2	6685.9078	3342.9539	9.90	0.0029
Location	1	3578.5800	3578.5800	10.59	0.0069
Speed×location	2	2088.0300	1044.0150	3.09	0.0827

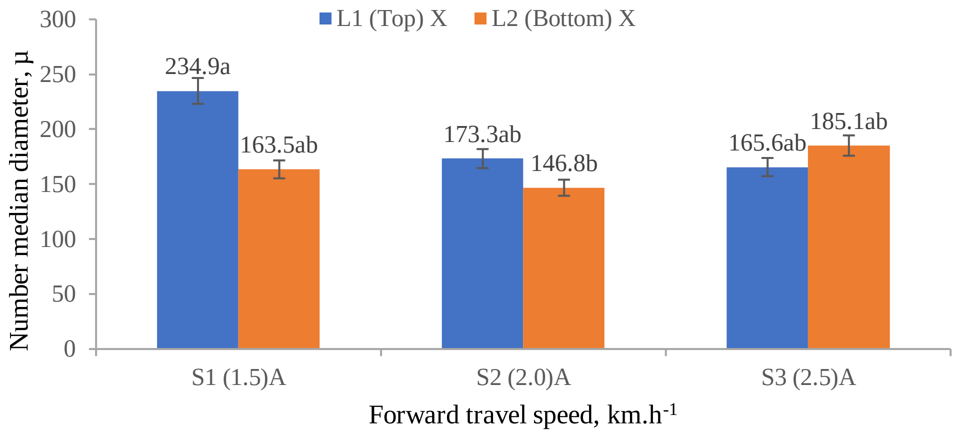

(Mean values and independent parameters with same letters are not significantly different, $p>0.05$)

Fig. 8: Effect of forward speed on number median diameter

Table 4. ANOVA table on the effect of operating speed and location on NMD of droplets

Source	DF	Type III SS	Mean Square	F value	p value
Speed	2	4678.5344	2339.2672	2.32	0.1409
Location	1	3068.0556	3068.0556	3.04	0.1068
Speed×location	2	6206.5411	3103.2706	3.07	0.0836

Leaf area coverage

Forward travel speed and location of tag hada significant effect ($p<0.05$) on the leaf area coverage (Fig. 9 and Table 5), whereas their interaction was non-significant ($p>0.05$). The leaf area coverage reduced from 30.30 % to 4.12 % with increasing forward speed from 1.5 km.h^{-1} to 2.5 km.h^{-1} for both top and bottom locations of the tag of the plantcanopy. It was due to the constant rate of application (fixed pressure of 2.5 kgf.cm^{-2}) at all forward travel speeds, thereby reducing the duration of spray and strike of droplets with increasing speed. This indicated that a lower forward travel speed of 1.5 km.h^{-1} would give better performance (30.30- 20.01 % coverage) when there are more pest infestations and dense canopy. Coverage obtained on the top portions of the plant canopies were higher from the bottom parts by 51.42 %, 107.68 % and 273.05 %, respectively, at all operating speeds. It might be due to obstructions on the path of droplets (leaves, branches, etc.) from the hollow cone nozzle causing low coverage on bottom sides.

Droplet density

From the ANOVA results, the effect of operating speed and location of tags on droplet density is presented in Fig. 10 and Table 6, respectively. The forward speed, location of the tag, and their interaction were statistically significant ($p<0.05$) on droplet density. The interaction S3L2 was significantly lower (78.44 droplet.cm^{-2}) droplet density from its neighbouring values. Droplet density on top portions of the plant canopies was higher as compared to the bottom parts, but the result was not significantly different.The droplet densities on the leaf surface were compared with the recommended droplet densities for various operations and were observed to satisfy the recommended conditions. With these nozzle combinations, the desired droplet density could eradicate pests and diseases. The droplet densities at three forward travel speeds were also compared with the previous researches and recommendations. Observed droplet density fulfilled the criteria that with medium-size droplets, insecticides should have 20-30 droplet.cm^{-2}, herbicides 20-40 droplet.cm^{-2}, and fungicides with 50-70 droplet.cm^{-2} (Hoffman, 2018). The results also satisfied the recommended number of droplets(20-30 droplet.cm^{-2} for spraying insecticides and 50-70 droplet.cm^{-2}) for spraying fungicides (Zhu *et al.*, 2006).

Relative standard deviation (RSD) values of the four parameters are represented in Fig. 11. The least relative standard deviation for leaf area coverage was at forward speed of 1.5 km.h^{-1} for the top portion of leaves (30.30 ± 14.50 %). Relative standard deviation was minimum for droplet densities (243.30 ± 9.44 %), mean droplet

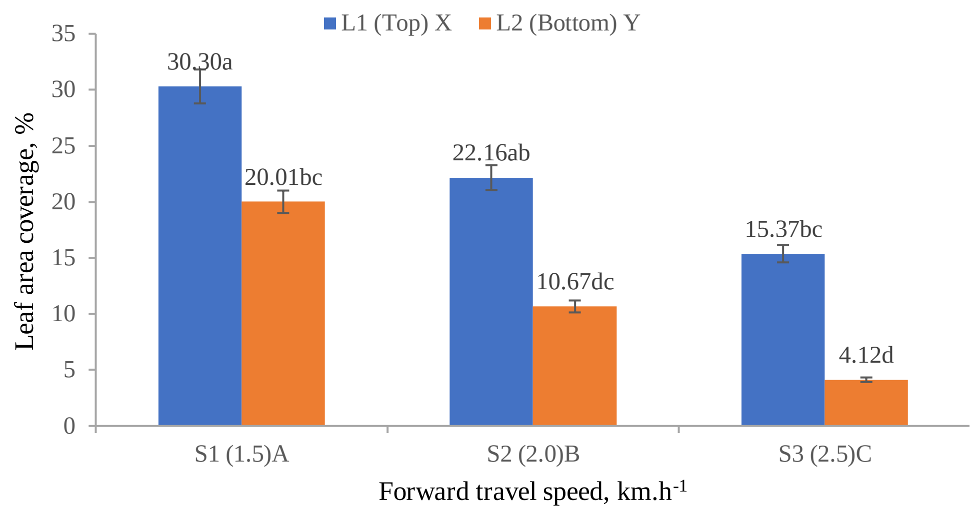

(Mean values and independent parameters with same letters are not significantly different, p>0.05)

Fig. 9: Effect of forward speed on leaf area coverage

Table 5. ANOVA table on the effect of operating speed and location on leaf area coverage

Source	DF	Type III SS	Mean Square	F value	p value
Speed	2	715.8900	357.9450	30.36	<.0001
Location	1	544.5000	544.5000	46.19	<.0001
Speed×location	2	1.1433	0.5717	0.05	0.9529

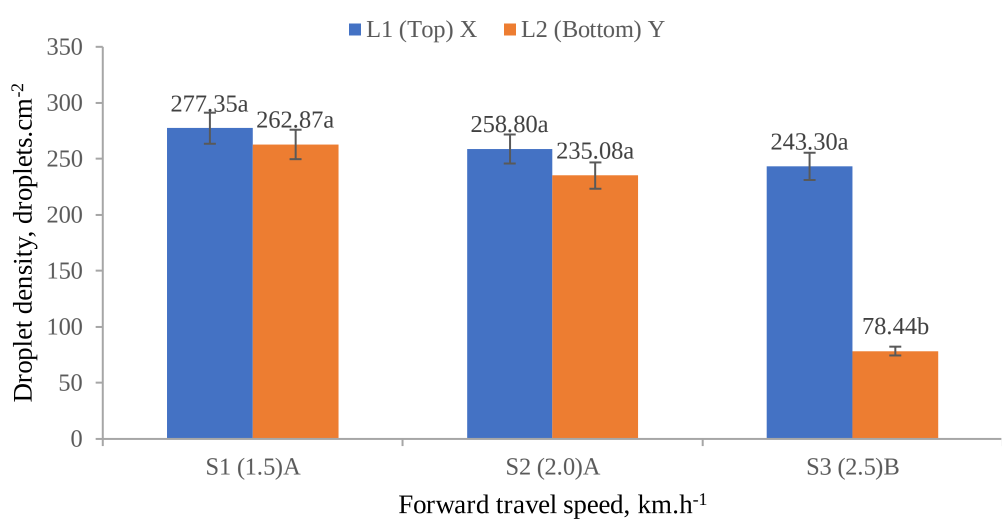

(Mean values and independent parameters with same letters are not significantly different, p>0.05)

Fig. 10: Effect of forward speed on droplet density

Table 6. ANOVA table on the effect of operating speed and location on droplet density

Source	DF	Type III SS	Mean Square	F value	p value
Speed	2	39765.6411	21316.7211	24.69	<.0001
Location	1	20611.2672	20611.2672	25.59	0.0003
Speed×location	2	21316.7211	10658.3606	13.23	0.0009

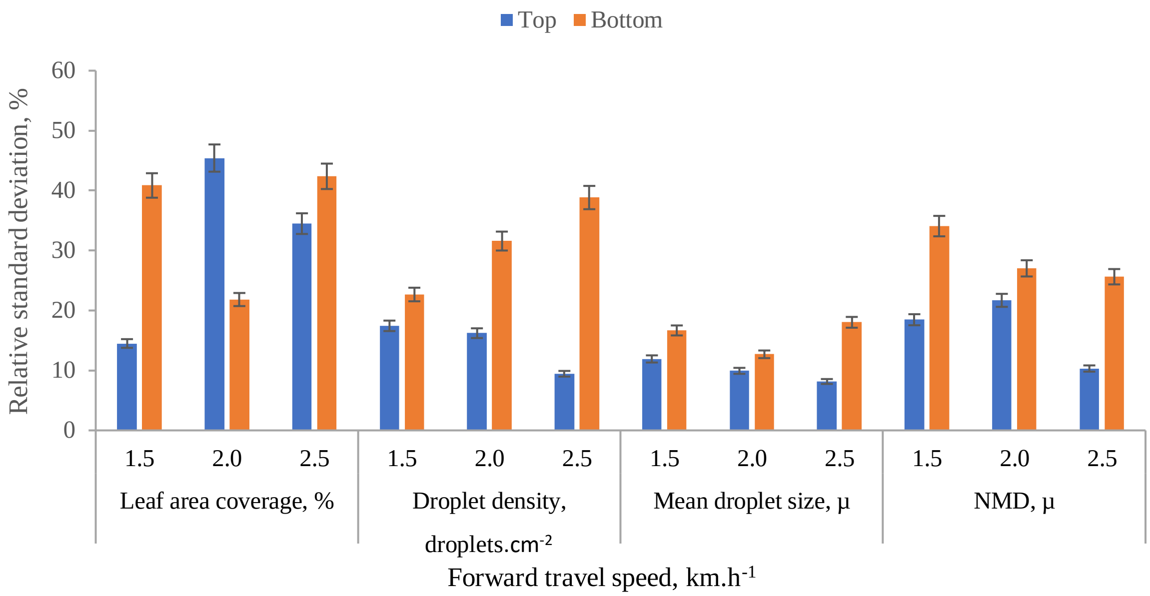

Fig. 11: Relative Standard deviation of dependent parameters of the spraying system

sizes (199.28 ± 8.15 %), and NMD of droplets (165.56 ± 10.32 %) at forward speed of 2.5 $km.h^{-1}$. The top portion of leaves received more uniform droplets as compared to the bottom part of leaves, and forward speed of 2.5 $km.h^{-1}$ exhibited least RSD values. The total volume of spray liquid consumed during the field trial varied between 400 to 675 $l.ha^{-1}$ with increasing travel speedfrom 1.5 to 2.5 $km.h^{-1}$.

Manoeuvrability and operational recommendations

The manoeuvrability of the spraying system was better for soybean crops as compared to cowpea due to well-maintained row spacing in soybean crops, while the cowpea crops caused some hindrance to the movement of the unit due to entangled branches and plants. The machine can be well suited for well-maintained row crops with a row-to-row spacing of up to 600 mm. A minimum of 60 mm space between the rows is necessary for easy movement of the spraying system. The spraying system requires a minimum of 1.5 m head lands for successive turning in the field. The machine can accommodate a wide range of row crops (Soybean, cowpea, green gram, black gram, groundnut, vegetable crops) whose crop geometry lie within the operating range of the machine.

CONCLUSIONS

Leaf area coverage on the top side of the leaves was higher as compared to the bottom sideat forward travel speeds between 1.5 $km.h^{-1}$ and 2.5 $km.h^{-1}$. Mean droplet size on the top and bottom leaf surface reduced from 263.8 µ to 199 µ and 208.5 µ to 196.7 µ, respectively, with increase in forward travel speed of the spraying system. Droplet densities on top leaf surfaces reduced from 277.35 $droplet.cm^{-2}$ to 243.30 $droplet.cm^{-2}$ and 262.87 $droplet.cm^{-2}$ to 78.44 $droplet.cm^{-2}$ at bottom surface with increasing operating speed, and satisfied the required droplet density application criteria at forward travel speed between 1.5 $km.h^{-1}$ and 2.5 $km.h^{-1}$. The slow and medium forward travel speed (1.5 and 2.0 $km.h^{-1}$) gave higher (158.13 % and 68.45 %) coverage as compared to the forward speed of 2.5 $km.h^{-1}$, and hence can be used for spraying for crops with dense canopy or higher pest infestation. Higher forward travel speed of 2.5 $km.h^{-1}$ could provide sufficient droplet density to kill insects / pests, and spraying at this speed could also be performed effectively for less dense crops or crops with less pest infestation. Operation at forward speed of 1.5 $km.h^{-1}$ was thus recommended for proper leaf area coverage, while speed of 2.5 $km.h^{-1}$ produced better droplet density, mean droplet size, and NMD.

ACKNOWLEDGMENT

The first author is thankful to TEQIP-II, College of Technology, GBPUA&T, Pantnagar, Uttarakhand for providing fellowship during his M. Tech. degree programme. The authors are grateful to GBPUA&T, Pantnagar, for providing the funding and necessary research facilities for fabrication and testing. Authors are also thankful to the Head, Department of Farm Machinery and Power Engineering, PAU, Ludhiana, Punjab, India and the Director, Central Institute of

Agricultural Engineering, Bhopal, India, for providing necessary laboratory facilities during research work.

REFERENCES

Anon. 2016a. Next Generation Indian Agriculture-Role of Crop Protection Solutions. A Report on Indian Agrochemical Industry. FICCI, July 2016, 5-12.

Anon. 2016b. Five Decades of Soybean Research at Pantnagar. GBPUA&T, Pantnagar, Uttarakhand, India, pp: 26

Anon. 2018. Soybean. Package of Practices for Crop Management. ICAR- Indian Institute of Soybean Research, Khandwa Road, Indore-452001, Madhya Pradesh, India, 22, 44, 45.

Anon. 2019a. Agriculture Census, 2015-16. All India Report on Number and Area of Operational Holdings, Department of Agriculture, Co-operation and Farmers Welfare, Ministry of Agriculture and Farmers Welfare, Government of India, pp: 12.

Anon. 2019b. Crop Protection.TNAUAgritech Portal, Tamil Nadu Agricultural University, http://agritech.tnau.ac.in/crop_protection/crop_prot_plant_protection%20_equipments_types%20of%20nozzles.html (Accessed on 04.12.2019).

Anon. 2020a. Annual Report 2018-19. Department of Agriculture, Cooperation and Farmers Welfare, Ministry of Agriculture and Farmers Welfare, Government of India, Krishi Bhawan, New Delhi-110 001, pp: 220. (http://agricoop.nic.in/sites/default/files/AR_2018-19_Final_for_Print.pdf)

Anon. 2020b. Plant protection equipment. https://farmer.gov.in/dacdivision/Machinery1/chap4.pdf, 167-180 (Accessed on 10.09.2020).

Anon. 2020c. TeeJet Tech.https://www.sprayersupplies.com/tp8001e-teejet-a8471504 (Accessed on 11.09.2020).

Das N; Maske N; Khawas V; Chaudhary S K; Dhete R D. 2015. Agricultural fertilisers and pesticide sprayers- A review. Int. J. Innov. Res. Sci. Technol., 1, 249-252.

Dash B S. 2016. Development and performance evaluation of self-propelled boom sprayer for intra canopy spraying in row crops. Unpublished M. Tech. Thesis, GBPUA&T, Pantnagar, Uttarakhand, India. pp: 48.

Dhaliwal R J. 2018. Development and evaluation of engine operated walk type drop-down sprayer for cotton crop. Unpublished M. Tech. Thesis, Punjab Agricultural University, Ludhiana, India.

Hofman V. 2018. Spray Equipment and Calibration**.** Agricultural and Biosystems Engineering, North Dakota State University, Fargo, North Dakota, pp: 16.

Hoffmann W C; Hewitt A J. 2005. Comparison of three imaging systems for water-sensitive papers. Appl. Eng. Agric., 21(6), 961-964.

ISI. 1977. Test Code for Power-operated Hydraulic Sprayer. IS: 8548 -1977, Indian Standard Institution, New Dellhi, 7-8.

ISI. 1985. Methods for Calibration of Sprayers. IS:11429-1985, Indian Standard Institute, New Delhi, 6-7.

Mehta C R; Chandel N S; Jena P C; Jha A. 2019. Indian agriculture counting on farm mechanization. Agric. Mech. Asia Afr. Latin Am., 50(1), 84-89.

Mishra P K; Singh M; Sharma A; Sharma K; Singh B. 2014. Studies on effect of electrostatic spraying in orchards. Agric. Eng. Int.: CIGR J., 16(3), 60-69.

Modi R U; Manjunatha K; Gauam P V; Nageshkumar T; Sanodiya R; Chaudhary V; Murthy G R K; Srinivas I; Rao C S. 2020. Climate-smart technology-based farm mechanization for enhanced input use efficiency. In: Srinivasarao C; Srinivas T; Rao R V S; Rao N S; Vinayagam S S; Krishnan P (Eds.) Climate Change and Indian Agriculture: Challenges and Adaption Strategies, ICAR-National Academy of Agricultural Research and Management, Hyderabad, Telangana, India, 257-325.

Narang S; Agrawal K N; Singh R C. 2013. Development of power tiller operated intra canopy sprayer for cotton and pigeon pea crops. Agric. Eng. Today, 37(2), 17-22.

Negi A. 2018. Performance of soybean varieties under different land configurations in mollisols of Himalayan tarai. Unpublished M.Sc. Thesis, GBPUA&T, Pantnagar, Uttarakhand, India, 45-47.

Patel B; Singh M; Mishra P K; Manes G S; Sharma K; Mishra A. 2016. Comparative evaluation of electrostatic sprayer for cotton crop. Int. J. Bioresour. Stress Manage., *7*(5), 1049-1053.

Sharma D N; Mukesh S. 2013. Farm Machinery Design: Principles and Problems. Jain Brothers, pp: 217.

Singh A K; Manes G S; Dixit A; Singh S K; Singh M. 2019. Development and evaluation of multi nozzle backpack type power sprayer. Indian J. Agric. Sci., 89(6), 1005-1010.

Singh N R; Mishra H S; Tewari S K; Chaturvedi S. 2015. Suitability of soybean varieties under second year populus deltoides plantation in tarai region of Uttarakhand. Ind.For., 141(9), 981-984.

Singh S. 2011. Farm Machinery Principles and Applications. Indian Council of Agricultural Research, New Delhi, India, 158-161.

Varshney A C; Narang S; Kumar A. 2004. Plant protection equipment. In: Varshney A C; Tiwari P S; Narang S; Mehta C R. (Eds.) Data Book for Agricultural Machinery Design, Central Institute of Agricultural Engineering, Bhopal, Madhya Pradesh, India, 286-338.

Zhu H; Derksen R C; Guler H; Krause C R; Ozkan H E. 2006. Foliar deposition and off-target loss with different spray techniques in nursery applications. Trans. ASABE, 49(2), 325-334.

Zhu H; Salyani M; Fox R D. 2011. A portable scanning system for evaluation of spray deposit distribution. Comp. Electron. Agric., 76(1), 38-43.

http://www.isae.in / journal_jae.aspx

Journal of Agricultural Engineering

Vol. 57 (3): July-September, 2020

Enhancing Shelf-life of Fresh-cut Carrot and Cauliflower Floret with Combined Ozone and Ultraviolet-C Radiation Treatment

S. K. Giri[1], Sadvatha R. H.[2], M. K. Tripathi[1] and Dilip A. Pawar[2]

[1]Principal Scientist, [2]Scientist, Agro Produce Processing Division, ICAR-Central Institute of Agricultural Engineering, Bhopal, India. Corresponding author email address: giri.saroj@gmail.com

Article Info

Manuscript received:
August, 2019
Revised manuscript accepted:
July, 2020

Keywords: Ozone, carrot, cauliflower, cut-vegetable, texture, UV treatment

ABSTRACT

The effects of ozone and ultraviolet (UV-C) radiation on the quality parameters and microbiology of fresh-cut carrot and cauliflower were investigated. Carrot slices (3 mm thickness) and cauliflower florets were treated with ozonated water (1 ppm) for 10 min and also with sodium hypochlorite solution (100 ppm available chlorine) for comparison. The treated cut vegetables were sealed in polypropylene films and stored at a temperature of 5- 7 °C. In another group, the ozone treated and packed cut-vegetables were subsequently exposed under UV-C radiation for 5 minutes. Microbiological counts (total bacterial count and total fungal count), firmness, colour, TSS, pH and decay rate of products were determined just after treatment, and at regular intervals during storage. The population of microorganisms in the samples treated with both ozone and UV-C was lowest compared to that of other treatment samples. Both bacterial and fungal population of carrot and cauliflower samples with the ozone + UV-C treatment were less than 5 log CFU g^{-1} initially, and kept the lowest level among all treatments during their storage. Ozone and UV-C radiation significantly inhibited the decay rate and decrease in firmness and TSS, and increased the colour values in the fresh-cut carrots and cauliflowers.

Fresh-cut technology aims to provide consumers with a convenient and fresh-like fruits/vegetables with desirable nutritional and sensory qualities. Due to the increasing preferences of consumers towards ready-to-use foods, the economic relevance of fresh-cut fruit and vegetables industry is gaining importance. A huge expansion, both in terms of value and volume, of this market segment can be expected in the coming years, which is evidenced by the growing trend and desire towards such products.

Fresh-cut vegetables of commercial importance include peeled and sliced/grated carrot, baby corn, broccoli and cauliflower florets, shredded cabbage, cut-celery stalk, and cut-sweet potatoes. Carrot (*Daucas carota* L.) is a common root vegetable consumed as raw or in cooked form. Carrot is a rich source of β-carotene (precursor of vitamin A), minerals and some phenolic antioxidants (Ranjitha *et al*., 2017). Cauliflower (*Brassica oleracea*) is another important vegetable crop of India, and is a rich source of proteins, carbohydrates, vitamins and minerals (Singh *et al*., 2015). Fresh cauliflower can be stored for 2–4 weeks, and carrots can be stored for up to 6 months at storage temperature of 0 °C and relative humidity (RH) of 95 per cent. The preservation of carrots and cauliflower in native state can provide nutritional security to the large section of populations (Gupta and Sehgal, 2011; Singh *et al*., 2015).

However, maintaining quality and increasing shelf-life of fresh-cut products is a major challenge, as there are numerous factors which limit the quality and shelf-life. Fresh-cut fruits and vegetables are much more susceptible to deterioration than their corresponding whole fruits and vegetables due to their much larger cut surface and wounding during preparation (Yousuf and Srivastava, 2017; Zambrano-Zaragoza *et al.,* 2017). Furthermore, every step during the preparation of fresh-cut produce could have a potential effect on nutrients and quality of the prepared produce. Quality of fresh-cut produce can be affected both by internal factors including morphological, physiological, and biochemical defence mechanisms, type of fruit, genotype, stress-induced senescence programs and external factors representing environmental situations such as storage temperature, humidity, sharpness of cutting-knife, and chemical treatments (Hodges and Toivonen, 2008). Fresh-cut carrots and cauliflowers undergo deterioration, largely due to microbial spoilage, changes in colour, texture, odour and biochemical parameters. Cut surface whitening/white blush is another important characteristic associated with quality deterioration in fresh-cut carrots. Thus, techniques for reducing undesired microbial contamination and spoilage, and for maintaining the visual, textural and nutritional qualities of the cut-vegetables are required at all steps of the production and distribution chain.

Different approaches including physical, chemical, thermal and bio-preservation technologies have been investigated to reduce the detrimental changes such as microbial growth, desiccation and discoloration in fresh-cut fruits and vegetables including carrots and cauliflowers. Some of the previously published researches suggested the effectiveness of cellulose, casein or chitosan based coatings in shelf-life improvement of fresh-cut carrots (Villalobos-Carvajala *et al.,* 2009; Leceta *et al*., 2015); while a study by Rico *et al.* (2007) reported the use of hygroscopic salts, such as calcium lactate or calcium chloride for the preservation of freshness in fresh-cut carrots. Besides, application of chemical sanitizers such as hypochlorite and chlorine dioxide for extending the shelf-life of grated carrot has also been documented (Gómez-López *et al.,* 2007; Chung *et al.,* 2011). Some of these previous studies had reported a shelf-life of 7 days or less, even with the use of optimized pre-treatments. Chung *et al*. (2011) evaluated the bactericidal efficacy of chlorine dioxide (ClO_2) and sodium hypochlorite solution (NaOCl) for six kinds of fresh-cut vegetables and fruits (cucumber, lettuce, carrot, apple, tomato and guava). The results indicated that 100 ppm ClO_2 solution can reduce total bacterial and *coliform* counts to 3.5-4.0 logCFU.g^{-1} ($p < 0.05$) on lettuce, carrots and tomatoes, which is better than sodium hypochlorite solution. However, treatment with 200 ppm NaOCl resulted in residual trihalomethans (THMs) of 142 ppb, which is higher than the safe limit of 80 ppb. Ranjitha *et al.* (2017) found that shelf-life of fresh-cut carrots can be extended to 12 days by coating carrot slices with polyvinyl alcohol or pectin mainly through preventing formation of white blush and the changes in colour, texture and flavour during storage at 8 °C. Pectin-treated carrot slices showed significantly lower concentration of lignin precursors, and off-tastes causing flavonoids, such as myricetin and narenginin, compared to control.

Subjecting fresh-cut produces to a mild heat treatment has also been attempted with limited success (Lemoine *et al.*, 2009; Silveira *et al.,* 2011; Siddiq *et al.,* 2013; Wulfkuehler *et al.,* 2014). Nevertheless, mild heat treatment leads to reduction of nutritional components and browning of fresh-cut produce (Alegria *et al.,* 2012). Miceli *et al.* (2013) investigated the effect of hot air treatment and cold storage on minimally processed cauliflower. Fresh-cut cauliflower florets put in sealed polyethylene bags were treated at 48°C for 180 min and then stored at 4°C for 21 days. The hot air treatment reduced colour changes of minimally processed cauliflower, however, its increased weight loss during storage. Chlorine is commonly applied as hypochlorous acid and hypochlorite in the fresh-cut industry as a disinfectant at concentrations varying between 50 ppm and 200 ppm of free chlorine (Chung *et al.*, 2011; Goodburn and Wallace, 2013). However, these disinfectants can produce unhealthy by-products including carcinogenic and mutagenic chlorinated compounds, such as chloroform and other trihalomethanes, chloramines and halo-acetic acids, when reacting with organic molecules (Bull *et al.*, 2011). Furthermore, chlorine-based disinfectant can be easily inactivated by organic matter, and its action is highly pH dependent, which limits its efficiency in reducing microbial loads under certain circumstances (Meireles *et al.*, 2015; Ramos *et al.*, 2013). Hence, there is a global concern on developing alternative disinfection strategies to minimize its environmental and public health impacts (Gopal *et al.,* 2010). Relatively new disinfectant processes, such as ultraviolet (UV) illumination, ozone (O_3), and advanced oxidation technologies (AOT) do not present the problems associated with the use of chlorine (Meireles *et al*., 2016).

Ozone is a gas with a strong oxidant capacity that was granted GRAS (Generally Recognized as Safe) status in 1997 by the U.S. Food and Drug Administration, and approved for use as a disinfectant or sanitizer in food processing (Karaca, 2010; García-Martín *et al*., 2018; Tabakoglu and Karaca, 2018). Owing to its sterilization function, ozone has been applied to reduce microbial populations and extend the shelf-life of many fresh-cut fruits (Selma *et al.*, 2008; Ong *et al.,* 2013). Gaseous ozone has been reported to reduce populations of *Escherichia coli* O157, *Listeria monocytogenes* and

Salmonella enterica on fresh-cut bell pepper (Horvitz and Cantalejo, 2012) and anthracnose in papaya (Ong *et al.*, 2013). The increasing trend of consuming fresh-cut produce urges the need to further explore the promising potential of ozone for its effectiveness to control microbial population. However, fruits and vegetables are sometimes affected by the negative effects of ozone due to their high moisture content, enzymes and phenolic compounds (Gabler *et al.,* 2010; Sandhu *et al.,* 2011). Consequently, an optimization of the conditions for treatment is required to be studied for each food.

UV-C light treatment exploits the radiation from the electromagnetic spectrum from 200 nm to 280 nm. It is a powerful germicidal method, being fast, economic and environmentally friendly (Hägele *et al.,* 2016; Meireles *et al*., 2016). Moreover, it has not been reported to form known toxic or significant non-toxic by-products (Otto *et al.,* 2011). The antimicrobial effect of UV-C light is due to its ability to damage microbial DNA, leading to cell death (Birmpa *et al.*, 2013; Manzocco *et al.,* 2016; Sharma *et al.,* 2020). However, little information is currently available about the use of ozone and UV-C treatment for disinfection of cut-vegetables, and their effect on quality and shelf-life of cut-products. The aim of the present study was to evaluate the effectiveness of ozone alone, and in combination with UV-C radiation, in extending the shelf-life of fresh-cut carrot slices and cauliflower florets, and compare with conventional hypochlorite treatment.

MATERIALS AND METHODS

Freshly harvested cauliflower (Cv. C-6041) and carrots (Cv. Arka Suraj) were purchased from a local vegetable market in Bhopal, India. The vegetables were selected to remove defective ones. Carrots were sorted based on the quality characteristics like uniform size, bright orange colour, uniform tapering and minimal lateral roots. Cauliflowers of uniform curd size without any damage were chosen for the study.

Machinery for Production and Treatment of Cut Vegetables

A pilot plant unit was developed at ICAR-CIAE, Bhopal for production of minimally processed fresh-cut vegetables (capacity: 100 $kg.h^{-1}$). The unit consisted of a vegetable washer (bubble type)-cum-ozone treatment tank, cutter/slicer (for cutting vegetables to different size/shape), ozone production system, basket centrifuge, packaging machine, UV chamber and conveyors (Fig. 1). Machinery like the cauliflower floret cutter, washing-cum-ozone treatment tank, UV treatment chamber, basket centrifuge and conveyors were designed and developed by the authors. Detailed technical specifications of these units are given in Table 1. A few components of the plant viz. vegetable slicer, ozone generation system and packaging machine were purchased from commercial manufacturers. The flow diagram of the minimal processing cut vegetable plant is depicted in Fig. 2.

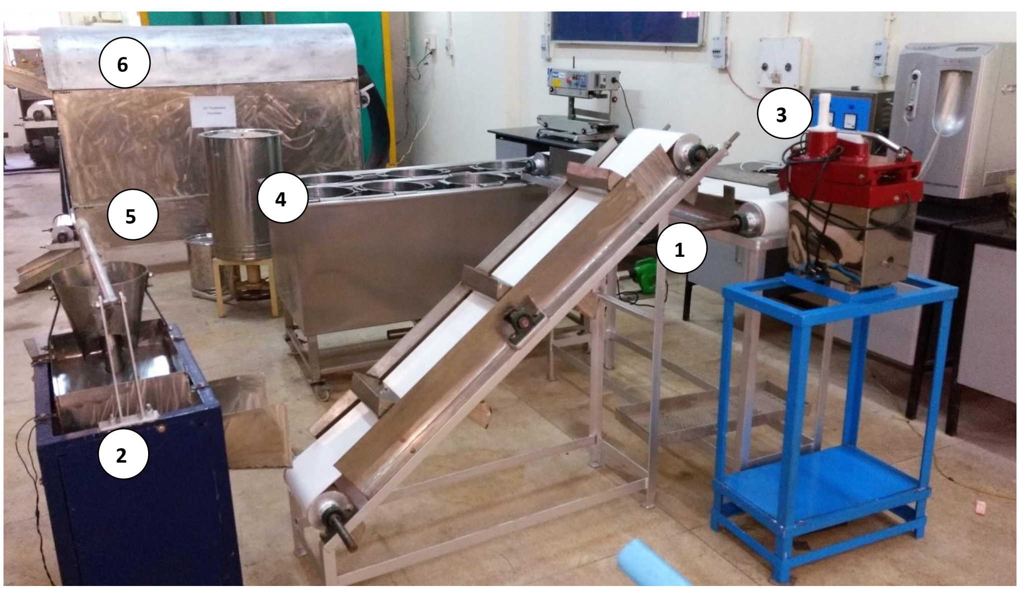

(1) Vegetable cutter, (2) Cauliflower floret cutter, (3) Ozone generation system, (4) Treatment tank, (5) Basket centrifuge, (6) UV chamber

Fig. 1: View of pilot plant for minimally processed cut-vegetables

Table 1. Technical specifications of cut-vegetable pilot plant machinery/equipment

Sl. No.	Name of macninery	Technical specifications
1.	Vegetable slicer (Make: Ponnmani Industries, Coimbatore, India)	Capacity: 100-150 kg.h^{-1} (depending upon type of vegetables) Power of prime mover: 0.75 kW motor (single phase) Voltage: 240 V Cutting blade material: Stainless steel (316) Weight of machine: 30 kg It can cut vegetables like carrot, potato, cabbage, onion, etc. into slices, dices, cubes and grates
2.	Cauliflower floret cutter	Capacity: 5-6 cauliflower per min (120-150 kg.h^{-1}) Power of prime mover: 0.37 kW motor (single phase) Speed of cutting shaft: 350 rpm Overall dimensions: 803 mm × 580 mm × 1095 mm Material of construction: Stainless steel (304)
3.	Washing-cum-Ozone treatment tank	Dimensions of tank: 1500 mm × 750 mm × 600mm Volume of tank: 0.675 m^3 Volume of water for treatment: 500 litre Dimensions of baskets: 500 mm x 310 mm (dia) Air blower speed: 16000 rpm Blower motor power: 0.7 kW
4.	UV Treatment chamber	Capacity: 100-150 kg.h^{-1} Length of the chamber: 2000 mm Width of the chamber: 500 mm Width of conveyor belt: 400 mm Belt material: UV stable PVC UV-c (germicidal) lamps: 30 W capacity (253.7 nm) Number of UV lamps: 04 Power of prime mover: 1.5 kW motor Belt speed: 0.25-2 m.min^{-1}
5.	Basket centrifuge	Basket dimensions: 500 mm × 310 mm(dia) Basket capacity: 10-12 kg of cut vegetables Overall dimensions: 760 mm× 650 mm× 1150 mm Power of driving motor: 0.75 kW Rotational speed: 750 and 1500 rpm
6.	Oxygen concentrator *(Make: Creative Oz-Air (I) Pvt., Ltd., Noida, India; Model HG 5-C)*	Capacity: 5 l.min^{-1} Oxygen concentration: 85-90% from ambient air Outlet pressure: 50 kPa Line voltage: 230 V AC; 50 HZ, single phase
7.	Ozone generator *(Make: Southern Electronics Pvt. Ltd., Bengaluru, India; Model: A-10*)	Ozone production rate: 10 g.h^{-1} or more Ozone concentration: 50 g.m^{-3} or more Operating temperature: 15° C - 40° C Line voltage: 230 V AC; 50 HZ, single phase Specified life: 20,000 working hours
8.	Titanium dome Diffuser *(Make: Creative Oz-Air (I) Pvt. Ltd., Noida, India)*	Dome diameter: 100 mm Height of dome: 25-30 mm Internally fitted with 12.7 mm pipe Life of diffuser: >5,000 working hours

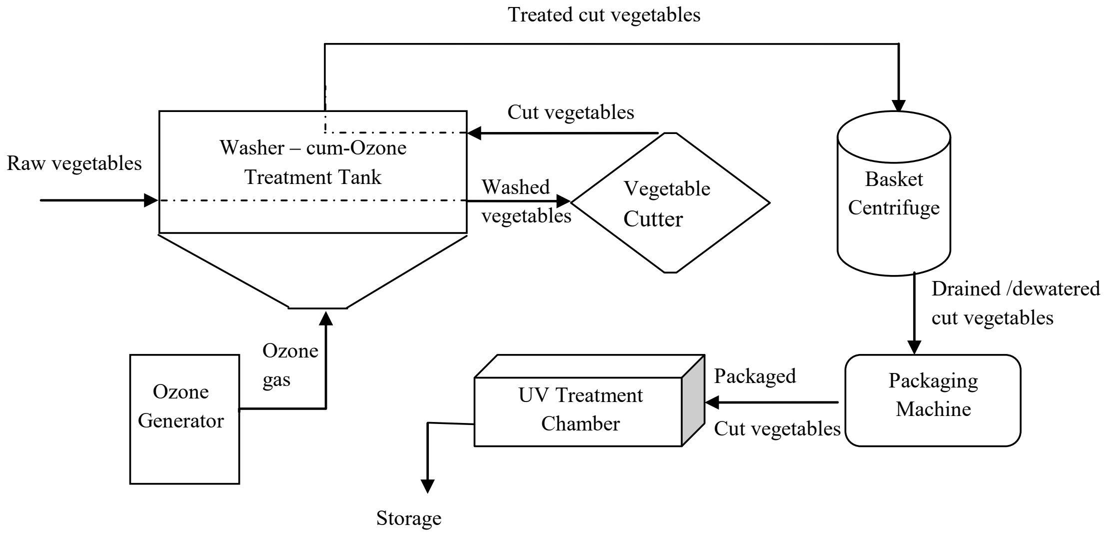

Fig. 2: Flow diagram of cut-vegetable pilot plant

The ozone generation system consisted of an ozone generator and an oxygen concentrator. The ozone generator (Model: A-10, Southern Electronics Pvt. Ltd., Bengaluru, India) used an oxygen flow of 5 $l.min^{-1}$ from an Oxygen Concentrator (Model HG 5-C, Creative Oz-Air (I) Pvt. Ltd., Noida, India) and produced ozone gas at the rate of 10 $g.h^{-1}$.

The UV treatment chamber contained four UV-C (germicidal) lamps of 30 W capacities each (253.7 nanometer light wave). Packaged products could be passed through the chamber continuously in conveyor belts, while exposing them to UV radiation. Detailed specifications of the chamber are given in Table 1. The distance between the products and UV-C lamps could be varied, thereby varying the radiation intensity. UV-C radiation intensity (irradiance) was found to increase from 0.2 $mW.cm^{-2}$ to 0.45 $mW.cm^{-2}$ when the distance was decreased from 450 mm to 250 mm.

Sample Preparation and Treatment

Whole carrots were cleaned with water and cut into 3 mm thick slices with a vegetable cutter (M/s Ponmanni Industries, Coimbatore). Working tables, vegetable cutter knives, containers and surfaces in contact with vegetables during processing were sanitized with chlorine (sodium hypochlorite) solution prior to an operation. Cauliflower florets were separated from the curd by using a motor operated cauliflower floret cutter developed by the authors (Fig. 3), wherein florets of about 30-50 mm head diameter and 40-50 mm length are cut from the cauliflower head. The equipment has following major components: rotating blade assembly, feeding hopper, discharge chute, electric motor and power transmission assembly. The machine is operated by a 0.5 hp electric motor, and a detailed specification of the machine is given in Table 1.

Fresh-cut carrot slices and cauliflower florets were subsequently collected in stainless steel containers. The independent variable in this study was treatment type and type of vegetable. The cut vegetables were divided into four groups of 7.5 kg each: Treatment 1: washing

Fig. 3: Cauliflower floret cutter in operation

with tap water without any sanitizer (i.e. control); Treatment 2: treatment with recommended dose of sodium hypochlorite solution; Treatment 3: Treatment with ozonated water; and Treatment 4: treatment with ozonated water and UV-C. The process parameters for ozone and UV-C treatment (ozone concentration and treatment time, UV-C radiation intensity and exposure time) were fixed at a particular level based on preliminary works.

For treatment-2, the cut samples were dipped in sodium hypochlorite solution (100 ppm available chlorine) for 5 min (Goodburn and Wallace, 2013; Jideani *et al.,* 2017). For treatment-3, cut vegetable samples were dipped in ozonated water (1 ppm). The treatment was carried out in a treatment tank made of food grade stainless steel containing 300 l of water. The ozone gas was dispersed in water with the help of a titanium dome diffuser placed at the centre of the tank. The cut-vegetables were placed in perforated SS baskets inside the tank for ozone treatment. Based on prior preliminary screening tests, the optimum duration of exposure was decided as 10 min, and ozone concentration of 1 ppm to control microbial population in the cut-vegetable samples. After ozonation, the cut-vegetables were withdrawn from water, centrifuged at 750 rpm for 3-4 min to remove the surface water, and allowed to dry at room temperature (25-30 °C) for around 30 min. The cut-samples were thereafter packed in polypropylene (40 micron) pouches weighing 250 g each. Treatment-4 involved exposing the packages of cut-vegetable samples obtained from treatment-3 under UV-C radiation to see its effectiveness in preventing post-treatment contamination. Samples were exposed under UV radiation for 5 min, leading to a radiation intensity of 1 $kJ.m^{-2}$ on the cut-vegetable surface.

Ozone concentration in water was quantified with the help of ozone detection kit (Prerana Laboratories, Pune, India). This residual Ozone Test Kit used DPD Colourimetric method to measure dissolved ozone levels in water up to 1.0 ppm. The kit included a Colour Comparator with least count of 0.1 ppm. Oxidation-Reduction Potential (ORP) of the ozonized water was also measured with the help of an ORP meter (Model: HI98201, Hanna Instruments, USA). The ORP range of the equipment was ±999 mV with a resolution of 1 mV. The ORP reading was correlated with concentration of ozone (ppm) in the water. A linear correlation was observed between the two with R^2 value of 0.93 (Fig. 4). UV-C radiation intensity inside the UV treatment chamber was measured with

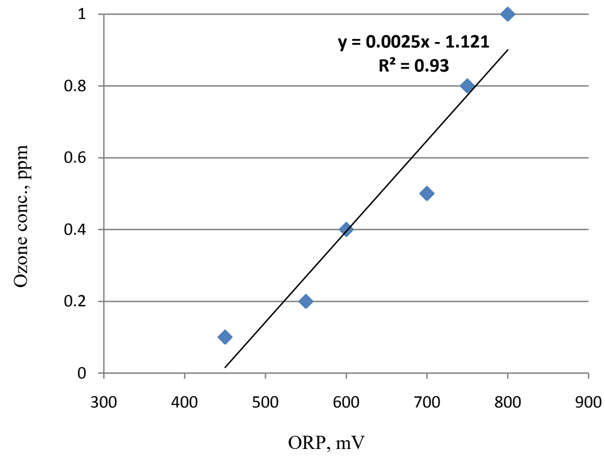

Fig. 4: Correlation between ORP and ozone concentration in water used for treatment of cut-vegetable

the help of a UVA/UVC Light Meter (Model Extech SDL470, FLIR Commercial Systems Inc. USA). The equipment used a UV-C probe that captured short-wave 254 nm UV irradiance measurements under an UV-C light source.

The control and treated cut vegetable samples were stored under refrigeration at 5-7 °C temperature for 14 days during which various quality parameters of the samples were analysed. Three replicates were used per treatment. The study was carried out at Agro Produce Processing Division, ICAR-CIAE Bhopal during 2018-19.

Microbiological Analysis

Total aerobic mesophilic bacteria, yeast and moulds, and coliform were used as microbial indices, and their populations in cut-samples were determined at every three-day interval during storage. Aliquots were taken from the wash water of each vegetable product, diluted in 0.85 % NaCl solution, and surface plated on different culture media. Total aerobic mesophilic bacteria were enumerated by the standard plate count method on plate count agar (PCA) (Himedia Laboratories, Mumbai, India) after incubation at 37 ±1°C for 48 h. Total fungal (yeast and mould) count was enumerated on potato dextrose agar after incubation at 25 ±1°C for 24-72 h. Finally, surviving microbial populations were counted and expressed as log CFU g^{-1} (Selma *et al*., 2008).

Measurement of Quality Parameters

Quality analyses of the cut-vegetables were performed immediately before and after treatments, and were conducted at regular interval of two days over the period of storage. The effects of different treatments on quality were investigated by measuring firmness, weight loss, total soluble solids (TSS), pH and colour parameters and decay of samples during storage.

Decay or spoilage incidences in cut-carrot slices and cauliflower florets were visually assessed during storage at every 2 days' interval. In order to measure per cent decay, three packages for each treated and control sample were drawn randomly from the refrigerator. Individual pieces of cut-samples with any sign of spoilage (soft and mushy consistency, mould growth, off-colour) were separated, weighed and calculated as percentage in relation to the totality of samples of each one of three packages. Firmness of cut-carrot slices and cauliflower florets was determined with a TA-XT2i Texture Analyzer (Stable Micro Systems Ltd., Surrey England, UK) by measuring the maximum force (N) required to cut the samples. A knife blade with 45^{o} chisel end was used at a speed of 2 mm.s^{-1} for the test (Jha *et al.,* 2013).

The colour of cut-vegetable samples was measured with a colour measurement spectrophotometer (Hunter Lab Color Lab Scan XE, Hunter Associates Laboratory Inc., Virginia, USA) in the reflectance mode (Jha *et al.,* 2010). It provided CIE L*, a*, and b* values.

For determination of the total soluble solid content, the samples were minced, crushed, and filtered through a Buchner filter by using two layers of filter papers. The total soluble solid content was measured with a digital refractometer (Model: PAL-1, Atago Co. Ltd., Tokyo, Japan) and expressed as ^{o}Bx. Three replicates of samples were conducted for each treatment to measure the content of total soluble solids. Measurement of pH was done using a hand held pH/mV/Temperature meter (Model pH 3110, WTW GmbH, Wilhelm, Germany) attached to a stainless-steel pH/temperature probe. Technical specifications of all measuring instruments used are listed in Table 2.

Table 2. Specifications of analytical/measuring instruments used for experiment

Sl. No.	Name	Specifications
1.	Colorimeter *(Make: HunterLab, USA;* *Model: Labscan LX16244)*	Geometry: Directional annular 45° illumination / 0° viewing Port diameter/View diameter: 31.8 mm illuminated/ 25.4 mm measured Spectral range: 400 nm - 700 nm Spectral resolution: < 3 nm Reporting interval: 10 nm Light source: Pulsed Xenon Lamp Flashes per measurement: 1 flash Measurement time: < 1 second from button push to measurement
2.	Digital refractometer *(Make: Atago Co. Ltd., Japan;* *Model: PAL-1)*	Range Brix: 0.0 to 53.0 % Resolution: 0.1% Accuracy: ±0.2 %
3.	UVA/UVC Light meter *(Make: FLIR Commercial Systems Inc. USA;* *Model Extech SDL470)*	UVA/UVC range: 2mW.cm^{-2} - 20mW/cm^{2} Resolution: 0.001 mW.cm^{-2} Accuracy: ±4% FS Frequency bandwidth: 365 nm (UVA); 254nm (UVC) Memory: Manual: 99 data readings; includes SD memory card for datalogging Dimensions/ Weight: 182 x 73 x 47.5 mm / 475g
4.	Ozone Test kit *(Make: Prerana Laboratories, Pune, India)*	Range: 0 to 1 ppm Least count: 0.1 ppm No. of tests: 50 Principle used: DPD Colourimetric method
5.	Digital colony counter *(Make: Labtronics, India; Model: LT-37)*	Digital display: 4 digits, 9999 Maximum count Dish size: 110 mm Magnification: x 1. 7 Power: 230v ± 10% AC, 50 Hz, 40 W
6.	pH/mV/Temperature meter *(Model pH 3110, WTW GmbH, Weilheim, Germany)*	pH: -2.000 to +19.999 ±0.005 pH mV: -1200.0 to +1200.0 ±0.3 mV Temperature: -5.0 to +105.0 ± 0.1 °C Power supply: 4 x 1.5 V AA oder 4 x 1.2 V NiMH-rechargeable battery Continuous operation time: up to 100 hours/800 hours w/o backlit

Statistical Analysis of Data

Statistical analyses of data (Tukeys HSD test and Duncan's multiple range test) were carried out to find out significance difference between different treatments and with storage period using SAS software (SAS Institute India Pvt. Ltd.).

RESULTS AND DISCUSSION

Effect of Different Treatments on Microbial Population

Microbial load in cut-fruits and vegetables is one of the critical quality parameters to evaluate their storage quality. Microbiological examination of the fresh-cut carrots revealed that the initial microbial counts in carrots were higher than those of cauliflower (Table 3), possibly because of contamination from soil in case of carrot. Microbial growths gradually increased in all samples when time of storage got extended. However, the rate of increase in microbial populations in control samples was significantly higher than those of treated samples. Treatment with combined Ozone + UV was most effective in restraining the microbial growth.

In case of carrot slices, the initial total bacterial count (TBC) and total fungal count (TFC) were 6.18. and 6.28 log CFU.g^{-1}, respectively, in control samples. Significant differences in microbial counts were observed between control and treated carrots and cauliflower throughout the storage periods (Table 3). After treatments, the TBC and TFC counts were found to be 4.69 and 4.34 log CFU.g^{-1}, 4.53 and 5.45 log CFU.g^{-1}, and 4.11 and 4.96 log CFU g^{-1} for chlorine, ozone, and Ozone + UV treated samples, respectively. Thus, there were about two log reductions in the values of TBC and TFC. TBC increased from an initial value of 1.5×10^6 to 8.4×10^9 CFU.g^{-1}, and TFC increased from an initial value of 1.9×10^6 to 2.7×10^8 CFU.g^{-1} in control carrot samples within 6 days of storage. During this period, distinct spoilage was also observed. However, the same level of TBC and TFC counts were observed after 12 days' storage in chlorine and ozone treated samples.

The population of microorganisms in the samples treated with ozone + UV was lowest compared to that of the other treatment samples. Both bacterial and fungal population of the carrot and cauliflower samples with ozone + UV treatment were less than 5 log CFU.g^{-1} on day 0, and maintained the lowest level among all treatment samples during storage up to 12 days (Table 3).

Literature on acceptable universal microbiological limits for spoilage organisms in fresh-cut fruits and vegetables are scarce. However, some countries have established legal limits for microbial population in minimally processed fresh fruits. The Spanish legal limit (RD 3484/ 2000, 2001) for microbial populations for minimally fresh-processed fruits for safe consumption

Table 3. Effects of treatments on microbial populations (log cfu.g^{-1}) of fresh-cut carrots and cauliflower during refrigerated storage at 5-7 °C

Treatment	Total bacterial count Storage period, days					Total fungal count Storage period, days				
Carrot	0	3	6	9	12	0	3	6	9	12
Control	6.18^{a}	7.38^{a}	9.92^{a}	10.66^{a}	10.86^{a}	6.28^{a}	6.92^{a}	8.43^{a}	9.26^{a}	9.72^{a}
Chlorine	4.69^{b}	5.51^{b}	6.82^{b}	8.64^{b}	9.54^{b}	4.34^{c}	4.58^{c}	6.85^{b}	7.56^{b}	7.93^{b}
Ozone	4.53^{b}	5.89^{b}	6.86^{b}	7.86^{b}	9.53^{b}	5.45^{b}	5.97^{b}	6.81^{b}	7.54^{b}	8.64^{c}
Ozone + UV	4.11^{b}	4.92^{c}	5.68^{c}	5.91^{c}	7.88^{c}	4.96^{bc}	5.38^{d}	5.89^{c}	5.91^{c}	7.66^{b}
CD value ($p \leq 0.05$)	0.56	0.43	0.65	0.86	1.03	0.64	0.52	0.38	0.67	0.63
Cauliflower										
Control	4.92^{e}	5.65^{e}	7.45^{e}	8.62^{e}	9.20^{e}	5.83^{e}	6.95^{e}	8.79^{e}	9.40^{e}	9.82^{e}
Chlorine	3.84^{f}	4.56^{f}	6.76^{f}	6.81^{f}	7.57^{f}	4.80^{f}	5.76^{g}	6.34^{g}	6.79^{f}	8.11^{f}
Ozone	3.75^{f}	3.79^{g}	5.94^{g}	6.80^{f}	6.92^{g}	4.73^{f}	6.53^{f}	6.94^{f}	7.00^{f}	7.81^{g}
Ozone + UV	3.65^{f}	3.94^{g}	5.41^{h}	6.62^{f}	6.72^{g}	4.49^{f}	5.78^{g}	6.92^{f}	7.71^{g}	7.56^{g}
CD value ($p \leq 0.05$)	0.21	0.43	0.38	0.55	0.40	0.38	0.33	0.42	0.57	0.44

Note: 1. Values represent the mean of three replicates

2. Different letters within each column indicate significant differences ($p < 0.05$) between treatments is 7 log CFU.g^{-1} for aerobic bacteria (Barth *et al.,* 2009), while it is 7.7 log CFU.g^{-1} (5×10^7 CFU.g^{-1}) for total microbial count in Germany. Debevere (1996) reported the population as 8 log CFU.g^{-1} for mesophilic aerobic bacteria; 7 log CFU.g^{-1} for lactic acid bacteria and 5 log CFU.g^{-1} for yeasts at the end of the shelf-life in fresh-cut vegetables. Garg *et al.* (1990) reported aerobic plate counts of shredded carrots ranging from 5.0–5.8 log CFU.g^{-1}. Carlin *et al.* (1989) observed initial counts of ~6.7 log CFU.g^{-1} and subsequent growth to 8.7 log10 CFU.g^{-1} after storage for 7 days in ready-to-use grated carrots. The microbial counts even after 12 days of storage in Ozone + UV treated carrot slices, reported in this study were in the range of 6.72-7.8 log CFU.g^{-1}. This indicated that combined ozone and UV treatment could inhibit the growth of bacterial populations in fresh-cut carrots and cauliflowers.

Effect of Treatments on Decay Rate of Cut-carrots and Cauliflower Florets

Ozone with UV treatment employed in this study resulted in a significant effect on the decay rate of cut-carrot and cauliflower (Fig. 5). No decay symptom was observed in the samples of treated groups during the first 6 days of storage. In control samples, decay was noticed on 4th day, and the degree of decay was significantly higher ($p \leq 0.05$) than the treated samples from fourth day onwards (Table 4). The results in Table 4 and Fig. 5a showed that decay symptoms were observed on the 8th day with 2 % and 3 % decay in ozone and chlorine treated carrot slices, respectively. However, decay was noticed on 10th day (only 2 % decay) in samples that were treated both with ozone and UV, whereas 36 % decay occurred in control sample by that time. Decay initiated after 8 days in all treated samples in case of cauliflower (Fig. 5b). After 12 days of storage 33 % of control samples were spoiled but combined ozone and UV-C treated samples had only 7 % spoilage (Table 4). Whangchai *et al.* (2006) and Han *et al.* (2017) stated that ozone destroyed microorganisms by oxidation of cellular components, such as sulfhydryl groups of amino acids in enzymes leading to cell membrane damage. The results here also suggested that Ozone + UV treatments could reduce the rate of decay in cut carrots and cauliflowers.

Treatment of fruits and vegetables either with gaseous ozone or ozone dissolved in water has been found to prevent their decay as reported in previous studies done in this field. Barth *et al.* (1995) reported that storage of blackberries under 0.1 mg.kg^{-1} or 0.3 mg.kg^{-1} ozone atmosphere for 12 days at 2 °C was effective

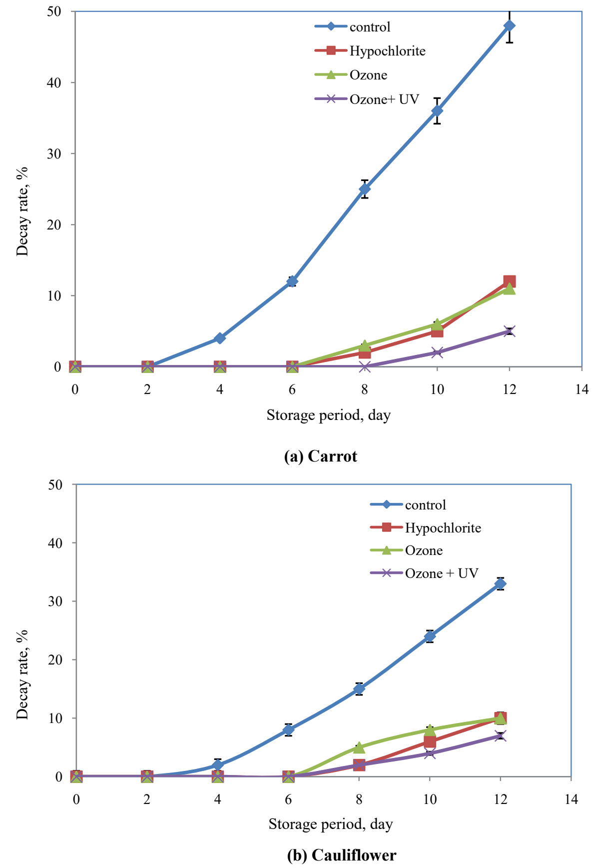

Fig. 5: Effect of different treatments on decay rate of (a) carrot slice, and (b) cauliflower floret during refrigerated storage (5 - 7 °C)

in preventing losses due to rotting. Sarig *et al.* (1996) observed that a short exposure to ozone (20 min) reduced the incidence decay in table grapes during cold storage and subsequent shelf-life. According to the authors, ozone not only had a sterilizing effect but also induced resistance against the development of fruit rot. Cayuela *et al.* (2009) concluded that 2 mg.kg^{-1} ozone treatment for 72 days considerably reduced decay of cold stored grapes compared to those kept in air. García *et al.* (2016) showed that the effectiveness of exposure to ozone as pre-treatment for improving citrus shelf-life is superior to that of heat treatments both at laboratory (water dipping) and industrial scale (heat water showers system).

Effect of Treatments on Different Quality Parameters of Cut-Carrot and Cauliflower

Firmness

Fruits and vegetables with a firm texture have high desirability as consumers associate these textural

Table 4. Effects of treatments on decay percentage, firmness value and colour parameters of fresh-cut carrots and cauliflower during refrigerated storage at 5-7 °C

Storage Period, day	Carrot				Cauliflower			
	Control	Chlorine	Ozone	Ozone + UV	Control	Chlorine	Ozone	Ozone + UV
				Decay, %				
0	0	0	0	0	0	0	0	0
2	0	0	0	0	0	0	0	0
4	4^{a}	0^{b}	0^{b}	0^{b}	2^{a}	0^{b}	0^{b}	0^{b}
6	12^{a}	0^{b}	0^{b}	0^{b}	8^{a}	0^{b}	0^{b}	0^{b}
8	25^{a}	2^{b}	3^{b}	0^{c}	15^{a}	2^{b}	5^{c}	2^{b}
10	36^{a}	5^{b}	6^{b}	2^{c}	24^{a}	6^{b}	8^{c}	4^{d}
12	48^{a}	12^{b}	11^{b}	5^{c}	33^{a}	10^{b}	10^{b}	7^{c}
				Firmness, N				
0	84.5^{a}	84.5^{a}	84.5^{a}	84.5^{a}	61.8^{e}	60.5^{e}	61.4^{e}	60.2^{e}
2	82.6^{a}	82.8^{a}	83.7^{a}	83.5^{a}	58.4^{e}	57.2^{e}	58.6^{e}	58.2^{e}
4	78.3^{a}	78.6^{a}	81.6^{b}	82.6^{b}	52.7^{e}	55.6^{f}	58.7^{g}	58.6^{g}
6	72.4^{a}	77.5^{b}	80.9^{c}	81.5^{c}	46.2^{e}	52.3^{f}	56.5^{g}	57.8^{h}
8	62.4^{a}	65.7^{b}	76.4^{c}	75.2^{c}	33.0^{e}	47.5^{f}	55.9^{g}	55.2^{g}
10	57.8^{a}	60.5^{b}	71.8^{c}	72.8^{c}	30.5^{e}	48.6^{f}	54.8^{g}	55.6^{g}
12	-	-	-	-	-	46.5^{f}	54.5^{g}	55.2^{g}
		Colour 'a' value					Colour 'L' value	
0	25.32^{a}	25.72^{a}	25.32^{a}	25.11^{a}	87.05^{e}	87.24^{e}	87.22^{e}	87.14^{e}
2	23.54^{a}	24.36^{b}	23.82^{a}	23.58^{a}	85.23^{e}	86.24^{e}	85.87^{e}	86.35^{e}
4	21.48^{a}	22.57^{b}	21.35^{a}	22.68^{b}	82.57^{e}	85.36^{f}	83.64^{e}	84.31^{f}
6	18.54^{a}	21.64^{b}	19.07^{a}	20.14^{b}	80.75^{e}	82.65^{f}	81.90^{f}	82.47^{f}
8	16.34^{a}	19.87^{b}	18.65^{c}	17.48^{ac}	79.50^{e}	81.36^{f}	80.41^{f}	80.73^{f}
10	15.32^{a}	19.18^{b}	18.32^{b}	17.04^{c}	78.94^{e}	81.02^{f}	80.13^{f}	79.44^{f}
12	-	-	-	-	-	80.78^{f}	80.34^{f}	79.37^{f}

Note: 1. Values represent the mean of three replicates
2. Different letters within each row (on the same day) for carrots and cauliflowers separately indicate significant differences ($p \leq 0.05$) between treatments

attributes with freshness and wholesomeness (Rico *et al.*, 2007). Firmness of the fresh-cut carrot slices showed a decreasing trend during storage up to 12 days, but the firmness values of control samples decreased at a faster rate compared to those of ozone and UV treated samples (Fig. 6). In case of control (untreated) carrot, the firmness value reduced to 68.4 % of its initial value after 10 days, whereas treated sample retained 86.15% of initial firmness value. Similarly, in case of cauliflower the firmness values were 49.35% and 92.3% of initial values after 10 days of storage for control and ozone + UV-C treated samples, respectively (Table 4). However, there was no significant difference ($p \leq 0.05$) between samples treated with ozone alone and ozone + UV (Table 4). Treatment with hypochlorite solution resulted in softer texture as compared to the ozone treated samples. The cut-carrot and cauliflower treated with ozone and UV-C retained firmness better than the untreated and chlorine treated samples during storage up to 12 days. Similar observations for firmness in tomatoes were made by Liu *et al.* (1993). Allendea *et al.* (2006) had observed that a higher dose (7.11 $kJ.m^{-2}$) of UV-C radiation might result in softening of lettuce, which could be related to the production of free radicals as a result of increase in senescence.

There is contradiction regarding effect of ozone in maintaining firmness of fruits and vegetables. A few studies showed that ozone did not have any effect on the change in firmness of apples, grapes, pears and rocket leaves (Skog and Chu, 2001; Sharpe *et al.*, 2009; Horvitz and Cantalejo, 2014). D'Souza *et al.* (2018) reported that

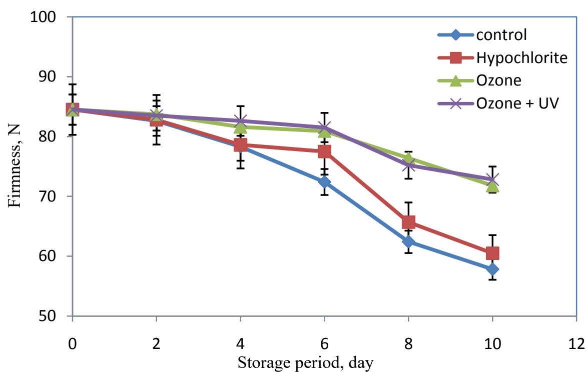

(a) Carrot

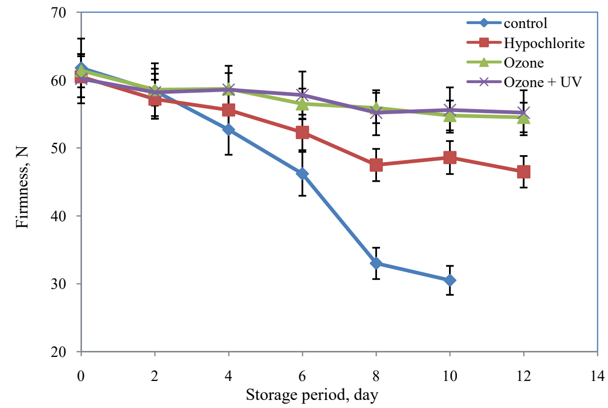

(b) Cauliflower

Fig. 6: Effect of different treatments on firmness of a) carrot slice, and b) cauliflower floret during refrigerated storage (5 - 7 °C)

the average firmness of carrots was neither influenced by different ozone treatments nor by the storage time for up to five days. However, several other studies showed that there was better firmness retention in kiwi, papaya, strawberries and tomatoes (Tzortzakis *et al.,* 2011; Ali *et al.,* 2014; Kying and Ali, 2016) in response to ozone treatment. Ozone treatment delayed the tissue toughening in carrot sticks (Forney *et al.*, 2007; Chauhan *et al.*, 2011). These changes were associated with changes in cellulose, hemicellulose and lignin content, mainly due to the reduced lignification of the cell walls.

Colour

The visual quality of a cut-product is important, as any colour alteration might be recognized as a symptom of senescence.

The lightness L' value of cauliflower floret and carrot slice as well as a-value (redness) of carrot decreased gradually throughout the storage period (Fig. 7). As compared to the control group, cut-vegetables of treated groups showed a distinctly higher colour (L and a- value) during longer storage time. There was no significant difference ($P < 0.05$) in colour values of samples treated with ozone and Ozone + UV at initial stage of storage. The lightness (L-value) and redness (a- value) of sodium hypochlorite treated carrot samples were significantly ($P < 0.05$) higher than those of other samples (Table 4). Similar result was obtained by Chung *et al.* (2011) who reported that chlorine treatment significantly increased the L- value of fresh-cut apples due to the bleaching effect of chlorine.

According to Sandhu *et al.* (2011), ozone may react with the conjugated double bonds in the carotenoids,

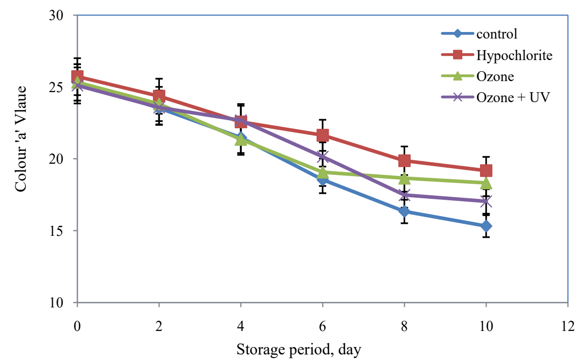

(a) Colour 'a' value of carrot

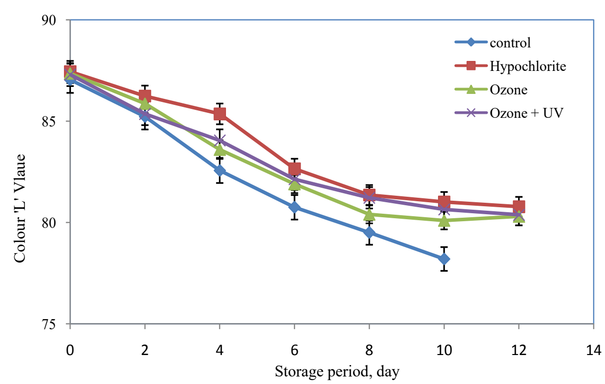

(b) Colour 'L' value of cauliflower

Fig. 7: Effect of different treatments on colour values of cut-vegetables during refrigerated storage (5 - 7 °C)

thereby decreasing the yellowness. In carrots treated with ozone at concentrations from 10 - 115 µg. l^{-1}, the lightness value increased significantly. Conversely, ozone treatment at 0.8 µg.l^{-1} had no effect on the colour of carrot (Sharpe *et al.,* 2009). Ozone treatment had no effect on the change in colour of papaya (Kying and

Ali, 2016), apple (Sharpe *et al.,* 2009), and tomato (Bermudez-Aguirre and Barbosa-Canovas, 2013) during storage. Our results showed that treatment with ozone and UV was effective in maintaining colour of cut-carrot slices and cauliflower florets during storage up to 10 and 12 days, respectively.

pH and total soluble solid (TSS) content

The pH values of cut carrot and cauliflower did not change significantly during storage up to 12 days. The pH remained between 5.4 and 6.3 for various treatments in case of carrot, and between 5.75 and 6.18 in cauliflower (Table 5). However, the rate of decline in pH was less (3-4 %) in ozone and UV-C treated samples compared to the control (10-15%) and chlorine treated samples (7-8 %). D'Souza *et al.* (2018) had also reported that the pH values of the carrot treated in ozonated water remained approximately 6.0 during storage up to 5 days. The pH values of fresh-cut carrot and lettuce were considered to be adequate in a range of 5-6.5 for quality retention (Rico *et al.,* 2007).

Pan and Zu (2012) observed that UV-C radiation slowed the rise in titratable acidity of fresh-cut pineapple. The titratable acidity in the slices radiated for 60 s and 90 s was obviously lower than that in the control group. The authors correlated the result with the number of microorganisms present in the samples. As the titratable acidity always increased accompanying with an ascend trend of microbe (Zu *et al.,* 2009), therefore the less increase in titratable acidity of UV-C radiated samples might be due to UV-C irradiation reducing the number of microorganisms in the fresh-cut pineapple. In general, pH declines as the values of titratable acidity increases. In this study, we also observed less decrease in pH from an initial value of 6.48 to 6.3 in case of UV treated cut-carrots, and from 6.41 to 6.18 in case of cauliflower after 12 days of storage. Hence, the results obtained in the present study corroborated the previous findings on the effect of UV treatment on pH and titratable acidity of cut-vegetables.

The TSS of cut-carrot slices showed an upward trend during storage, while for cauliflower TSS of all treated samples remained almost constant except that of control. TSS of untreated carrots increased from an initial value of 6.1 ^{o}Bx to a final value of 9.4 ^{o}Bx after 12 days of storage. During this period, treated cut-carrot showed a less increase in value of TSS (up to 8.1 ^{o}Bx), with lowest increase (7.7 ^{o}Bx) in case of combined

Table 5. Effects of treatments on pH and total soluble solids(TSS) of fresh-cut carrot and cauliflower during refrigerated storage at 5-7 °C

Storage period, day	Carrot				Cauliflower			
	Control	Chlorine	Ozone	Ozone + UV	Control	Chlorine	Ozone	Ozone + UV
				pH				
0	6.54±0.11^{a}	6.37±0.14^{a}	6.51±0.08^{a}	6.48±0.13^{a}	6.31±0.07^{e}	6.45±0.09^{e}	6.37±0.11^{e}	6.41±0.12^{e}
2	6.35±0.09^{a}	6.25±0.10^{a}	6.36±0.12^{a}	6.44±0.11^{a}	6.24±0.12^{e}	6.38±0.15^{e}	6.25±0.09^{e}	6.42±0.14^{e}
4	6.21±0.07^{a}	5.84±0.09^{b}	6.25±0.14^{a}	6.35±0.08^{a}	6.08±0.09^{e}	6.41±0.13^{e}	6.30±0.11^{e}	6.28±0.08^{e}
6	5.87±0.12^{b}	5.74±0.12^{b}	6.23±0.08^{a}	6.28±0.14^{a}	5.84±0.12^{f}	6.20±0.08^{e}	6.24±0.14^{e}	6.24±0.10^{e}
9	5.35±0.07^{b}	5.36±0.08^{b}	6.14±0.12^{a}	6.32±0.11^{a}	5.77±0.14^{f}	5.96±0.11^{e}	6.12±0.15^{e}	6.27±0.06^{e}
12	5.44±0.09^{b}	5.65±0.11^{b}	5.98±0.17^{ab}	6.30±0.08^{a}	5.75±0.10^{f}	5.82±0.13^{f}	6.10±0.08^{e}	6.18±0.07^{e}
				TSS, ^{o}Bx				
0	6.1±0.06^{a}	6.3±0.08^{a}	6.1±0.12^{a}	6.2±0.09^{a}	4.0±0.04^{p}	4.8±0.08^{r}	4.4±0.06^{q}	4.2±0.06^{pq}
2	6.7±0.08^{b}	6.5±0.09^{b}	6.3±0.08^{a}	6.4±0.07^{ab}	4.2±0.08^{p}	5.0±0.05^{r}	4.3±0.06^{q}	4.0±0.09^{p}
4	7.0±0.08^{c}	6.9±0.11^{c}	6.8±0.08^{bc}	6.5±0.11^{b}	4.1±0.06^{p}	4.9±0.09^{r}	4.6±0.08^{r}	4.3±0.04^{q}
6	7.8±0.09^{e}	7.4±0.05^{d}	7.4±0.06^{d}	6.8±0.07^{c}	4.3±0.07^{q}	4.8±0.08^{r}	4.5±0.04^{s}	4.2±0.08^{q}
9	8.9±0.05^{f}	7.7±0.07^{d}	7.6±0.05^{d}	7.3±0.05^{d}	4.7±0.05^{r}	5.1±0.05^{t}	4.2±0.06^{p}	4.4±0.07^{q}
12	9.4±0.06^{h}	8.0±0.05^{g}	8.1±0.09^{g}	7.7±0.06^{j}	4.7±0.09^{r}	5.0±0.07^{t}	4.5±0.09^{s}	4.5±0.05^{s}

Note: 1. Values represent the mean ± SD of three replicates

2. Different letters within each row (on the same day) for carrots and cauliflowers separately indicate significant differences (p < 0.05) between treatments ozone and UV treated sample. At the end of storage (12 days), there was a significant difference ($p < 0.05$) in TSS contents of the control and treated samples, but not among different treatments (Table 5). TSS values of cauliflower floret oscillated within the range of 4 - 5 °Bx up for all treatments. Initially, the treated samples showed higher values of TSS compared to control. At the end of 12 days, however, there was no significant difference in the values of TSS for different samples.

The results on pH and TSS changes found in this study (higher changes in control samples than in ozone/UV treated samples) were in agreement with previous studies (Pan and Zu, 2012; Carbone and Mencarelli, 2015; García-Martín *et al.,* 2018). Pan and Zu (2012) observed a significant difference in TSS values of the UV radiated and un-radiated pineapple slices. However, UV treatment had only a small and insignificant effect on the TSS of tomato during the post-treatment storage and ripening (Charles *et al.,* 2005). Similarly, García-Martín *et al.* (2018) reported that the application of 60 $mg.kg^{-1}$ ozone-enriched atmosphere during cold storage of citrus did not induce any effect on their juice content, pH, soluble solids and titratable acidity; which meant that exposure to ozone was not detrimental to these citrus quality parameters. Carbone and Mencarelli (2015) on the exposition of grapes to ozone gas in air atmosphere for 12 h at 10 °C, concluded that the use of ozone in air or nitrogen does not alter the fruit quality attributes.

D'Souza *et al.* (2018) observed that the alteration in pH of ozone treated carrot is a temporary effect of the treatment, and the effect of ozone on pH is temperature dependent. It was verified that the temperature associated with the ozone concentration could affect the pH of carrots. The authors observed that increasing the ozone concentration to above 5 mg. l^{-1}, prevented immediate changes in the pH of carrots when they were exposed to treatment with ozonated water at temperatures above 14 °C. Moreover, pH values of samples were similar throughout the storage time, being close to 6.0. These values are the expected values for carrot in storage (Mastromatteo *et al.,* 2012). The treatment with ozone (2.5 and 5 $mg.l^{-1}$) as gas also prevented the total soluble solid concentration of carrot from increasing from the fourth day of storage (D'Souza *et al.,* 2018). The authors opined that the action of ozone might have suppressed the microorganisms on fruits/vegetable surfaces, which could inhibit internal physiological changes in carrot, resulting in smaller variation in the pH and TSS values. Thus, the ozone and UV treatment could prevent the deterioration of the product and increase its shelf-life. Ozone and UV-C treated carrot slices and cauliflower florets could be stored for 10 and 12 days, respectively under refrigerated conditions. During this period, less changes in colour parameters, firmness, pH and TSS of the cut-products occurred as compared to untreated control samples. Total bacterial count and fungal count remained under the acceptable range of 6.7-7.8 log $CFU.g^{-1}$ in the treated samples, resulting in less decay.

CONCLUSIONS

The results of this study explained the usefulness of treating fresh-cut carrot slices and cauliflower florets with ozone and UV-C radiation for quality maintenance during storage. Treatment with ozone and UV-C reduced the decay rate, maintain colour, and delay softening of cut carrots and cauliflower, thus extending their shelf-life during refrigerated storage. The shelf-life of treated cut-carrot and cauliflower were observed to be 10 and 12 days, respectively, when stored under refrigerated conditions (5-7 °C), whereas untreated control samples had shelf-life of 5 and 8 days, respectively. The delayed senescence by ozone and UV-C radiation might be related to its impact on the degradation of cell wall substance. Considering the better-quality parameters (colour and texture), less decay in treated samples and non-thermal/non-chemical nature of the treatment, use of ozone and UV-C could be recommended for improving the shelf-life of fresh-cut carrot and cauliflower.

REFERENCES

Alegria C; Pinheiro J; Duthoit M; Gonçalves E M; Moldáo-Martins M; Abreu M. 2012. Fresh-cut carrot (cv. Nantes) quality as affected by abiotic stress (heat shock and UV-C irradiation) pretreatments. LWT- Food Sci. Technol., 48(2), 189-208.

Allendea A; McEvoyb J L; Luo Y; Artesc F; Wang C Y. 2006. Effectiveness of two-sided UV-C treatments in inhibiting natural microflora and extending the shelf-life of minimally processed 'Red Oak Leaf' lettuce. Food Microbiol., 23, 241-249.

Ali A; Ong M K; Forney C F. 2014. Effect of ozone pre-conditioning on quality and antioxidant capacity of papaya fruit during ambient storage. Food Chem., 142, 19-26.

Barth M; Zhou C; Mercier J; Payne F A. 1995.

Ozone storage effects on anthocyanin and fungal growth in blackberries. J. Food Sci., 60, 1286-1288.

Barth M; Hankinson T R; Zhuang H; Breidt F. 2009. Microbiological Spoilage of Fruits and Vegetables. In: Speber W H; Doyle M P. (Eds.) Compendium of the Microbiological Spoilage of Foods and Beverages, Food Microbiology and Safety, Springer Science + Business Media, Germany, LLC 2009, 135-183. DOI 10.1007/978-1-4419-0826- 1_6.

Bermudez-Aguirre D; Barbosa-Canovas G V. 2013. Disinfection of selected vegetables under nonthermal treatments: Chlorine, acid citric, ultraviolet light and ozone. Food Control, 9(1), 82-90.

Birmpa A; Sfika V; Vantarakis A. 2013. Ultraviolet light and ultrasound as nonthermal treatments for the inactivation of microorganisms in fresh ready-to-eat foods. Int. J. Food Microbiol., 167(1), 96-102.

Bull R J; Reckhow D A; Li X; Humpage A R; Joll C; Hrudey S E. 2011. Potential carcinogenic hazards of non-regulated disinfection by-products: Haloquinones, halo-cyclopentene and cyclohexene derivatives, N-halamines, halonitriles, and heterocyclic amines. Toxicol., 286 (1–3), 1-19.

Carbone K; Mencarelli F. 2015. Influence of short-term postharvest ozone treatments in nitrogen or air atmosphere on the metabolic response of white wine grapes. Food Bioprocess Technol., 8(8), 1739-1749.

Carlin F; Nguyen-the C; Cudennec P; Reich M. 1989. Microbiological spoilage of fresh, ready-to-use grated carrots. Sci. Aliments., 9, 371-386.

Cayuela J A; Vázquez A; García Martos A G. 2009. Control of table grapes postharvest decay by ozone treatment and resveratrol induction. Food Sci. Technol. Int., 15 (5), 495–502.

Charles M T; Kalantari R; Corcuff R; Arul J. 2005. Postharvest quality and sensory evaluation of UV-treated tomato fruit. Acta Hort., 682, 537-542.

Chauhan O P; Raju P S; Ravi N; Singh A; Bawa A S. 2011. Effectiveness of ozone in combination with controlled atmosphere on quality characteristics including lignification of carrot sticks. J. Food Eng., 102, 43-48.

Chung C C; Huang T C; Yu C H; Shen F Y; Chen H H. 2011. Bactericidal effects of fresh-cut vegetables and fruits after subsequent washing with chlorine dioxide. Int. Conf. Food Eng. Biotechnol. IPCBEE, 9, 107-112.

D'Souza L P; Faronia L R D; Helenoa F F; Ceconb P R; Danielle T. 2018. Effects of ozone treatment on postharvest carrot quality. LWT - Food Sci. Technol., 90, 53-60.

Debevere J. 1996. Criteria en praktische methoden voir de bepaling van de houdbaarheidsdatum. In de etikettering. Etikettering, houdbaarheid en bewaring (voedingsmiddelen en recht 2), Belgium, Die Keure, Brugge, 37-64.

Forney C F; Song J; Hildebrand P D; Fan L; McRae K B. 2007. Interactive effects of ozone and 1-methylcyclopropene on decay resistance and quality of stored carrots. Postharvest Biol. Technol., 45, 341-348.

Gabler F M; Smilanick J L; Mansour M F; Karaca H. 2010. Influence of fumigation with high concentrations of ozone gas on postharvest grey mold and fungicide residues on table grapes. Postharvest Biol. Technol., 55, 85-90.

García J F; Olmo M; García J M. 2016. Decay incidence and quality of different citrus varieties after postharvest heat treatment at laboratory and industrial scale. Postharvest Biol. Technol., 118, 96-102.

García-Martín J F; Olmo M; García J M. 2018. Effect of ozone treatment on postharvest disease and quality of different citrus varieties at laboratory and at industrial facility. Postharvest Biol. Technol., 137, 77-85.

Garg N; Churey J J; Splittstoesser D F. 1990. Effect of processing conditions on the microflora of fresh-cut vegetables. J. Food Prot., 53, 701-703.

Gómez-López V M; Devlieghere F; Ragaert P; Debevere J. 2007. Shelf-life extension of minimally processed carrots by gaseous chlorine dioxide. Int. J. Food Microbiol., 10, 221-227.

Goodburn C; Wallace C A. 2013. The microbiological efficacy of decontamination methodologies for fresh produce: A review. Food Control., 32(2), 418-427.

Gopal A; Coventry J; Wan J; Roginski H; Ajlouni S. 2010. Alternative disinfection techniques to extend the shelf life of minimally processed iceberg lettuce. Food Microbiol., 27(2), 210-219.

Gupta M K; Sehgal V K. 2011. Drying kinetics of cauliflower in a hot air dryer. J. Agric. Eng., 48(3), 26-31.

Hägele F; Nübling S; Schweiggert R M; Baur S;

Weiss A; Schmidt H; Menegat A; Gerhards R; Carle R. 2016. Quality improvement of fresh-cut endive (cichorium endivia l.) and recycling of washing water by low-dose UV-C irradiation. Food Bioprocess Technol., 9 (12), 1979-1990.

Han Q; Gao H; Chen H; Fang X; Wu W. 2017. Precooling and ozone treatments affects postharvest quality of black mulberry (Morus nigra) fruits. Food Chem., 221, 1947-1953.

Hodges D M; Toivonen P M A. 2008. Quality of fresh-cut fruits and vegetables as affected by exposure to abiotic stress. Postharvest Biol. Technol., 48, 155-162.

Horvitz S; Cantalejo M J. 2012. Effects of ozone and chlorine postharvest treatments on quality of fresh-cut red bell peppers. Int. J. Food Sci. Technol., 47(9), 1935-1943.

Horvitz S; Cantalejo M J. 2014. Application of ozone for the postharvest treatment of fruits and vegetables. Crit. Rev. Food Sci. Nutr., 54(3), 312-339.

Jideani A I O; Anyasi T A; Mchau G R A; Udoro E O; Onipe O O. 2017. Processing and preservation of fresh-cut fruit and vegetable products. In: Post Harvest Handling, Ibrahim Kahramanoglu (Ed.), IntechOpen, 47-73. Available at: https://www.intechopen.com/books/ postharvest-handling/processing-and-preservation-of-fresh-cut-fruit-and-vegetable-products.

Jha S N; Rai D R; Gunasekaran S. 2010. Visual spectroscopy and colour modelling for non-destructive quality evaluation of apple. J. Agric. Eng., 47 (2), 9-13.

Jha S N; Jaiswal P; Narsaiah K; Kaur P P; Singh A K; Kumar R. 2013. Textural properties of mango cultivars during ripening. J. Food Sci. Technol., 50 (6), 1047-1057.

Karaca H. 2010. Use of ozone in the citrus industry. Ozone Sci. Eng., 32 (2), 122-129.

Kying O M; Ali A. 2016. Effect of ozone exposure on microbial flora and quality attributes of papaya (Carica papaya L) fruit. J. Agron. Agric. Aspects, JAAA-104. 1(1), 1-7.

Leceta I; Molinaro S; Guerreroa J P; Kerry K; de la Caba. 2015. Quality attributes of map packaged ready-to-eat baby carrots by using chitosan-based coatings. Postharvest Biol. Technol., 100, 142–150.

Lemoine M L; Civello P; Chaves A; Martínez G. 2009. Hot air treatment delays senescence and maintains quality of fresh-cut broccoli florets during refrigerated storage. LWT- Food Sci. Technol., 42(6), 1072-1081.

Liu J; Stevens C; Khan V A; Lu J Y; Wilson C L; Adeyeye O. 1993. Application of ultraviolet-C light on storage rots and ripening of tomatoes. J. Food Prot., 56, 868-872.

Manzocco L; Plazzotta S; Maifreni M; Calligaris S; Anese M; Nicoli M C. 2016. Impact of UV-C light on storage quality of fresh-cut pineapple in two different packages. LWT - Food Sci. Technol., 65, 1138-1143.

Mastromatteo M; Conte A; Del Nobile M A. 2012. Packaging strategies to prolong the shelf life of fresh carrots (*Daucus carota* L.). Innov. Food Sci. Emerg. Technol., 13, 215-220.

Meireles A; Giaouris E; Simões M. 2016. Alternative disinfection methods to chlorine for use in the fresh-cut industry. Food Res. Int., 82, 71–85.

Meireles A; Machado I; Fulgêncio R; Mergulhão F; Melo L; Simões M. 2015. Efficacy of antimicrobial combinations to reduce the use of sodiumhypochlorite in the control of planktonic and sessile Escherichia coli. Biochem. Eng. J., 104, 115-122.

Miceli A; Vetrano F; Romano C. 2013. Effect of hot air treatment on minimally processed cauliflower. Acta Hort., 1005, 309-314.

Ong M K; Kazi F K; Forney C F; Ali A. 2013. Effect of gaseous ozone on papaya anthracnose, Food Bioprocess. Technol., 6(11), 2996–3005.

Otto C; Zahn S; Rost F; Zahn P; Jaros D; Rohm H. 2011. Physical methods for cleaning and disinfection of surfaces. Food Eng. Rev., 3(3–4), 171–188.

Pan Y G; Zu H. 2012. Effect of UV-C radiation on the quality of fresh-cut pineapples. Procedia Eng., 37, 113-119.

Ramos B; Miller F A; Brandão T R S; Teixeira P; Silva C L M. 2013. Fresh fruits and vegetables — An overview on applied methodologies to improve its quality and safety. Innov. Food Sci. Emerg. Technol., 20, 1-15.

Ranjitha K; Rao D V S; Shivashankara K S; Oberoi H S; Roy T K; Bharathamm H. 2017. Shelf-life extension and quality retention in fresh-cut carrots coated with pectin. Innov. Food Sci. Emerg. Technol., 42, 91-100.

Rico D; Martin-Diana A B; Barat J; Barry-Ryan C. 2007. Extending and measuring the quality of fresh-cut fruit and vegetables: A review. Trends Food Sci. Technol., 18(7), 373-386.

Sandhu H P S; Manthey F A; Simsek S. 2011. Quality of bread made from ozonated wheat (Triticum aestivum L.) flour. J. Sci. Food Agric., 91, 1576-1584.

Sarig P; Zahavi T; Zutkhi Y; Yannai S; Lisker N; Ben-Arie R. 1996. Ozone for control of post-harvest decay of table grapes caused by Rhizopus stolonifer. Physiol. Mol. Plant Pathol., 48, 403-415.

Selma M V; Allende A; Lo´ pez-Ga´ lvez F; Conesa M A; Gil M I. 2008. Heterogeneous photocatalytic disinfection of wash water from the fresh-cut vegetable industry. J. Food Prot., 71, 286-292.

Sharma P; Sharma S R; Mittal T C. 2020. Effects and application of ionizing radiation on fruits and vegetables: A review. J. Agric. Eng., 57 (2), 97-126.

Sharpe D; Fan L; McRae K; Walker B; MacKay R; Doucette C. 2009. Effects of ozone treatment on Botrytis cinerea and Sclerotinia sclerotiorum in relation to horticultural product quality. J. Food Sci., 74, M250-M257.

Siddiq M; Roidoung S; Sogi D S; Dolan K D. 2013. Total phenolics, antioxidant properties and quality of fresh-cut onions (Allium cepa L.) treated with mild-heat. Food Chem., 136(2), 804-806.

Silveira A C; Aguayo E; Escalona V H; Artés F. 2011. Hot water treatment and per acetic acid to maintain fresh-cut Galiame lonquality. Innov. Food Sci. Emerg. Technol., 12(4), 570–576.

Singh S; Singh A; Singh V; Khemariya P; Rai A; Pandey A K. 2015**.** Steeping preservation of cauliflower with hurdle concept. J. Food Sci. Technol., 52(3), 1350-1360.

Skog L J; Chu C L. 2001. Effect of ozone on qualities of fruits and vegetables in cold storage. Can. J. Plant Sci., 81, 773-778.

Tabakoglu N; Karaca H. 2018. Effects of ozone-enriched storage atmosphere on postharvest quality of black mulberry fruits (Morus nigra L.). LWT - Food Sci. Technol., 92, 276-281.

Tzortzakis N; Taybi T; Roberts R; Singleton I; Borland A; Barnes J. 2011. Low level atmospheric ozone exposure induces protection against Botrytis cinerea with down-regulation of ethylene-, jasmonate and pathogenesis-related genes in tomato fruit. Postharvest Biol. Technol., 61, 152-159.

Villalobos-Carvajala R; Hernandez-Munozb P; Alborsc A; Chiralt A. 2009. Barrier and optical properties of edible hydroxypropyl methylcellulose coatings containing surfactants applied to fresh cut carrot slices. Food Hydrocolloids, 23, 526-535.

Whangchai K; Saengnil K; Uthaibutra J. 2006. Effect of ozone in combination with some organic acids on the control of postharvest decay and pericarp browning of longan fruit. Crop Prot., 25(8), 821-825.

Wulfkuehler S; Stark S; Dietz J; Schmidt H; Weiss A; Carle R. 2014. Effect of water jet cutting and moderate heat treatment on quality of fresh-cut red oak leaf lettuce (Lactuca sativa L. Var. crispa). Food Bioprocess. Technol., 7(12), 3478-3492.

Yousuf B; Srivastava A K. 2017. A novel approach for quality maintenance and shelf life extension of fresh-cut Kajari melon: Effect of treatments with honey and soy protein isolate. LWT-Food Sci. Technol., 79, 568-578.

Zambrano-Zaragoza M L; Quintanar-Guerrero D; Real A D; Pinon-Segundo E; Zambrano-Zaragoza J F. 2017. The release kinetics of β-carotene nanocapsules/ xanthan gum coating and quality changes in fresh-cut melon. Carbohydr. Polymers., 157, 1874-1882.

Zu H; Pan Y G; Chen W X; Liu X H; Shao Y Z. 2009. Effect of UV-C radiation on microbial indexes of fresh-cut pineapples. Food Sci., 30, 67-69.

http://www.isae.in / journal_jae.aspx

Journal of Agricultural Engineering

Vol. 57 (3): July-September, 2020

Qualitative Analysis of Roasted and Germinated Green Chickpea for Snack Food: Proximate, Functional and Pasting Properties

Yogesh Kumar[1], Vijay Singh Sharanagat[2], Lochan Singh[3], Promita Gundev[4], Saravanan Mani[5] and Prabhat K. Nema[6]

[1]M. Tech Student, [2]Assistant Professor, Department of Food Engineering, [3]Ph. D. Scholar, Department of Agriculture and Environmental Sciences, [4]Ph. D. Scholar, Department of Food Science and Technology, [5]Lab In-charge, Biochemistry Laboratory, Department of Basic and Applied Sciences, [6]Associate Professor, Department of Food Engineering, NIFTEM, Haryana, India. *Corresponding author email address: vijaysinghs42@gmail.com

Article Info

Manuscript received: December, 2018
Revised manuscript accepted: June, 2020

***Keywords*:** Germination, roasting, pasting properties, functional characteristics, TPC

ABSTRACT

In this study, the change in quality of green chickpea (GC) apropos to roasting and germination were analyzed. Significant ($p<0.05$) increase in surface area of GC occurred upon roasting (130.98-143.59 mm^2) and germination (130.98-224.51 mm^2), whereas, a slight increase in sphericity was observed with roasting. Both the treatments increased the fibre and protein content and reduced the carbohydrate content. Fat and ash content decreased by 1.88 % and 12 %, respectively, upon roasting but increased by 3.97 % and 29.84 %, respectively, on germination. 'L*' value decrease on roasting (91.02-65.28) but increased with germination (91.02-93.32). The starch and amylose-lipid complex gelatinization temperature reduced with both the treatments with higher reduction in roasted GC. The highest oil (0.82 g.g^{-1}) and water (1.4 g.g^{-1}) absorption capacity were found in germinated and roasted samples, respectively, while the highest pasting temperature (74.05 ºC) was observed for control. Total phenolic content increased on roasting (50.05 %), but decreased with germination (25.22 %).

Germination, roasting, drying, frying, steaming and extrusion are the commonly used methods for the preparation of snack foods (Saldivar, 2015; Jogihalli *et al.*, 2017; Pedreschia *et al.*, 2018). The most commonly prepared and consumed snack food in different parts of the world are roasted peanuts (Lykomitros *et al.*, 2016), popcorn (Andrade *et al.*, 2018), pretzels (Tal and Wansink, 2015), corn chips (Yuksel *et al.*, 2017), tortillas (Liu *et al.*, 2016), pita bread (Alu'datt *et al.*, 2012), roasted flour (*sattu*) and *sattu* drink (Jogihalli *et al.*, 2017), etc. Among these, roasted and germinated snack foods are popular due the ease of preparation and superior health benefits such as increased anti-oxidant activity, increased protein and starch digestibility, reduction of anti-nutrientsand bioavailability of minerals (Schoeman *et al.*, 2017; Kaczmarska *et al.*, 2018). Addition of food legumes (such as chickpea, soybean, groundnut, pea) or their use as snacks has multifaceted advantages like richness in bio-actives (Lopez-Martinez *et al.*, 2017), protein (Kaczmarska *et al.*, 2018), anti-carcinogenic properties (Clemente and Olias, 2017), resistance to digestion (Clemente and Olias, 2017), glycemic control (Becerra-Tomas *et al.*, 2018).

India is the largest producer of chickpea, holding around 67 % of global production (FAO, 2019). In India, chickpea is cultivated on 40 % of total area under pulse production and shares 50 % of total pulse production (Rampal, 2017). Madhya Pradesh is the largest producer of chickpea; whereas Punjab, Haryana, Bihar and Maharashtra are the highest consumer of chickpea (Rampal, 2017). The most used varieties in southern and central India are JG 11, Vijay, JG 16, Vikas, Vishal, JGK-1, KAK 2, ICCV 2, and ICCV-10. Pusa 372, Udai, RSG 963, BGM 547 and Rajas varieties are commonly grown in Uttar Pradesh, Bihar, Jharkhand, Haryana and Punjab (Dixit *et al.*, 2019). Green chickpea is one of the major food legumes of countries like India, Egypt, Ethiopia and Turkey

(Baburao *et al.,* 2019). In comparison to dark brown chickpeas that are rich in starch, the green garbanzo beans are rich in dietary fibres, vitamin B and good carbs; and possess superiorhypercholesteraemic and hypolipidemic effects (Baburao *et al.,* 2019). It has become a smart food and better alternative for snack food development due to ease in availability, sweet taste, good nutrition value, presence of important unsaturated fatty acids and low in cost (Kaur *et al*., 2005; Veena and Bhattacharaya, 2012; Bai *et al.,* 2018). The most common preparations of green chickpea are *dhal*, roasted and fried snacks, extruded and germinated snacks, especially in countries like India, USA and Egypt (Sofi *et al.,* 2020).

Despite all these benefits, few studies have focused on green chickpea and its flour (Rajiv *et al.,* 2012; Veena and Bhattacharya, 2012; Basha and Rao, 2017). Limited emphasis has been given on the effect of roasting and germination treatments of green chickpea. Owing to the importance of germinated and roasted green chickpea in the snack basket and the differences in basic nature as well as mechanism of the two treatments, it was considered essential to comparatively evaluate their effects on various qualitative characteristics. Both the processes exhibit advantages such as enhanced anti-oxidant activity and micronutrients' bio-availability, but have their own importance and limitation. Hence, a study was performed with the objective to characterize germinated and roasted green chickpea apropos to their physico-chemical, thermal and functional properties.

MATERIALS AND METHODS

Sample Preparation

Unprocessed Raw green chickpea (GC) grains (500 kg) were procured from a Reliance fresh store, Sonepat, Haryana, India. The grains were manually cleaned and its initial moisture content (11.2 g.100g^{-1}) was determined using the hot air oven method.Roasting of GC grains (200 g in three batch) was performed using a microwave oven (Samsung CE104VD-B microwave of 2450 MHz, 230 V-50 Hz AC, 100-900 W-6 levels) at 600W for 10 min. For germination, GC grains (200 g) were soaked in water for 10 h at room temperature. Thereafter, the water was drained out and the samples were kept in a jute bag for 12 h to allow germination. Germinated grains were dried in a hot air dryer at 45 °C for 24 h. Germinated (after drying) and roasted grains were ground using a mixer grinder. The flour was passed through 250-micron (IS 460-I) sieve and stored in aluminium pouches at room temperature for further analysis. All experiments were performed at NIFTEM, Kundali, Sonepat (Haryana).

Physical Properties of Grain

Surface area (S) and sphericity (ϕ) of control, roasted and germinated GC grains were calculated by the method described by Nimesh and Sharanagat (2016). In brief, the dimensions of six random grains were measured using a digital micro-meter having an accuracy of 0.001 mm. The surface area was calculated using average geometric diameter of the grains.The proximate composition (moisture, protein, fibre, fat, and ash content) of the control, roasted and germinated GC flour were analysed using AOAC (1984) method.

Colour measurement

The colour parameters as L*, a*, b* and total colour difference (ΔE) of control, germinated and roasted flour samples were determined by CIE colour scales using a hand held Chroma meter (KONICA MINOLTA, CR-400, Japan, Display range: Y:0.1 to160.00 per cent. Chroma meter was calibrated with the standard white board, and experiments were performed in triplicate.

Thermal properties

Thermal properties of control, germinated and roasted GC flour were analysed by the method described by Jogihalli *et al.* (2017) using a differential scanning calorimeter (DSC-200, NETZSCH, Germany, Temperature range:170 - 600 °C, heating rate: 0.001 - 100 K.min^{-1}, cooling rate: 20 K.min^{-1} down to 100 °C).

Functional properties

Two functional properties,water absorption capacity (WAC) and oil absorption capacity (OAC), of control, germinated and roasted sample flours were determined by the method described by Sharanagat *et al.* (2019).

Pasting properties

Pasting properties such as Peak viscosity (cP), Holding viscosity (cP), Pasting viscosity (cP), Breakdown viscosity (cP), Final viscosity (cP), Setback from through (cP), Setback from peak (cP) and Pasting temperature (ºC) of control, germinated and roasted green chickpea flours were determined using a rheometer (MCR 302, Anton Paar, Austria, Temperature range: 5 °C to 160 °C, max heating rate: 60 K.min^{-1}, Max cooling rate: 45 K.min^{-1}). A sample flour suspension was prepared by adding 16.66 g of water in 2 g of sample. The suspension was equilibrated at 50ºC for 1 min, and then heated from 50 ºC to 95 ºC

(6 ºC per min), and subsequently held at 95 ºC for 5 min. The sample was then cooled to 50 ºC (6 ºC per min) and was finally held at 50 ºC for 2 min.

Estimation of Total Phenolic Content (TPC)

A 200 mg of green chickpea flour sample was added to 4 ml acidified methanol (Methanol:HCl: Water, 80:1:9) and kept in a shaking incubator at 40 ºC for 2 h. Afterwards, the clear extract was collected and stored at room temperature for further analysis.The TPC of the extracts were determined by the Folin–Ciocalteu method (Cornejo *et al.,* 2015). A 0.2 ml of sample extract was added with 2.5 ml of freshly diluted (10-fold) Folin–Ciocalteu reagent and allowed to stand for 5 min. A 2 ml of sodium carbonate solution (7.5 g in100 ml) was then added. The mixture was then allowed to stand for 30 min at room temperature. Absorbance was then measured at 760 nm against reagent blank using an UV/VIS spectrophotometer (Shimadzu, UV-2600, Japan, Wave length: 195-800nm, Abs. Range: 2.3-3.7).

The TPC of a sample was estimated using a Gallic acid calibration curve, and the results were expressed as mg of Gallic acid equivalent per gram dry weight. For the calibration curve, standard series of known concentration of Gallic acid (0-60 mg.l^{-1}) were prepared and then treated in the manner similar to the samples.

Statistical Analysis

All experimental runs were carried out in triplicates, and the data were analysed using statistical analysis software SPSS (SPSS 17.0 for Window, SPSS Inc, Chicago, IL). The significance ($p \leq 0.5$) of variation in data and mean values were determined using analysis of variance (ANOVA) and Duncan's multiple range tests, respectively.

RESULT AND DISCUSSION

Physical Characteristics of Grains

Germination and roasting treatments significantly ($p<0.05$) affected the surface area of GC. The surface area of native GC grain was found to be 130.98 mm^2, which increased by 9.63 % upon roasting and by 71.41 % upon germination (Table 1). The higher increase in surface area through germination compared to roasting process can be attributed to the imbibing of water in the cells of grain, followed by the increase in moisture content and in swelling of grain structure.

Higher the temperature employed during roasting process, initiated drying accompanied by complex energy transfer to grain from roaster and mass transfer from grain to environment involving initial endothermic changes, dehydration, rapid removal of moisture from food grains and faster release of steam resulting in expansion (Oliveros *et al.,* 2017; Bustos-Vanegas *et al.,* 2018).

Table 1. Physical, colour, functional and antioxidant properties of raw, germinated and roasted green chickpea

Sl. No.	Property	Green chickpea		
		Raw	Germinated	Roasted
1.	S, mm^2	130.98±10.82^a	224.51±18.78^b	143.59±8.98^a
2.	S_p	0.79±0.05^a	0.79±0.02^a	0.84±0.01^a
3.	L^*	91.02±0.17^a	93.32±0.22^b	65.28±0.71^c
4.	a^*	-10.36±0.23^a	-7.30±0.23^b	7.08±0.29^c
5.	b^*	25.54±0.44^a	16.41±0.51^b	26.82±0.07^c
6.	ΔE	27.65±0.46^a	18.79±0.59^b	35.11±0.55^c
7.	BD, g.ml^{-1}	0.66±0.01^a	0.51±0.00^b	0.58±0.01^c
8.	WAC, g.g^{-1}	0.81±0.01^a	0.96±0.04^b	1.49±0.01^c
9.	OAC, g.g^{-1}	0.72±0.00^a	0.82±0.02^b	0.78±0.02^c
10.	TPC, mg GA/g dry weight	10.43±2.55^a	7.80±0.70^b	15.65±0.93^c

**Mean values within the column followed by the a, b and c superscript letter were significantly different at $p<0.05$. Mean ±SD (n=10)*

S_p= Sphericity, S= Surface area, L^*= Lightness, a^*=Redness, b^*=Yellowness, ΔE=Total colour change, BD=Bulk density, WAC=Water absorption capacity, OAC= Oil absorption capacity, TPC= Total phenolic content

Sphericity, which is another important physical characteristic, did not differ significantly with germination and roasting. However, a slight increase from 0.79 to 0.84 was observed during roasting. This might be attributed to higher expansion of food grains' width and thickness as compared to length. The findings were supported by Jogihalli *et al.* (2017) and Sharanagat *et al.* (2018) for the hydration of mung bean and roasting of chickpea, respectively.

Proximate Analysis of Flour

Green chickpea flour was found to be rich in carbohydrates (68.08 g.100g^{-1} dry matter), protein (13.72 g.100 g^{-1} dry matter) and fibre (10.16 g.100 g^{-1} dry matter). According to Hashimoto *et al.* (2016), diet having less than 10 % carbohydrates can be considered as low carbohydrates diet, 40 % as mid, and more than 40 % as rich. However, diets with 40-50 % carbohydrates are recommended for people having metabolic condition (Giugliano *et al.*, 2018). An increase in protein, fat, fibre and ash content by 8.96 %, 3.97 %, 12.20 % and 29.84 %, respectively, occurred during germination whereas a reduction of 5.33 % was observed in carbohydrate content (Table 2). Proteins are polypeptides and hydrolyse to oligopeptides during germination and further break into amino acids.

Degradation of starch takes place providing sugar to embryo for further growth (Nonogaki and Nonogaki, 2017). Increased fibre content might be attributed to growing carbohydrate metabolism, formation of new polysaccharides and cellulose, and change in matrix of cell walls (Ma *et al.*, 2018); while loss of starch might have resulted in increased ash content (Devi *et al.*, 2015). Benitez *et al.* (2013) also reported a decrease in total starch and increase in dietary fibre upon germination of different legumes such as cowpea, jack bean, mucuna and dolichos. Contrarily, roasting process decreased fat (1.88 %), ash (12 %) and carbohydrate content (2.27 %), and increased fibre (14.46 %) and protein (3.26 %) content of GC. The increased fibre content upon roasting might be attributed to formation of protein-fibre complex due to chemical modifications induced at high temperature (Ma *et al.*, 2017). The reduction in carbohydrate content upon roasting might be due to higher rupturing of starch granules. This change is responsible for increased digestibility of starch in roasted samples compared to raw samples (Ma *et al.*, 2017). The reduction of fat indicated destruction of fat upon roasting,which meant that the control sample was more susceptible to rancidity than roasted sample (Obadina *et al.*, 2016). As observed (Table 2), germination contributed to higher increase in protein, fat and ash content while higher fibre and carbohydrate content were found in roasted sample. Reported results were also supported by Olanipekun *et al.* (2015) for roasting of kidney beans.

Colour Analysis

Significant effect of roasting and germination was observed on the colour characteristics of GC (Table 1, Fig. 1). Reduction in 'L*' value from 91.02 to 65.28 occurred upon roasting, while 'L*' value increased from 91.02 to 93.32 during germination. During germination, the natural colour of GCdarkened, resulting in an increase in 'L*' value. Contrarily, discolouration of natural pigments and formation of brown pigment as a result of mallard reaction in grains upon roasting reduced the 'L*' value (Kaur *et al.*, 2005). Similar observations were reported by Shi *et al.* (2017) for dry roasting, oil roasting, and blister frying of peanuts; and by Raigar and Mishra (2018) for roasted maize. The trend of increase in 'a*' value were in the order of Control<Germinated<Roasted, whereas the trend followed by 'b*' value were Germinated<Control<Roasted. The total colour change (ΔE) also varied with roasting and germination process. The germination of green chickpea led to a decrease in ΔE (32.04 %), while roasting exhibited an opposite trend and increased the ΔE (26.98 %). Finally, the germination led to the development of an appealing dark green colour, while roasted grains were brown in colour losing the attraction.

Table 2. Effect of germination and roasting on proximate composition of green chickpea (g.100g^{-1} dry matter)

Sl. No.	Sample	Proximate composition				
		Protein	Fat	Fibre content	Ash content	Carbohydrate content
1.	Raw	13.72±0.49	4.78±0.50	10.16±0.14	3.25±0.72	68.08±0.92
2.	Germinated	14.95±0.74	4.97±0.34	11.40±0.99	4.22±1.00	64.45±0.00
3.	Roasted	14.18±0.12	4.69±0.63	11.63±0.71	2.86±0.99	66.53±1.05

**Sample data presented in mean ±SD (n=2)*

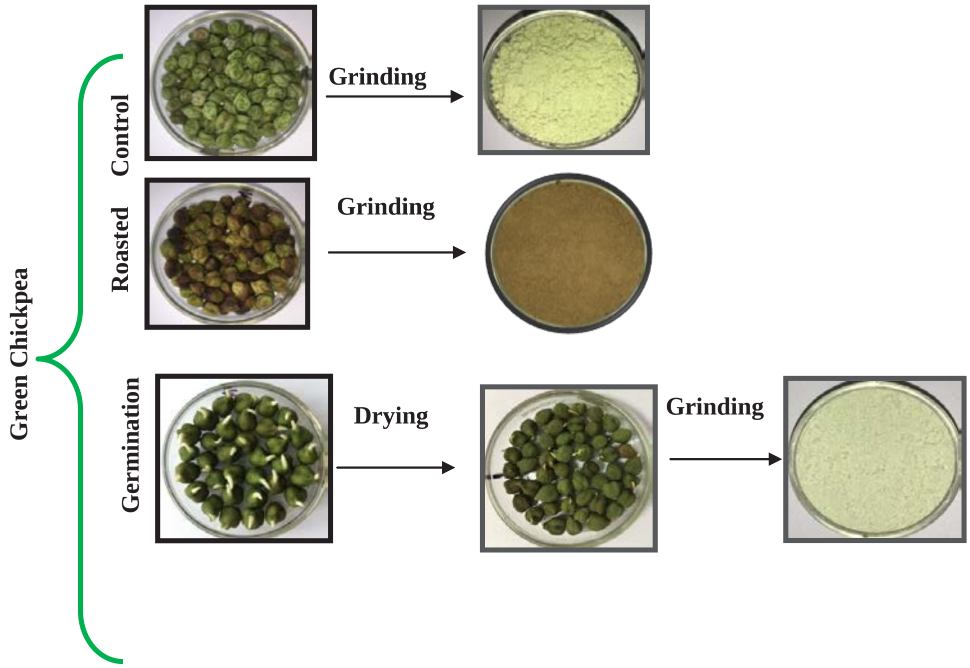

Fig. 1: Effect of germination and roasting on colour of chickpea

Thermal Properties

Table 3 shows the thermal properties of control, germinated and roasted GC.The first peak and second peak represented gelatinization of starch and amylose lipid complex, respectively. The peak onset temperature (T_o), mid temperature (T_m) and end temperature (T_e) for starch gelatinization of control sample was 55.5 ºC, 67.9 ºC and 62.2 ºC, respectively. Similarly, onset, mid and end temperature for amylose lipid complex (ALC) peaks were 114.8 ºC, 117.3 ºC and 120.4ºC, respectively for control sample. Both roasting and germination treatments reduced the onset, mid and end temperatures for both peaks. The reduction in starch gelatinization and amylose lipid complex in heat treated samples, as compared to control sample, exhibits easy achievement of gelatinization owing to lesser energy requirements for intermolecular bond breakage in protein bodies and starch (Ma *et al.*, 2017; Ma *et al.*, 2018). It might also be related to the reduced composition of carbohydrates found in heat treated samples, and illustrated the fact that the protein and starch molecules exposed to heat treatments were more vulnerable to intermolecular bond breaking. Except for T_m and $T_e$temperature of starch gelatinization, all values for the two peaks followed the trend in order of control>germinated>roasted. Higher reduction in roasted sample compared to germinated samples might be a result of high energy and temperature used in the process. T_m and T_e of starch gelatinization were higher for roasted samples as compared to germinated samples. Results were supported by germination and roasting of yellow field cowpea (Ma *et al.*, 2017; Ma *et al.*, 2018).

Functional Properties

Functional characteristics as oil absorption capacity (OAC) and water absorption capacity (WAC) play an important role in determining the effect of processing

Table 3. Thermal properties of raw, germinated and roasted green chickpea

Sl. No.	Sample	Starch gelatinization			Amylose-lipid complex		
		T_o, °C	T_m, °C	T_e, °C	T_o, °C	T_m, °C	T_e, °C
1.	Raw	55.5	67.9	62.2	114.8	117.3	120.4
2.	Germinated	51.7	50.8	52.4	105.8	111.3	117.7
3.	Roasted	45.6	53.3	58.8	103.2	109.7	115.9

To= Onset temperature, Tm= Mid temperature, Te= End temperature on interaction with oil and water. The WAC and OAC of green chickpea increased with both treatments (Table 1). Highest value of OAC (0.82 $g.g^{-1}$) was observed for germinated sample, while lowest value was found for control sample (0.72 $g.g^{-1}$). On the other hand, roasted sample had highest water absorption capacity (1.4 $g.g^{-1}$), followed by germinated (0.96 $g.g^{-1}$) and raw samples (0.81$g.g^{-1}$).

Germination increased the OAC of grains by enhancing the quality of protein, protein surface hydrophobicity and its' fat globule holding capacity. Similarly, WAC increased on germination because of the polysaccharide breakdown and increase in sites for interaction with water molecules (Sibian *et al*., 2017). Both the properties were affected due to the biochemical changes taking place in grains during germination. Similar results have been reported by Sibian *et al.* (2017) for wheat, triticale and brown rice; and by Benitez *et al.* (2013) for cowpea, mucuna pruriens and dolichos.On the other hand, roasting increased WAC by denaturizing protein, swelling crude fibre and gelatinizing starch. Induced breakdown and volumetric expansion of starch during the high temperature treatment also increased the WAC of flour in the presence of adequate moisture (Raigar and Mishra, 2018). High temperature or power used in roasting resulted in denaturation of proteins, their solubilisation and dissociation; thereby exposing non-polar amino acids present inside protein molecules, favouring hydrophobicity and interaction with fats (Raigar and Mishra, 2018). Similar trend has been reported for flaxseed (Khan and Saini, 2016) and maize (Raigar and Mishra, 2018).

It could be concluded that germinated samples are mostly suitable for food products requiring better mouth feel and flavour retention, while roasted samples are suitable for food products such as complementary foods, weaning foods and cereal blended formulations. Hence, incorporation of treated green chickpea in low-protein and composite flours to make buns, biscuits, cookies, muffins, sauces, sausages etc. may aid in eradicating protein malnutrition.

Pasting Properties

Peak viscosity represents characteristics of starch to absorb the water, and swell indicates the water binding capacity of starch (Mariotti *et al.*, 2006; Ingbian and Adegoke, 2007). Breakdown viscosity represents the stability of suspension under stress and temperature,while final viscosity represents the ability of suspension to form a paste (Mariotti *et al.*, 2006; Ingbian and Adegoke, 2007).

The pasting properties (peak viscosity, holding viscosity, pasting viscosity, breakdown viscosity, setback from through, final viscosity, setback from peak and pasting temperature) of roasted, germinated and control GC flour are shown in Table 4. The trends followed by samples for peak viscosity, pasting viscosity, holding viscosity, breakdown viscosity, final viscosity and setback from trough viscosity in increasing order were roasted<raw<germination. An opposite trend was seen for setback from peak. Pasting temperature, on the other hand, was highest for raw samples and lowest for roasted flour samples.

Increase in peak viscosity, holding viscosity, pasting viscosity, breakdown viscosity, final viscosity and setback from trough viscosity of green chickpeas upon germination showed higher ability of its starch to form viscous paste than roasted and raw samples. These results varied from those reported by Xu *et al*. (2017) for adlay seeds who reported significant reduction in peak viscosity (1844 to 822 cP) after 24 h of germination. Moreover, Kumar *et al*. (2020) reported similar reduction in peak viscosity (1020 to 50.66 cP) of microwave roasted black chickpea. However, Ma *et al.* (2017) reported an increase in peak viscosity (162 to 185 cP) for oven-roasted yellow field peas. The observed deviations might be due to the difference in germination stages studied and molecular structures apropos to species and cultivars (Li *et al.*, 2017). There are three important stages in germination: initial rapid water imbibition by grains, secondly reactivation of metabolism; and finally, radicle protrusion. The increase in pasting properties might also be attributed

Table 4. Pasting properties of raw, germinated and roasted green chickpea

Sl. No.	Sample	Peak viscosity, cP	Pasting viscosity, cP	Holding viscosity, cP	Breakdown viscosity, cP	Final viscosity, cP	Setback from through, cP	Setback from peak, cP	Pasting temperature, ˚C
1.	Raw	450.00	35.15	333.60	126.50	988.70	655.00	(-)528.50	74.05
2.	Germinated	650.10	124.40	439.90	210.20	1405.00	965.30	(-)755.1	72.78
3.	Roasted	48.49	29.48	33.21	15.28	65.86	32.65	(-)17.37	60.39

to increased starch content due to loss of protein and lipids (Sandhu *et al.*, 2018), conversion to reducing sugar and presence of higher amylose (Sandhu *et al.*, 2018). On the other hand, decreases in these viscosities on roasting might be attributed to ease in hydration and rapid swelling of partially gelatinized, damaged and loosely packed starch granules (formed after roasting) in presence of heat, which resulted in low viscosities (Ma *et al.*, 2017). Decreased setback viscosity illustrated the fact that starch will retrograde slowly due to its' gelling tendency. Sharma *et al.* (2011) also reported the reduction in the final (15-57 %), peak (53-78 %), setback (18-47 %) and breakdown (64-92 %) viscosities of roasted barley.

The decreases in pasting temperature (from 74.05 ^{o}C to 72.78 ^{o}C and 60.39 ^{o}C) upon both treatments(germination and roasting, respectively) compared to control sample were due to the decrease in gelatinization time (Kaur *et al.*, 2007). These reductions were also supported by our results on thermal properties of green chickpea where gelatinization temperature decreased from 67.9 ^{o}C (control) to 50.8 ^{o}C (germinated) and 53.3 ^{o}C (roasted) (Table 3). Decrease in pasting temperature has been also reported for germinated amaranth flour (Chauhan *et al.*, 2015). Conclusively, these results indicated that the germinated sample suspension had higher stability and paste forming capacity with lower gelatinization temperature compared to roasted sample suspension, and thus can be utilized for the preparation of different sausages and liquid food-based products.

Total Phenolic Content

Total phenolic content (TPC) of control sample was found to be 10.43 mg of GAE/ g dry weight (Table 1). Germination process resulted in reduction of TPC to 7.80 mg GAE/ g dry weight),whereas increase in TPC was observed with roasting process (15.56 mg of GA equivalent per g dry weight). Reduction in total polyphenol content during germination was also observed by Khandelwal *et al.* (2010) in various pulses. Aguilera *et al*. (2015) made similar observations for lentils and kidney beans. Segev *et al.* (2011) reported reduction in TPC up to 45 % with hydration. The reduction in TPC with germination might be attributed to the breakdown and decrease in phenolic compounds (Xu and Chang, 2008), owing to the increase in activity of polyphenol oxidase and other catabolic enzymes. Increase in TPC during roasting on the other hand might be because of the breakdown of cellular compounds, disruption of cell wall and the liberation of bounded phenolics from cell matrix (Lee *et al.*, 2006). Similar observations of increased TPC with roasting were reported by Mrad *et al.* (2015) and Segev *et al.* (2011) for chickpea where the increase might be due to the formation of Maillard reaction products.

CONCLUSIONS

Germination and roasting of green chickpea had increasing effect on physical properties, but germination resulted in higher surface area (224.51 mm^2) compared to roasted (143.59 mm^2) and control sample (130.98 mm^2). The green natural colour of green chickpea darkened upon germination, while the colour changed to dark brown after roasting due to high temperature favouring Maillard reaction and flavour generation. Results of thermal and pasting study demonstrated that the gelatinization in roasted and germinated green chickpea flour samples may be easily achieved in comparison to untreated flour, making them suitable for development of low temperature-based functional foods. Higher WAC and OAC also found in roasted (WAC-1.49 g.g^{-1}, OAC-0.78 g.g^{-1}) and germinated (WAC-0.96 g.g^{-1}, OAC-0.82 g.g^{-1}) flour compared to control flour (WAC-0.81 g.g^{-1}, OAC-0.72 g.g^{-1}) showed their higher capacity for incorporation in low-protein and cereal blend formulations, weaning foods and complementary foods. The germinated samples exhibiting higher stability and paste forming capacity also shows its suitability for incorporation and development sausages and liquid-based formulations.

ACKNOWLEDGEMENT

Authors are thankful to the National Institute of Food Technology, Entrepreneurship and Management, Haryana, India, for providing instrumental facility to conduct the research.

REFERENCES

Aguilera Y; Herrera T; Liébana R; Rebollo-Hernanz M; Sanchez-Puelles C; Martín-Cabrejas M A. 2015. Impact of melatonin enrichment during germination of legumes on bioactive compounds and antioxidant activity. J. Agric. Food Chem., 63(36), 7967-7974.

Alu'datt M H; Rababah T; Ereifej K; Alli I; Alrababah M A; Almajwal A; Masadeh N; Alhamad M N. 2012. Effects of barley flour and barley protein isolate on chemical, functional, nutritional and biological properties of Pita bread. Food Hydrol., 26(1), 135-146.

Andrade G C R M; Pimpinato R F; Francisco J G; Monteiro S H; Calori-Domingues M A; Tornisielo V L. 2018. Evaluation of mycotoxins and their estimated daily intake in popcorn and cornflakes using LC-MS techniques. LWT - Food Sci. Technol., 95, 240-246.

AOAC. 1984. Proximate Composition. In: Official Methods of Analysis (14th Ed.), Arlington, VA: Association of Official Analytical Chemists, 249-252.

Baburao K K; Kamble D K; Patange D D; Yadav M M; Londhe-Patil P B. 2019. Process standardization for preparation of green chickpea (Cicer arietinum L.) Burfi. Pharma.Innov. J., 8(11), 201-206.

Bai T; Nosworthy M G; House J D; Nickerson M T. 2018. Effect of tempering moisture and infrared heating temperature on the nutritional properties of desi chickpea and hull-less barley flours, and their blends. Food Res. Int., 108, 430-439.

Basha S A; Rao U J S P. 2017. Bioactivities of fractions obtained from green gram (*Vigna radiata*) milled by-products. Food Biosyst., 19, 134-141.

Becerra-Tomás N; Díaz-López A; Rosique-Esteban N; Ros E Buil-Cosiale P; Corella D; Estruch R; Fitó M; Serra-Majem L; Arós F; Lamuela-Raventós R M; Fiol M; Santos-LozanoJ M; Díez-EspinoJ; Portoles O; Salas-Salvadó J. 2018. Legume consumption is inversely associated with type 2 diabetes incidence in adults: A prospective assessment from the PREDIMED study. Clinical Nutr., 37(3), 906-913.

Benítez V; Cantera S; Aguilera Y; Mollá E; Esteban R M; Díaz M F; Martín-Cabrejas M A. 2013. Impact of germination on starch, dietary fibre and physicochemical properties in non-conventional legumes. Food Res. Int., 50 (1), 64-69.

Bustos-Vanegas J D; Corrêa P C; Martins M A; Baptestini F M; Campos R C; de Oliveira G H H; Nunes E H M. 2018. Developing predictive models for determining physical properties of coffee beans during the roasting process. Indian Crops Prod., 112, 839-845.

Chauhan A; Saxena D C; Singh S. 2015. Total dietary fibre and antioxidant activity of gluten free cookies made from raw and germinated amaranth (Amaranthus spp.) flour. LWT - Food Sci. Technol., 63 (2), 939-945.

Clemente A; Olias R. 2017. Beneficial effects of legumes in gut health. Curr. Opin. Food Sci., 14, 32-36.

Cornejo F; Rosell C M. 2015. Influence of germination time of brown rice in relation to flour and gluten free bread quality. J. Food Sci. Technol., 52, 6591-6598.

Devi C B; Kushwaha A; Kumar A. 2015. Sprouting characteristics and associated changes in nutritional composition of cowpea (*Vigna unguiculata*). J. Food Sci. Technol., 52(10), 6821-6827.

Dixit G P; Srivastava A K; Singh N P. 2019. Marching towards self-sufficiency in chickpea. Curr. Sci., 116(2), 239-242.

FAO. 2019. The Global Economy of Pulses. Creative commons, Food and Agriculture Organization, United Nations, Rome, Italy, FISBN 978-92-5-109730-4, pp: 190.

Giugliano D; Maiorino M I; Bellastella G; Esposito K. 2018. More sugar? No, thank you! The elusive nature of low carbohydrate diets. Endocrine, 61(3), 383-387.

Hashimoto Y; Fukuda T; Oyabu C; Tanaka M; Asano M; Yamazaki M; Fukui M. 2016. Impact of low-carbohydrate diet on body composition: meta-analysis of randomized controlled studies. Obesity Rev., 17(6), 499-509.

Ingbian E K; Adegoke G O. 2007. Proximate compositions, pasting and rheological properties of mumu–A roasted maize meal. Int. J. Food Sci. Technol., 42(6), 762-767.

Jogihalli P; Singh L; Kumar K; Sharanagat V S. 2017. Novel continuous roasting of chickpea (Cicer arietinum): Study on physico-functional, antioxidant and roasting characteristics. LWT - Food Sci. Technol., 86, 456-464.

KaczmarskaK T; Chandra-Hioe M V; Frank D; Arcot J. 2018. Aroma characteristics of lupin and soybean after germination and effect of fermentation on lupin aroma. LWT - Food Sci. Technol., 87, 225-233.

Kaur M; Singh N; Sodhi N S. 2005. Physicochemical, cooking, textural and roasting characteristics of chickpea (Cicer arietinum L.) cultivars. J. Food Eng., 69(4), 511-517.

Kaur R; Gill B S; Sogi D S. 2007. Studies on the effect of aqueous hydrochloric acid on properties of wheat starch. J. Food Sci. Technol., 44(4), 386-390.

Khan A; Saini C S. 2016. Effect of roasting on physicochemical and functional properties of flaxseed flour. Cogent Eng., 3(1), 1145566.

Khandelwal S; Udipi S A; Ghugre P. 2010. Polyphenols and tannins in Indian pulses: Effect of soaking, germination and pressure cooking. Food Res. Int., 43(2), 526-530.

Kumar Y; Sharanagat V S; Singh L; Mani S. 2020. Effect of germination and roasting on the proximate composition, total phenolics, and functional properties of black chickpea (Cicer arietinum). Legume Sci., *2*(1), e20.

Lee S C; Jeong S M; Kim S Y; Park H R; Nam K C; Ahn D U. 2006. Effect of far-infrared radiation and heat treatment on the antioxidant activity of water extracts from peanut hulls. Food Chem., 94(4), 489-493.

Li C; Oh S G; Lee D H; Baik H W; Chung H J. 2017. Effect of germination on the structures and physicochemical properties of starches from brown rice, oat, sorghum, and millet. Int. J. Biol. Macromol., 105, 931-939.

Liu T; Hou G G; Lee B; Marquart L; Dubat A. 2016. Effects of particle size on the quality attributes of reconstituted whole-wheat flour and tortillas made from it. J. Cereal Sci., 71, 145-152.

López-Martínez L X; Leyva-López N; Gutiérrez-Grijalva Erick P; Heredia J B. 2017. Effect of cooking and germination on bioactive compounds in pulses and their health benefits. J. Funct. Foods, 38 (B), 624-634.

Lykomitros D; Fogliano V; Capuano E. 2016. Flavour of roasted peanuts (Arachis hypogaea) - Part I: Effect of raw material and processing technology on flavour, colour and fatty acid composition of peanuts. Food Res. Int., 89(1), 860-869.

Ma Z; Boye J I; Hu X. 2017. *In vitro* digestibility, protein composition and techno-functional properties of Saskatchewan grown yellow field peas (*Pisum sativum* L.) as affected by processing. Food Res. Int., 92, 64-78.

Ma Z; Boye J I; Hu X. 2018. Nutritional quality and techno-functional changes in raw, germinated and fermented yellow field pea (Pisum sativum L.) upon pasteurization. LWT - Food Sci. Technol., 92,147-154.

Mariotti M; Alamprese C; Pagani M A; Lucisano M. 2006. Effect of puffing on ultrastructure and physical characteristics of cereal grains and flours. J. Cereal Sci., 43(1), 47-56.

Mrad R; El Rammouz R; Maroun R G; Louka N. 2015. Effect of intensification of vaporization by decompression to the vacuum as a pretreatment for roasting a ustralian chickpea: Multiple optimization by response surface methodology of chemical, textural and colour parameters. J. Food Quality, 38(2), 139-152.

Nimesh A; Sharanagat V S. 2016. Effect of moisture content on engineering properties of chickpea seed. Agric. Eng. Today, 40(1), 13-21.

Nonogaki M; Nonogaki H. 2017. Germination. Encycl. Appl. Plant. Sci., 1, 509-512.

Obadina A O; Ishola I O; Adekoya I O; Soares A G; Carvalho C W P D; Barboza H T. 2016. Nutritional and physico-chemical properties of flour from native and roasted whole grain pearl millet (*Pennisetumglaucum* [L.]R. Br.). J. Cereal Sci., 70, 247-252.

Olanipekun O T; Omenna E C; Olapade OA; Suleiman P; Omodara O G. 2015. Effect of boiling and roasting on the nutrient composition of kidney beans seed flour. Sky J. Food Sci., 4(2), 24-29.

Oliveros N O; Hernández J A; Sierra-Espinosa F Z; Guardián-Tapia R; Pliego-Solórzano R. 2017. Experimental study of dynamic porosity and its effects on simulation of the coffee beans roasting. J. Food Eng., 199, 100-112.

Pedreschia F; Cortésa P; Mariottib M S. 2018. Potato crisps and snack foods. Reference Module Food Sci., Elsevier, doi.org/10.1016/B978-0-08-100596-5.21137-2.

Raigar R K; Mishra H N. 2018. Study on the effect of pilot scale roasting conditions on the physicochemical and functional properties of maize flour (Cv. *Bio 22027)*. J. Food Pro. Preserv., 42(5), e13602.

Rajiv J; Lobo S; Jyothi L A; Venkateswara R G. 2012. Influence of green gram flour (Phaseolus aureus) on the rheology, microstructure and quality of cookies. J. Text. Stud., 43(5), 350-360.

Rampal P. 2017. Situational Analysis of Pulse Production and Consumption in India. Leveraging Agriculture for Nutrition in South Asia (LANSA), 20, pp: 46.

Saldivar S O S. 2015. Snack Foods: Types and Composition. Reference Module in Food Science Encyclopedia of Food and Health, Elsevier, 13-18. doi.org/10.1016/B978-0-12-384947-2.00633-4

Sandhu R S; Singh N; Kaler R S S; Kaur A; Shevkani K. 2018. Effect of degree of milling on physicochemical, structural, pasting and cooking properties of short and long grain Indica rice cultivars. Food Chem., 260, 231-238.

Schoeman L; Plessis A; Verboven P;Nicolaï B M; Cantre D; Manley M. 2017. Effect of oven and forced convection continuous tumble (FCCT) roasting on the microstructure and dry milling properties of white maize. Innov. Food Sci. Emerg. Technol., 44, 54-66.

Segev A; Badani H; Galili L; Hovav R; Kapulnik Y; Shomer I; Galili S. 2011. Total phenolic content and antioxidant activity of chickpea (*Cicer arietinum* L.) as affected by soaking and cooking conditions. Food Nutr.Sci., 2, 724-730.

Sharanagat V S; Kansal V; Kumar K. 2018. Modeling the effect of temperature on the hydration kinetic whole moong grain. J. Saudi Soc. Agric. Sci., 17(3), 268-274.

Sharanagat V S; Suhag R; Anand P; Deswal G; Kumar R; Chaudhary A; Singh L; Kushwah O S; Mani S; Kumar Y; Nema P K. 2019. Physico-functional, thermo-pasting and antioxidant properties of microwave roasted sorghum [Sorghum bicolor (L.) Moench]. J. Cereal Sci., 85, 111-119.

Sharma P; Gujral H S; Rosell C M. 2011. Effects of roasting on barley β-glucan, thermal, textural and pasting properties. J. Cereal Sci., 53 (1), 25-30.

Shi X; Davis J P; Xia Z; Sandeep K P; Sanders T H; Dean L O. 2017. Characterization of peanuts after dry roasting, oil roasting, and blister frying. LWT - Food Sci. Technol., 75, 520-528.

Sibian M S; Saxena D C; Riar C S. 2017. Effect of germination on chemical, functional and nutritional characteristics of wheat, brown rice and triticale: a comparative study. J. Sci. Food Agric., 97 (13), 4643-4651.

Sofi S A; Muzaffar K; Ashraf S; Gupta I; Mir S A. 2020. Chickpea. In: Pulses, Springer, Cham, 55-76.

Tal A; Wansink B. 2015. Variety increases satiety: eating different- (vs same-) shaped pretzels increases satiety. J. Nutr. Educ. Behav., 47(4), S42. doi. org/10.1016/j.jneb.2015.04.111

Veena R; Bhattacharya S. 2012. Rheological characterization of raw and roasted green gram pastes. LWT - Food Sci. Technol., 46(1), 260-266.

Xu B; Chang S K. 2008. Total phenolics, phenolic acids, isoflavones, and anthocyanins and antioxidant properties of yellow and black soybeans as affected by thermal processing. J. Agric. Food Chem., 56(16), 7165-7175.

Xu L; Chen L; Ali B; Yang N; Chen Y; Wu F; Jin Z; Xu X. 2017. Impact of germination on nutritional and physicochemical properties of adlay seed (*Coixlachryma-jobi* L.). Food Chem., 229, 312-318.

Yuksel F; Safa Y; Melek K; Mehmet G; Hasan H; Mahmut Y; Mahmut D; Kayacier A. 2017. Production of deep-fried corn chips using stale bread powder: Effect of frying time, temperature and concentration. LWT - Food Sci. Technol., 83, 235-242.

http://www.isae.in / journal_jae.aspx

Journal of Agricultural Engineering

Vol. 57 (3): July-September, 2020

Rheological and Surface Properties of Edible Coating Solution Prepared from Vasa Plant (*Justicia Adhatoda* L.) Leaf Extract

Hanumantharaju K. N.[1], Thangavel K.[2] and Ganapathy S.[3]

[1]Research Scholar, Department of Food and Agricultural Process Engineering; [2]Professor and Head, Post-Harvest Technology Centre; [3]Professor and Head, Department of Food and Agricultural Process Engineering, TNAU, Coimbatore, Tamil Nadu, India. Corresponding author e-mail address: rajuknhgowda@gmail.com

Article Info

Manuscript received:
August, 2018
Revised manuscript accepted:
July, 2020

Keywords: Edible coating solution, *Justicia adhatoda*, antioxidant property, rheological properties, surface tension

ABSTRACT

Incorporation of plant extract into edible coating solution (ECS) enhances the antimicrobial and antioxidant property of the coating solution. Vasa plant (*Justicia adhatoda*) was selected and tested for total antioxidant capacity using phosphomolybdate method. Ethanolic extract of Vasa plant was found to contain 94.47 mg.ml^{-1} in equivalence of ascorbic acid for 24 hours of maceration. ECS suspension using ethanolic extract of vasa plant (3 %, 6 %, 9 %) was prepared with starch (4 %), sucrose (1 %, 1.25 %, 5 %) and glycerol (10 %, 15 %, 20 %) as base material at different proportions; and the rheological and physico-chemical properties of the ECS were determined. Prepared ECS followed Herschel-Bulkley flow curve having yield stress of 2.37-4.74 Pa and n-value in the range of 0.26-0.95. Further, the pH (6.2-6.9) and surface tension (58.10- 81.90 m. N.m^{-1}) of the ECS significantly ($p<0.05$) decreased by the increase in *Justicia adhatoda* extract. Electrical conductivity and total soluble solid of the formulated ECS ranged from 0.17-0.36 dS.m^{-1} and 1.7-3.9 °Brix. respectively, and both of them significantly ($p<0.05$) increased with increase in sucrose and *Justicia adhatoda* extract. Optimized ECS contained 1.04 % sucrose, 18.44 % glycerol and 9.00 % *Justicia adhatoda* extract.

Vasa plant (*Justicia adhatoda* L.), a tropical branched shrub, with lance shaped leaves. Leaves are oppositely arranged, smooth edged and borne on short petioles. Vasa plant, commonly known as malbar nut,is one of the mostly used medicinal plant for treating cough, cold and asthma in India. It is widespread in South-eastern Asia. The plant is generally cultivated for the purpose of living fencing, especially in northern Himalaya and southern India (Karthikeyan *et al*., 2009; Pa and Mathew, 2012; Nouri and Nafchi, 2014; Barth *et al*., 2015). It is commonly known as *malbar* nut or vasa plant. It has high antioxidant and antimicrobial properties due to presence of quinazoline alkaloids, betaine, steroids carbohydrate and alkanes (Pa and Mathew, 2012). Hence, *Justicia adhatoda* extract can be utilized in edible coating as a functional component.

Edible coating is the integrated form of protective layer on a food material. It protects the coated food material by preventing moisture, oxygen, light, and ethylene transmission from it. Additionally, edible coating films may deliver the functional ingredients to the target (Nouri and Nafchi, 2014). Hence, plant extracts are also incorporated into the edible coating solution (ECS) in order to increase antimicrobial and antioxidant property of the solution. Incorporation of antioxidant rich *Justicia adhatoda* extract into ECS formulation enhances the functional property of the solution (Bhattacharyya *et al*., 2005). Bitter taste and unpleasant smell of vasa plant makes it unsuitable for normal usage (Kaur *et al*., 2013). In order to overcome this bitter taste while preparing an ECS, sucrose can be added along with *Justicia adhatoda* extract, which can reduce bitterness and also increase the edible film elongation (Veiga-Santos *et al*., 2007). Sucrose acts as a plasticizer by interacting with the base material, and decreases the viscosity of the ECS. Since sucrose causes crystallinity, glycerol can be used to retard the crystallinity (Oliveira and Cereda, 2007; Veiga-Santos *et al*., 2007; Fadini *et al*., 2013). Glycerol is one of the most promising plasticizers for increasing the extensibility and flexibility of the film prepared from the ECS (Franssen and Krochta, 2003). Glycerol is more compatible with starch, because starch has good mechanical properties and brittle in nature (Muscat *et al*., 2012). This brittleness can be reduced by addition of glycerol. The proportion of plasticizer (glycerol and sucrose) affects the spreadability and uniformity of the ECS on fruit coatings (Izbassarov and Muradoglu, 2016; Jones *et al*., 2016). Uniformity of coating on fruits determines the effectiveness of the internal gas modification, which mainly depends on the surface tension and rheological properties of the ECS (Debeaufort and Voilley, 2009; Andrade and Osorio, 2012a).

Surface tension, viscosity and electrical conductivity of the ECS is responsible for the wettability, spreadability atomization and electrostatic spraying of the solution (Jaworek, 2007). Properties as pH and total soluble solids of the solution play a major role in interaction with the food on which it is coated (Ruenroengklin *et al*., 2008; Andrade *et al*., 2012b). With this background, the present study was undertaken with the objective of formulation of ECS using *Justicia adhatoda* extract, starch, sucrose and glycerol; and to analyse its physico-chemical, electrical and surface properties.

MATERIALS AND METHODS

Collection of Plant Material and Ethanolic Extract Preparation

Vasa plant (*Justicia adhatoda* L.) leaves were collected from the Department of Medicinal and Aromatic Crops,Tamil Nadu Agricultural University, Coimbatore, India. The experiment was carried out in the Department of Food Process Engineering, AEC & RI, TNAU Coimbatore.

The unnecessary plant portions (except leaves) were removed, and the leaves were washed thoroughly under running tap water. The leaves were chopped and shade-dried until it attained a constant moisture content (6-7 %, w.b.). The material was regularly inspected to check anyfungal growth orrotting. Dried plant material was powdered using an electric mixer (Bajaj India, Model: Classic-750 W, 4 blades-18000 rpm) at 15000 rpm for 90 s. Powdered plant material was sieved to get a particle size of 60 µm, and stored in HDPE polyethylene cover under refrigerated condition at 4 °C until they were used.

Dried fine powder (10 g) was soaked in 100 ml of ethanol for 24 hr at room temperature (28-35 ˚C) under dark condition. Extract was filtered after soaking time intervals of 6, 12, 18 and 24 h through Whatman's No.1 filter paper (11 µm) to get an ethanolic plant extract (Pa and Mathew, 2012).

Total Antioxidant Capacity

Antioxidant capacity of a sample was determined using spectroscopic method, using a phospomolybdate reagent following the procedure described by Prieto *et al*. (1999). Phospomolybdate reagent was prepared by mixing equal quantities of 0.028 M sodium phosphate, 0.004 M ammonium molybdate and 0.6 M sulfuric acid solution. An amount of 0.3 ml of plant ethanolic extract was mixed in a test tube with 3 ml of the reagent. The test tube was covered with aluminium foil and incubated in a boiling water bath at 95^{0}C for 90 min. After cooling the sample to room temperature, the absorbance of the aqueous solution was measured at 695 nm against blank in an UV-VIS spectrophotometer (Shimadzu Japan, Model: UV-1800, Spectral width: 1ηm-100 µm). A typical blank solution contained 3 ml of reagent solution and appropriate volume (0.3 ml) of the same solvent used for the sample; and it was incubated under same conditions as rest of the sample. Ascorbic acid was used as a standard. Standard ascorbic acid curve was obtained by plotting various concentrations (10, 20, 30, 40, 50, 60, 70, 80, 90, 100 $\mu g.ml^{-1}$) of ascorbic acid (X) against absorbance (Y). The antioxidant capacity of each sample was expressed as micrograms per ml of ascorbic acid equivalents using the following linear equation established using ascorbic acid standard curve (Fig. 1):

$$Y = 0.111X - 0.0416; \quad R^2 = 0.9917 \qquad \ldots(1)$$

Where,
Y = Absorbance at 695 nm, and
X = Concentration as ascorbic acid equivalent, $\mu g.ml^{-1}$.

The values are presented as the mean (±) standard deviation of triplicate analysis.

Preparation of Edible Coating Solution Containing *Justicia adhatoda* extract

Different concentration levels of independent variables were selected based on the preliminary study, and are presented in Table 1. Vasa plant (*Justicia adhatoda* L.) is shown in Fig. 2(a).

Corn starch (4 %, w/w) and sucrose (1-1.5 % w/w) were dispersed uniformly in a 100 ml of distilled water using stirrer at room temperature (28-35 ˚C). The

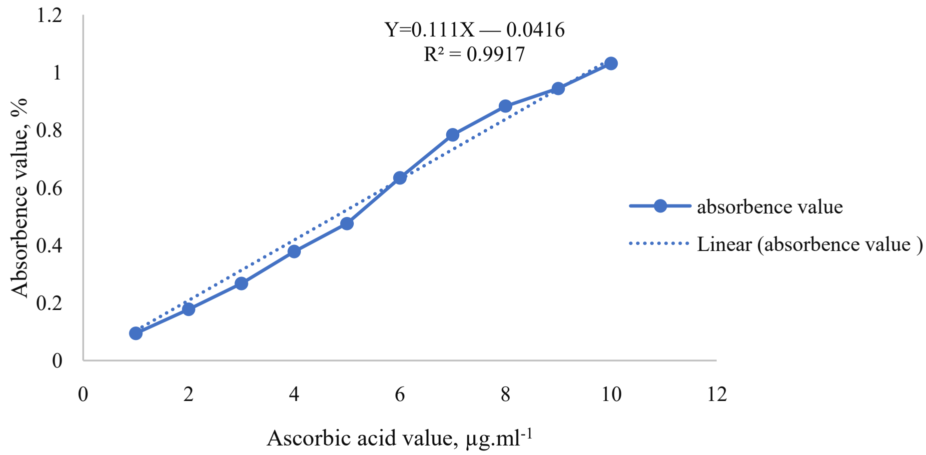

Fig. 1: Standard ascorbic acid curve prepared at 695 ηm

Fig. 2(a): Vasa plant (*Justicia adhatoda* L.)

Table 1. Different concentration levels of variables

Sl. No.	Constituent	Concentration level, %		
1.	Sucrose (X)	1.00	1.25	1.50
2.	Glycerol (Y) (for each gram of starch)	10.00	15.00	20.00
3.	*Justicia adhatoda* (Z)	3.00	6.00	9.00

dispersion was incubated at 85 ˚C in a hot water bath, for 30 minutes to induce starch gelatinization and then it was cooled down to room temperature (Moreno *et al*., 2014). Glycerol (10-20 %, for each gram of starch) was added to the suspension and it was again incubated for 15 mins at 90 ˚C in a water bath. This mixture was cooled down to room temperature. Plant extract (3-9 %, v/v) was added at required proportion and stirred for 2 min to get a uniform solution (Nouri and Nafchi, 2014).

Box Behnken method was used for statistical design, and response surface methodology was used for optimizing the constituents of the edible coating solution (ECS). Based on preliminary study sucrose (X; 1.00, 1.25, and 1.50 %), glycerol (Y; 10, 15, and 20 %) and plant extract (Z; 3, 6, and 9 %) were selected for preparing edible coating solutions. The Box-Behnken method consisted of 13 experiments in total (Table 2). Prepared edible coating solution using plant extract image is shown in Fig. 2(b).

Rheological Properties of Edible Coating Solution

Steady shear rheological properties

The rheological behaviour of the prepared ECS was analysed by utilizing a Rheometer (Anton PaarOstfildern, Germany, Model: Physica MCR 502, Torque: 100-300 µ Nm, GMBH). The PP50 probe (Plate and plate geometry, 50 mm diameter) was used for the flow curve measurements. Test gap for the sample was fixed at 1.0 mm. The shear rate tests were conducted over a shear rate ramp of 1-100 s^{-1}. The shear stress and viscosity changes were recorded at 30 °C. Data of all rheological measurements were analysed with supporting software Rhizopus/322 v 2.81 (Anton Paar, Germany). A sample volume of approximately 2 ml of

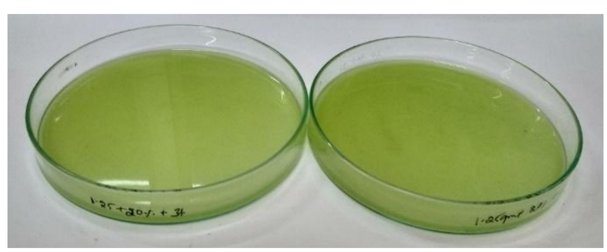

Fig. 2(b): Prepared edible coating solution using plant extract

Table 2. Response surface method design with coded values for film forming materials of sucrose (X), glycerol (Y), and *Justicia adhatoda* (Z) leaf extract

Sl. No.	Sucrose, w/w, % (X)	Glycerol, w/w, % (Y)	*Justicia adhatoda* extract v/v, % (Z)	Coded value
1.	1.00	10.00	6.00	1X10Y6Z
2.	1.00	15.00	3.00	1X15Y3Z
3.	1.00	15.00	9.00	1X15Y9Z
4.	1.00	20.00	6.00	1X20Y6Z
5.	1.25	10.00	3.00	1.25X10Y3Z
6.	1.25	10.00	9.00	1.25X10Y9Z
7.	1.25	15.00	6.00	1.25X15Y6Z
8.	1.25	20.00	3.00	1.25X20Y3Z
9.	1.25	20.00	9.00	1.25X20Y9Z
10.	1.50	10.00	6.00	1.5X10Y6Z
11.	1.50	15.00	3.00	1.5X15Y3Z
12.	1.50	15.00	9.00	1.5X15Y9Z
13.	1.50	20.00	6.00	1.5X20Y6Z

ECS was placed in between the plates and subjected to a programmed shear rate ramp which linearly increased from 1 to 100 s^{-1}. Based on the flow curve behaviour, the experimental data was fitted to Herschel Bulkley model as shown in Eq. (2).

$$\tau = \tau_0 + k\gamma^n \quad \text{…(2)}$$

Where,
τ = Shear stress, Pa,
τ_0 = Yield stress, Pa,
k = Consistency coefficient,
γ = Shear rate, s^{-1}, and
n = Flow behaviour index.

pH measurement

A digital pH meter (Elice France, Model: LI165, pH range: 0 -14) was used to measure the pH of the ECS. The pH electrode measures in the range of 0-13. If the pH changed beyond the set range, 0.1 N HCl or 0.1 N NaOH was added based on the measured value (Mazumdar and Majumder, 2003).

Electrical conductivity

Pre-calibrated electrical conductance testing instrument (Elice France, Model: LT51, Range: 0-200 $\mu S.cm^{-1}$) was used for measuring the electrical conductance ($dS.m^{-1}$) of the ECS. Fifty ml of ECS was taken in a beaker and stirred for 30 min. Electrodes washed with distilled water were inserted into the sample and the electrical conductance recorded (Mazumdar and Majumder, 2003).

Surface tension

Drop weight method was used to determine the surface tension properties of the ECS by forming cylindrical drops at the tip of a burette nozzle as described by Saha *et al.* (2011). Initial mass of the empty beaker (M1) was determined using a balance (Essae, India, Model: DC-50, Range: 10 g to 3 kg). The burette was filled with acoating solution sample, and its stopper adjusted such that the flow rate of liquid was about six drops per min. Fifty such drops were collected in the pre-weighed beaker, and the mass (M2) was noted. An additional 50 drops were then collected in the beaker taking the total number of drops to 100, and its mass (M3) was noted. Once again 50 more drops were collected, and the mass (M4) of the beaker corresponding to 150 drops was recorded. The mass of a single drop (M) was determined by dividing the total number of droplets by weight. Using a screw gauge (Eisco, France, Model: PH0086A, Range: 0 to 25x0.01 mm), the diameter of the tip of the burette nozzle was measured at different points along the tip, and the average radius of the tip (R) was calculated.

Surface tension of the liquid was calculated by using the relation presented in Eq. (3) (Saha *et al.,* 2011):

$$\sigma = \frac{Mg}{3.8R} \quad \text{…(3)}$$

Where,
σ = Surface tension, $m.N.m^{-1}$,
M = Average mass of single drop of the liquid, kg,
g = Acceleration due to gravity, 9.8 $m.s^{-1}$, and
R = Radius of the tip of burette, 0.75×10^{-3} m.

Total soluble solids

Total soluble solids in the prepared ECS samples were determined using a hand-held reflectometer (ATAGO, Co Ltd Japan, Model: PR-201ὰ, Range: 0.0-60.0 %) by the principle of total refraction. Total reflection was calibrated at 0^o Brix at 20 °C with the help of a temperature correction correlation chart. A few drops of ECS from each sample were dropped on the plate to record the Refractometer reading in Brix. (Mazumdar and Majumder, 2003).

Statistical Method

Box-Behnken method under response surface methodology was used to determine the interaction of independent variables on dependent parameters. Optimization of edible coating formulation (sucrose, glycerine and plant extract) was done by considering desirable solution properties such as lower yield stress (< 3.00Pa), surface tension (< 70 $m.N.m^{-1}$), and TSS (< 2.5 ^{o}Brix), neutral pH (6-7) and higher electrical conductivity (>0.1 $dS.m^{-1}$). Design Expert Version 6.0.8.1 software was used for analysing the data related to ECS, for statistical significance.

One-way ANOVA on MS Excel was used for analysing antioxidant property. All treatments were analysed at 0.05 % level of significance.

RESULTS AND DISCUSSION

Total Antioxidant Capacity

Total antioxidant capacity of the ethanolic extract of *Justicia adhatoda* at different time intervals (h) is presented in Fig. 3. Data was analysed using one-way Anova statistical tool (Table 3). There was a significant ($p<0.05$) difference between the total antioxidant capacity of the extract obtained at different time intervals (presented in equivalence of ascorbic acid). Ethanolic extract obtained at 6th hour showed lower antioxidant capacity (63.77 $\mu g.ml^{-1}$); whereas, at 24th hour the antioxidant capacity of 94.47 $\mu g.ml^{-1}$ was the highest. Higher antioxidant capacity of the extract after 24 hours might be due to availability of more time for diffusion of phytochemicals from the plant material to the ethanol. Karthikeyan *et al*. (2009) reported that antioxidant property of the *Justicia adhatoda* extract was mainly due to the presence of phytochemicals such as phenols, tannins, alkaloids, saponins flavonoids.

Rheological Properties of ECS

Steady-state flow curves were obtained by increasing the shear rate (0-100 s^{-1}) for formulated ECS. Viscosity versus shear rate of the formulated solution is presented in Fig. 4(a). It was observed that initially viscosity was maximum, and then gradually decreased with increasing shear rate, described as shear thinning behaviour of fluids. It was observed that increase in plant extract concentration decreased the viscosity of the formulated ECS.

After initial decrease, viscosity maintained an equilibrium at 65 s^{-1} to 75 s^{-1} shear rates. In case of lower plant extract, stable phase was reached little later as compared to that in higher plant extract incorporated sample. It might be due to the presence of polyphenolic

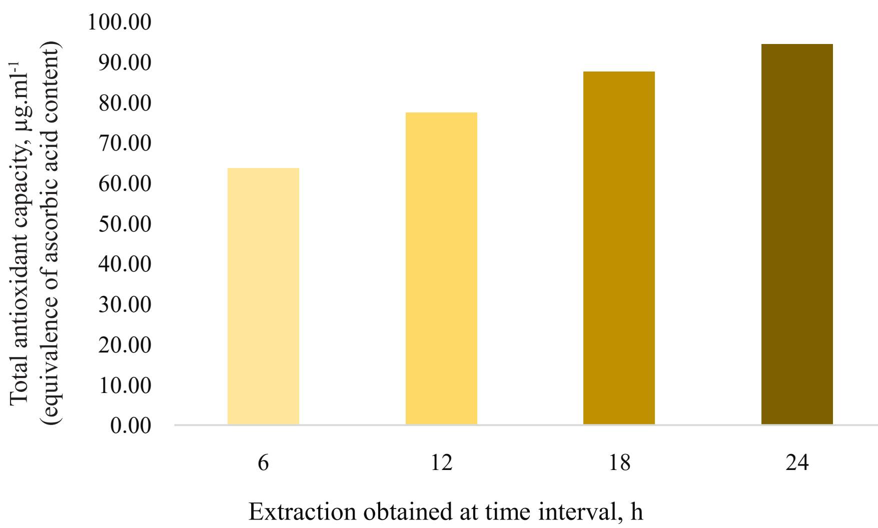

Fig. 3: Total antioxidant capacity of ethanolic extract of *Justicia adhatoda* at different time intervals

Table 3. ANOVA for total antioxidant capacity

Sl.No.	Source of variation	SS	Df	MS	F	P-value	F critical
1.	Between groups	1990.85	4	497.71	1140.60	3×10^{-13}	3.47
2.	Within groups	4.36	10	0.43			
3.	Total	1995.22	14				

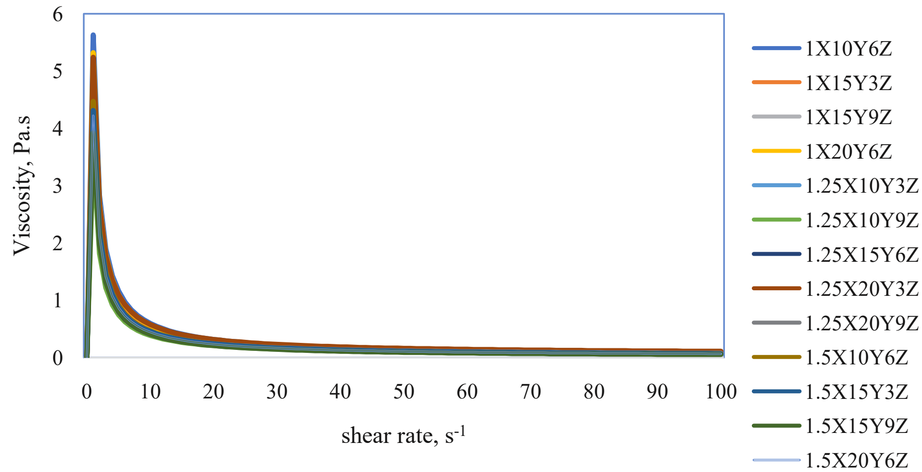

Fig. 4(a): Variations of viscosity with shear rate of ECS

compounds in the extract that influenced in structural breakdown, and in turn decreased viscosity of the ECS.

Flow curves of shear stress against shear rate of the ECS obtained from the rheometer are presented in Fig. 4(b). It was observed that all samples follow non-Newtonian fluid behaviour due to presence of yield stress, and their shear stress increased with shear rate but n-value was less than one. At lower shear stress, polymeric materials were coiled and entangled. As the shear rate increased, the polymeric materials disentangled and became straightened along the path of flow causing the material to behave in shear thinning manner. This type of behaviour was observed in the Herschel–Bulkley fluids (Rajesh and Thirupathi, 2014). Further, the flow curve data obtained from the rheometer was fitted to Herschel Bulkley model. The parameters obtained from the analysis are listed in the Table 4. The obtained data for different ECS fitted well to the Herschel Bulkley model with R^2-value ranging from 0.91 to 0.99. The flow index (n-value) of the obtained solution varied between 0.26 to 0.95. Since all the n-values obtained

Table 4. Parameters of Herschel Bulkley model for formulated ECS

Sl. No.	ECS formulation	Consistency index	n-Value	R^2	Yield stress, Pa
1.	1X10Y6Z	0.22	0.64	0.98	4.74
2.	1X15Y3Z	0.48	0.52	0.99	3.55
3.	1X15Y9Z	0.28	0.62	0.98	3.25
4.	1X20Y6Z	0.89	0.38	0.99	2.86
5.	1.25X10Y3Z	0.05	0.86	0.98	4.03
6.	1.25X10Y9Z	0.26	0.92	0.98	3.59
7.	1.25X15Y6Z	0.22	0.62	0.99	3.27
8.	1.25X20Y3Z	0.44	0.59	1.00	3.65
9.	1.25X20Y9Z	0.53	0.46	0.99	2.67
10.	1.5X10Y6Z	0.81	0.26	0.95	2.38
11.	1.5X15Y3Z	0.03	0.95	0.98	4.24
12.	1.5X15Y9Z	0.01	0.61	0.92	3.94
13.	1.5X20Y6Z	0.13	0.67	0.97	3.70

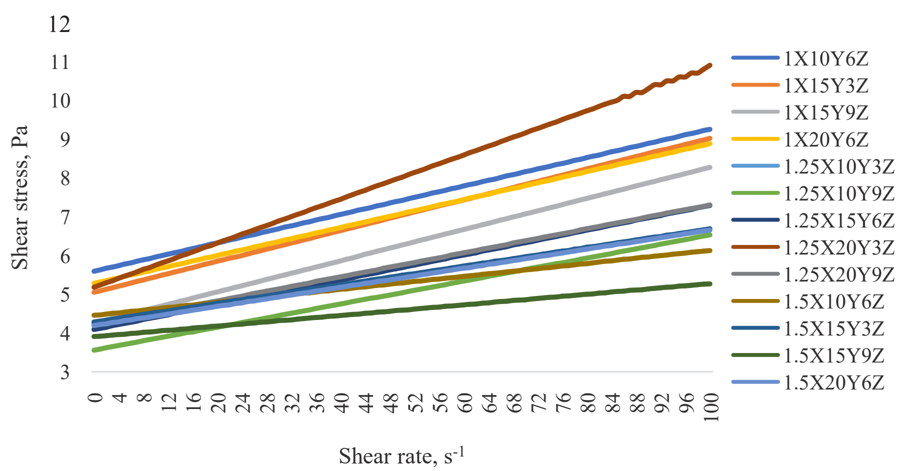

Fig. 4(b): Variations in shear stress with shear rate of ECS

for the formulated solutions were less than one, it confirmed that the prepared solution hadshear thinning behaviour. This might be due to the re-orientation of branched and randomly oriented micro-structure of the particles in the polymer solution under increase in the shear rate (Grigelmo-Miguel *et al*., 1999). Consistency index of the ECS varied from 0.03 to 0.89, which confirms the liquidity of the solution (Rajesh and Thirupathi, 2014).

Yield stress values varied from 2.38 Pa to 4.74 Pa at varying levels of glycerol, sucrose andplant extract as shown in Fig. 4(c). ANNOVA values for pH of ECS under the influence of individual parameters are given in Table 5. Yield stress values of the formulated solutions were significantly ($p<0.05$) affected by the interactions of sucrose and glycerol. This might be due to the water retention property of the plasticizer, which required more shear stress for initialization of fluid flow. Yield stress value of the liquid indicates the initial power required to initiate the flow of a liquid. Hence, liquid with lower yield stress had better flowability and atomisation possibility for spray coating.

pH of formulated ECS

Figure 5 shows the variations in pH of the ECS due to interaction of glycerol and *Justicia adhatoda* extract. pH of the formulated ECS varied from 6.2 to 6.9. pH increased non-significantly ($p <0.05$) with increase in glycerol concentration (Table 6). Increase in ethanolic extract of *Justicia adhatoda* had significantly ($p<0.05$) decreased the pH of the formulated solution. Since the

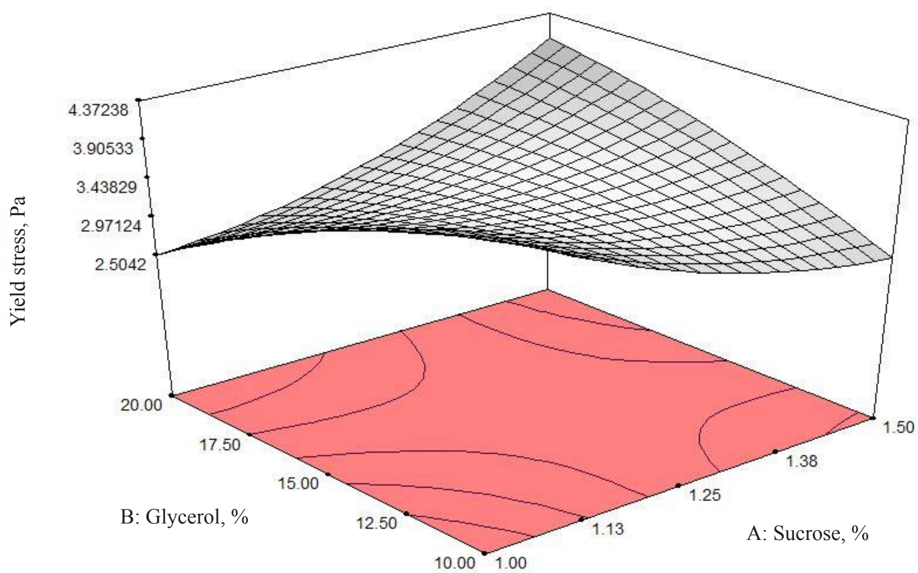

Fig. 4(c): Yield stresses at different concentrations of sucrose, glycerol and 6 % plant extract

Table 5. ANOVA for yield stress of ECS

Sl. No.	Source	SS	DF	MS	F-Value	Prob>F	Significance
1.	Model	3.34	6	0.56	3.35	0.04	*
2.	Sucrose	2.60×10^{-03}	1	2.60×10^{-03}	0.01	0.90	NN
3.	Glycerol	0.14	1	0.14	0.86	0.38	NN
4.	Plant extract	0.19	1	0.19	1.15	0.31	NN
5.	Sucrose and glycerol	2.56	1	2.56	15.42	2.00×10^{-03}	**
6.	Std. Dev.	0.41					
7.	Mean	3.42					
8.	C.V.	11.93					
9.	R-square	0.67					

*** - Significant at <0.01; * - Significant at <0.05; NN- non significant*

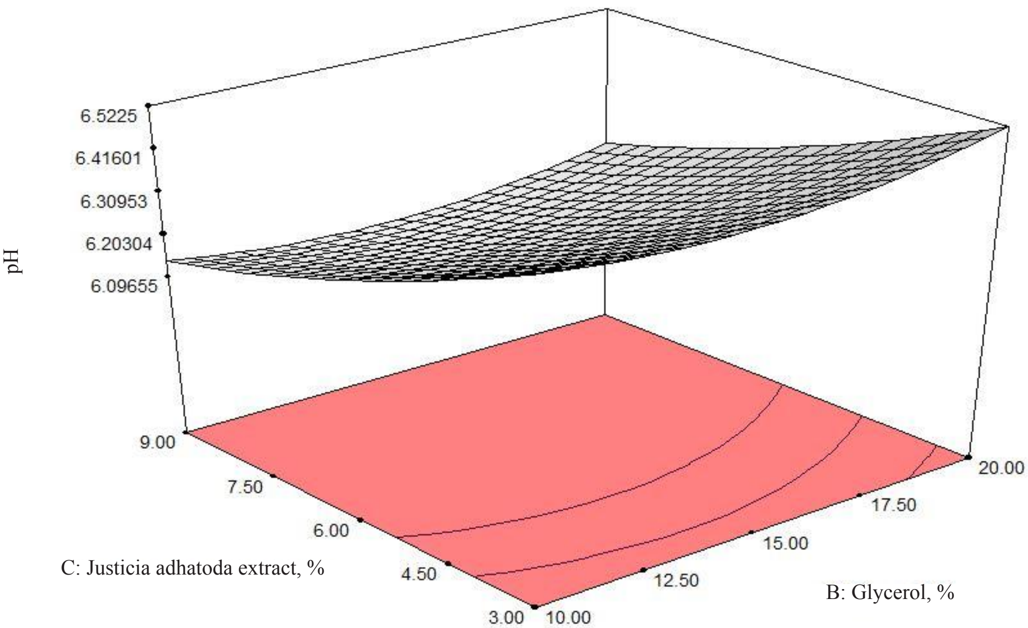

Fig. 5: Variation in pH of formulated edible coating solution at different concentrations of plant extract, glycerol and 1.25 % sucrose

Table 6. ANOVA table for pH of ECS

Sl. No.	Source	SS	DF	MS	F-Value	Prob>F	Significance
1.	Model	0.68	9	0.07	3.56	0.04	*
2.	Sucrose	1.25 x10^{-03}	1	1.25 x10^{-03}	0.06	0.81	NN
3.	Glycerol	3.20 x10^{-03}	1	3.20 x10^{-03}	0.15	0.70	NN
4.	Plant extract	0.24	1	0.24	11.30	0.01	*
5.	Std. Deviation	0.15					
6.	Mean	6.41					
7.	C.V.	2.26					
8.	R-square	0.82					

*** - Significant at <0.01; * - Significant at <0.05; NN- non significant*

pH of the ethanolic extract lied in the acidic range, it might have decreased the overall pH of the solution.

Electrical conductivity of formulated ECS

Electrical conductivity of the ECS samples was maximum (0.36 dS.m^{-1}) for 1.5 % sucrose, 15 % glycerol and 9 % *Justicia adhatoda* extract formulation; and minimum (0.17 dS.m^{-1}) for 1 % sucrose,10 % glycerol, and 6 % *Justicia adhatoda* extract formulation. It was observed from the Fig. 6 that the increase in sucrose and *Justicia adhatoda* extract concentration in the formulated solution significantly ($p<0.05$) increased the electrical conductivity due to increase in soluble constituents and phytochemicals in the extract. Since the ethanolic extract was rich in phytochemicals, it might have increased the ionic concentration of extract, and in turn the electrical conductivity. Electrical conductivity of the solutions mainly depended on the ionic concentration of the solution (Yusof *et al.*, 2014). Glycerol had non-significant ($p<0.05$) effect on electrical conductivity of the formulated solution (Table 7).

Surface tension of formulated ECS

Effect of *Justicia adhatoda* extract and glycerol on surface tension of the coating solution is presented in Fig. 7. Surface tension of the formulated solution varied from 58.10 mm.N.m^{-1}to 81.90 mm.N.m^{-1}.

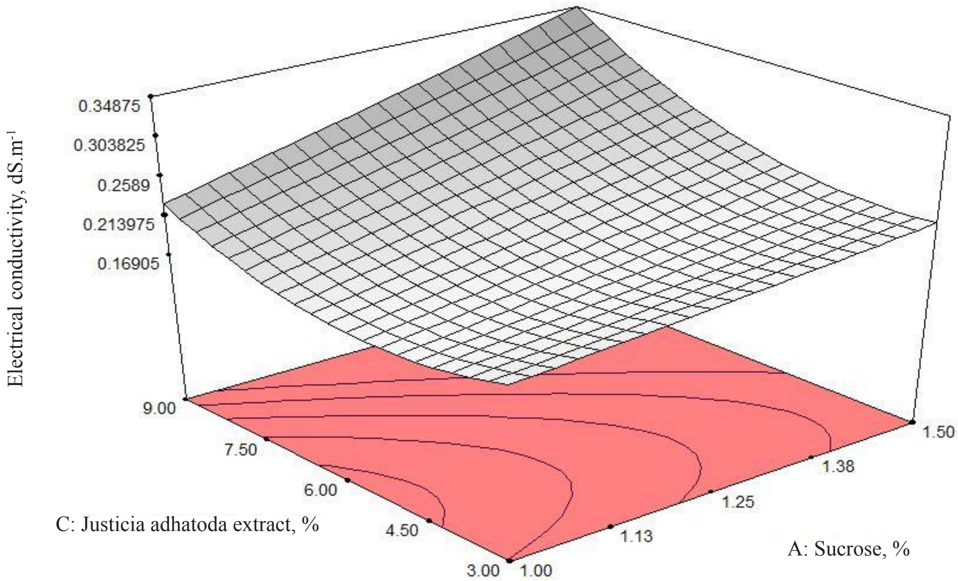

Fig. 6: Electrical conductivity of formulated edible coating solution at different concentration of sucrose, plant extract and 15 % glycerol

Table 7. ANOVA for electrical conductivity of ECS

Sl. No.	Source	SS	DF	MS	F-Value	Prob>F	Significance
1.	Model	0.03	9	3.75 x10^{-03}	12.98	14x10^{-03}	**
2.	Sucrose	0.01	1	0.013	44.25	3x10^{-04}	**
3.	Glycerol	3.13 x10^{-04}	1	3.13 x10^{-04}	1.08	0.33	NN
4.	Plant extract	0.01	1	0.01	41.52	4x10^{-03}	**
5.	Std. Deviation	0.02					
6.	Mean	0.23					
7.	C.V.	7.53					
8.	R-square	0.94					

*** - Significant at <0.01; * - Significant at <0.05; NN- non significant*

Surface tension of the formulated solution increased significantly (p<0.05) with increase in glycerol concentration (Table 8). This was due to the increase in cohesive force of inter-molecules on the surface of the formulated solutions due to the bonding ability of glycerol. Increase in *Justicia adhatoda* extract significantly (p<0.05) decreased the surface tension of the formulated solution due to the presence of saponins thatmight have acted as a surfactant in decreasing the intermolecular bonds and cohesive nature of the solution (Chen *et al*., 2010). Sucrose had a non-significant (p<0.01) effect on surface tension of the solution.

Total soluble solids of formulated ECS

Total soluble solids of the formulated solutions varied from 1.7 °Brix to 3.9 °Brix, Fig. 8. Total soluble solids in the solution increased significantly (p<0.05) with increase in sucrose and *Justicia adhatoda* extract due to the increase in soluble constituents in the ECS (Table 9). Glycerol had not shown any significant(p<0.05) effect on the TSS of the solution.

Optimization of Formulated ECS

Numerical optimization of individual variables was done using Design Expert (6.0.8.1) software. Optimum values for independent variables were obtained assigning certain constraint values for independent variables. Optimum values of independent variables were as follows: sucrose 1.04 %, glycerol 18.44 %, and *Justicia adhatoda* extract 9.00 per cent. ECS

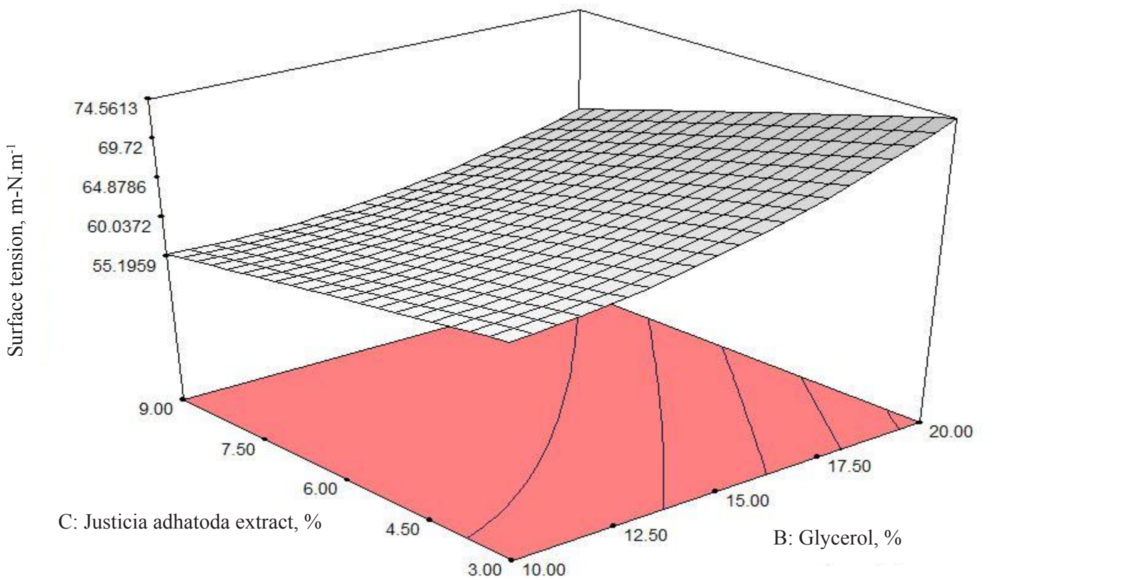

Fig. 7: Variations of surface tension of formulated edible coating solution at different concentrations of plant extract, glycerol and 1.25 % sucrose

Table 8. ANOVA for surface tension of ECS

Sl. No.	Source	SS	DF	MS	F-Value	Prob>F	Significance
1.	Model	660	9	73.33	4.73	0.03	*
2.	Sucrose	41.56	1	41.56	2.68	0.14	NN
3.	Glycerol	166.45	1	166.45	10.73	0.01	*
4.	Plant extract	201.17	1	201.17	12.96	8×10^{-02}	**
5.	Std. Deviation	3.94					
6.	Mean	65.40					
7.	C.V.	6.02					
8.	R-square	0.8587					

*** - Significant at <0.01; * - Significant at <0.05; NN- non significant*

formulation containing 1.04 % sucrose, 18.44 % glycerol and 9.00 % *Justicia adhatoda* extract showed yield stress, pH, electrical conductivity, surface tension and TSS values of 2.66 Pa, 6.29, 63.03 m.N.m^{-1}, 0.247 dS,m^{-1} and 1.86 °Brix, respectively, as the optimized solution.

Confirmative test for verification of model was carried out using optimum independent variables, and yield stress value obtained at optimum condition of independent variables was 2.66 Pa. In order to verify the reliability of the response surface results, the conformity experiment of the edible coating solution was carried out according to the optimal conditions obtained by the experiments. After three replicated experiments, the mean yield stress value obtained was 2.71 Pa. It confirmed a good correlation between the experimental and predicted yield value. Thus, the confirmation test validated the experimental results as well as the regression equation.

CONCLUSIONS

Vasa plant (*Justicia adhatoda*) extract was found to contain 94.47 µg.ml^{-1}of antioxidant capacity in equivalence of ascorbic acid. The ECS prepared from *Justicia adhatoda* extract followed non-Newtonion, Herschel-Bulkley curve having flow index less than 1, which confirmed viscous nature of the ECS. Increase in the concentration of plant extract decreased the pH, electrical conductivity and surface tension; while it increased the TSS of the ECS due to presence of

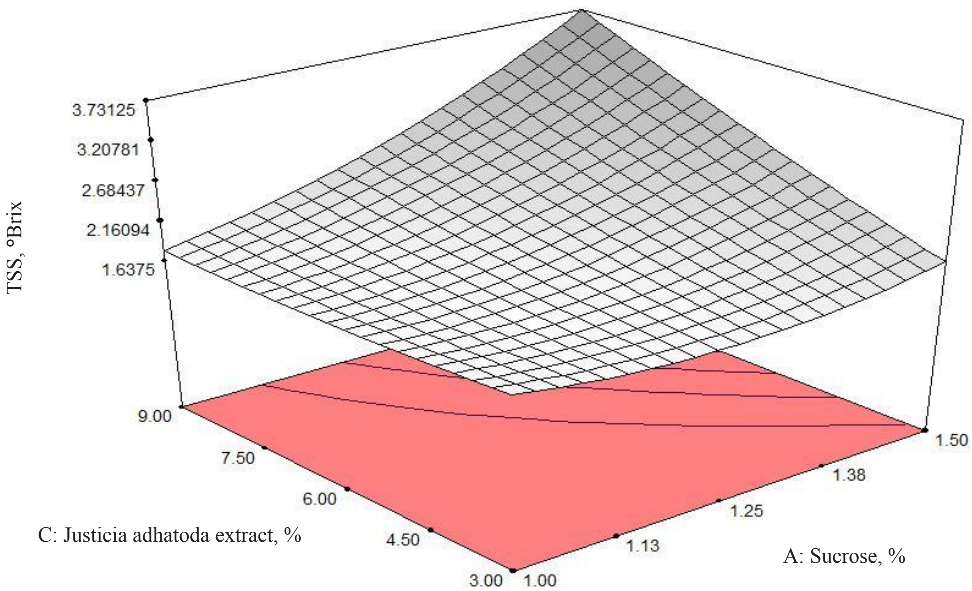

Fig. 8: Total soluble solids (°Brix) at different concentrations of plant extract, sucrose and 15 % glycerol

Table 9. ANOVA for TSS of ECS

Sl. No.	Source	SS	DF	MS	F-Value	Prob>F	Significance
1.	Model	5.30	6	0.88	8.23	$2x10^{-03}$	**
2.	Sucrose	2.00	1	2.00	18.65	$1x10^{-03}$	**
3.	Glycerol	0.34	1	0.34	3.17	0.10	NN
4.	Plant extract	1.49	1	1.49	13.87	$3x10^{-03}$	**
5.	Std. Deviation	0.33					
6.	Mean	2.21					
7.	C.V.	14.83					
8.	R-square	0.83					

*** - Significant at <0.01; * - Significant at <0.05; NN- non significant*

phytochemicals in the extract. The variation in the sucrose concentration showed a significant effect on the electrical conductivity due to change in the ionic concentration of the ECS. Further, the increase in glycerol concentration significantly increased the surface tension of ECS. TSS of the ECS varied based on the proportionate mixture of three base materials. Formulated ECS of 1.04 % sucrose, 18.44 % glycerol and 9.00 % *Justicia adhatoda* extract was found to provide optimum ECS by the design expert analysis.

REFERENCES

Andrade R; Osorio F. 2012a. Experimental study of drop impacts and spreading on epicarps : Effect of fluid properties.J. Food Eng., 109(3), 430-437.

Andrade R D; Skurtys O; Osorio F A. 2012b. Atomizing spray systems for application of edible coatings.Com. Rev. Food Sci. Food Saf., 11, 323-337.

Barth A; Hovhannisyan A; Jamalyan K; Narimanyan M. 2015. Phytomedicine antitussive effect of a fixed combination of Justicia adhatoda, Echinacea purpurea and Eleutherococcus senticosus extracts in patients with acute upper respiratory tract infection: A comparative, randomized, double-blind, placebo-contro. Phytomedicine, *22*(13), 1195-1200.

Bhattacharyya D; Pandit S; Jana U; Sen S; Sur T K. 2005. Hepatoprotective activity of Adhatoda vasica aqueous leaf extract on D -galactosamine-induced liver damage in rats. Fitoterapia,76(2), 223-225.

Chen Y F; Yang C H; Chang M S; Ciou Y P; Huang Y C. 2010. Foam properties and detergent abilities of the saponins from Camellia oleifera. Int. J. Mol. Sci., 11(11), 4417-4425.

Debeaufort F; Voilley A. 2009. Lipid-based Edible Films and Coatings. In: Huber K; Embuscado M (Eds.) Edible Films and Coating for Food Applications, Springer, New York, NY,135-168.

Fadini A; Rocha F; Alvim I; Sadahira M; Queiroz M; Alves R; Silva L. 2013. Mechanical properties and water vapour permeability of hydrolysed collagen–cocoa butter edible films plasticised with sucrose. Food Hydrocolloids, 30(2), 625-631.

Franssen L; Krochta J. 2003. Edible Coatings Containing Natural Antimicrobials for Processed Foods. In: Nat Antmicrobials Minimum Processing of Foods, Woodhead Publishing Series in Food Science, Technology and Nutrition, Elsevier, New York, NY, 250-262.

Grigelmo-Miguel N; Ibarz-Ribas A; Martín-Belloso O. 1999. Rheology of peach dietary fibre suspensions. J. Food Eng., 39(1), 91-99.

Izbassarov D; Muradoglu M. 2016. Effects of viscoelasticity on drop impact and spreading on a solid surface.Phy. Rev. Flu., 1(2), 1-18.

Jaworek A. 2007. Electrospray droplet sources for thin film deposition. J. Mat. Sci., 42(1), 266-297.

Jones J R; Paterson A; Pearce D L. 2016. Droplet impact and spreading : Droplet formulation effects. Chem. Eng. Sci., 62(9), 2336-2345.

Karthikeyan A; Shanthi V; Nagasathaya A. 2009. Preliminary phytochemical and antibacterial screening of crude extract of the leaf of Adhatoda vasica. L. Int. J. Green Pharm., 3(1),78-80.

Kaur R; Ruhil S; Balhara M; Dhankhar S; Chhillar A. 2013. A review on Justicia adhatoda: A potential source of natural medicine. Afr. J. Plant Sci., 5(11), 620-627.

Mazumdar B C; Majumder K. 2003. Methods on Physico-chemical Analysis of Fruit. Daya Publishing House, Delhi, 112-115.

Moreno O; Pastor C; Muller J; Atarés L; González C; Chiralt A. 2014. Physical and bioactive properties of corn starch – Buttermilk edible films. J. Food Eng., 141, 27-36.

Muscat D; Adhikari B; Adhikari R; Chaudhary D. 2012. Comparative study of film forming behaviour of low and high amylose starches using glycerol and xylitol as plasticizers. J. Food Eng., 109(2), 189-201.

Nouri L; Nafchi A M. 2014. Antibacterial, mechanical, and barrier properties of sago starch film incorporated with betel leaves extract. Int. J. Biol. Macromol., 66, 254-259.

Oliveira L M; Cereda M P. 2007. Sucrose and inverted sugar as plasticizer. Effect on cassava starch – gelatin film mechanical properties, hydrophilicity and water activity. Food Chem., 103(2), 255-262.

Pa R; Mathew L. 2012. Antimicrobial activity of leaf extracts of Justicia adhatoda L. in comparison with vasicine. Asian Pac. J. Trop. Biol., 2(3), S1556-S1560.

Prieto P; Pineda M; Aguilar M. 1999. Spectrophotometric quantitation of antioxidant capacity through the formation of a phosphomolybdenum complex: Specific application to the determination of vitamin E. Anal. Biochem., 269 (2), 337-341.

Rajesh G; Thirupathi V. 2014. Effect of plasticizers on rheology of banana flour and the mechanical and functional properties of banana flour composite films. Trends Biosci., 7(15), 2043-2048.

Ruenroengklin N; Zhong J; Duan X; Yang B; Li J. 2008. Effects of various temperatures and ph values on the extraction yield of phenolics from litchi fruit pericarp tissue and the antioxidant activity of the extracted anthocyanins. Int. J. Mol. Sci., 9(7), 1333-1341.

Saha D; Hait M; Patanwar M; Tamrakar A. 2011. Studies on surface tension of selected juice formulation by drop number method using Traube's Stalagmometer technique. Bul. Pharma. Res., 1(3), 1-3.

Veiga-Santos P; Oliveira L; Cereda M; Scamparini A R P. 2007. Sucrose and inverted sugar as plasticizer. Effect on cassava starch–gelatin film mechanical properties, hydrophilicity and water activity. Food Chem., 103(2), 255-262.

Yusof Y; Shukur M; Illias H; Kadir M. 2014. Conductivity and electrical properties of corn starch–chitosan blend biopolymer electrolyte incorporated with ammonium iodide. Phys. Scr., 89(3), 35701-35711.

http://www.isae.in / journal_jae.aspx

Journal of Agricultural Engineering

Vol. 57 (3): July-Sepember, 2020

Performance Evaluation of Subsurface Drainage System under Waterlogged Saline Vertisols for Sugarcane Crop in Ukai Kakrapar Canal Command, Gujarat

Anil R. Chinchmalatpure[1]*, Sagar D. Vibhute[2], M. J. Kaledhonkar[3], Sanjay Vasant Kad[4], Shrvan Kumar[5], David Camus[6], Indivar Prasad[7], S. K. Kamra[8] and P.C. Sharma[9]

[1]Head, [2]Scientist (Land and Water Management Engineering), [4]Scientist (Agriculture Extension), [5]Scientist (Soil Science), [6]Scientist (Agroforestry), ICAR-Central Soil Salinity Research Institute, Regional Research Station, Bharuch, Gujarat-392012, India; [3]Project Coordinator, AICRP on Management of Salt Affected Soils and Use of Saline Water in Agriculture, [8]Principal Scientist (Retd.), [9]Director, ICAR-Central Soil Salinity Research Institute, Karnal, Haryana-132001, India; [7]Scientist (Plant Breeding), ICAR-Indian Institute of Vegetable Research, Varanasi, Uttar Pradesh-221305, India. *Corresponding author email address: rcanil2014@gmail.com

Article Info

Manuscript received:
April, 2020
Revised manuscript accepted:
August, 2020

***Keywords*:** Agricultural drainage, subsurface drainage, canal command, salinity, sugarcane, Vertisols, waterlogging

ABSTRACT

Crop productivity in canal command areas of India is declining due to waterlogging and soil salinization problems, and it is posing a big threat to livelihood security of small and marginal farmers. Subsurface drainage (SSD) technology, which restores favourable condition in the crop root zone by reclaiming waterlogged saline soils, can be one of the options to restore the crop productivity in such areas. The SSD system was installed at Mulad village in the Ukai Kakrapar canal command area, Gujarat, in the year 2012 to address the problem of drastic yield reduction of sugarcane due to twin problems of waterlogging and soil salinity in Vertisols. It was found that the SSD helped in desalination of soil profile as soil electrical conductivity was reduced to a range of 0.42 to 3.90 $dS.m^{-1}$ from its initial range of 1.2 to 7.3 $dS.m^{-1}$. Electrical conductivity of drained water was in the range of 1.3 to 4.4 $dS.m^{-1}$. Further, there was reduction in waterlogging condition, both surface and sub-surface, as water table lowered below crop root zone depth (depth of 0.6 m) and surface water ponding duration reduced to 6-8 days from earlier 25-30 days during peak monsoon days. Overall performance of SSD system was satisfactory as average sugarcane yield in the study area increased significantly from 39.29 to 97.29 $t.ha^{-1}$ as result of reduction in soil salinity and waterlogging in drainage area. Economic analysis also indicated 114% increase in benefit-cost ratio after SSD installation. Thus, large scale installation of SSD system for reclamation of waterlogged saline Vertisols is economically viable in the state of Gujarat.

Irrigated agriculture in India as well as in the world is under stress due to twin problems of waterlogging and soil salinity (Valipour, 2014). Out of the world's total irrigated area of 299 Mha, only 22% area has drainage facilities (Ritzema, 2016). In different canal commands of India, around 3.0 Mha area suffers from irrigation induced waterlogging and soil salinization. It is slightly less than half of the salt affected area (6.74 Mha) in India (Kamra and Sharma, 2016). Out of 3.0 Mha waterlogged saline area, more than 1.1 Mha area is located in Vertisols (black cotton soils and associated soils) regions in different states of India. By nature, Vertisols are low in hydraulic conductivity due to more presence of micro pores than macro pores. Therefore, these soils are more suitable for dry land agriculture. These soils suffer from surface and subsurface waterlogging and soil salinity, if proper drainage facility is not provided along with provision of irrigation. Thus, provision of subsurface drainage is essential for economically viable crop production on irrigated Vertisols (Rao *et al.*, 2009).

Worldwide huge crop yield losses are reported due to waterlogging and salinity under irrigated agriculture.

In case of sugarcane crop, 15-20% reduction in the cane yield and sugar recovery has been reported due to waterlogging (Sanghera and Jamwal, 2019). Appropriate drainage measures are needed to reduce waterlogging and soil salinity, and to enhance water productivity in the canal command areas (Vibhute *et al*., 2016). The need of drainage provisions in irrigation projects has been well acknowledged by the researchers worldwide, and nowadays it is considered as an integral part of large irrigation schemes. Drainage helps in reducing soil submergence, soil salinity and improving root zone aeration and crop yields. Thus drainage improves land and water productivity and sometimes it creates new land available for agriculture, if land is abandoned due to waterlogging and soil salinity (Singh, 2019).

Subsurface drainage (SSD) has been practiced in 75-80% of irrigated area in Egypt, and 25-30% irrigated area in western USA (Tiwari and Goel, 2015). In India, SSD systems have been installed on about 61,084 ha area in different states till the year 2016 (Bundela *et al*., 2016, Sharma *et al*., 2016; Kamra *et al*., 2019), and has been found as an effective technology for reclamation and management of waterlogged saline soils. Design of SSD system has been standardized for alluvial soils of North-west India through experimentation at village Sampla in Haryana (Rao *et al*., 1986). The technology was widely adopted in the light textured soils of the states of Haryana and Punjab. Large scale SSD installations were done in India under Rajasthan Agricultural Drainage (RAJAD) project and Haryana Operational Pilot Project (HOPP) with Government support. The soils under RAJAD project were heavy. As far as Indian experience of managing waterlogging and soil salinity in heavy textured soils are concerned, first ever SSD system was tested in heavy textured soils of Maharashtra, much before Sampla study, at village Manjari located in Khadakwasala irrigation project near Pune (Anon., 1988). However, spread of SSD did not take place in Maharashtra and neighbouring states mainly because of high cost and lack of institutional support. Systematic studies conducted by Ritzema *et al*. (2008) under Indo-Dutch Network project in five different agro-climatic sub-regions of India proved the subsurface drainage (by pipe or by open drains) as technically feasible, cost-effective, and socially acceptable technology to reclaim waterlogged and saline land, and to sustain agriculture in irrigation commands under the prevailing soils, agro-climatic conditions and social settings.

An agreement between ICAR-Central Soil Salinity Research Institute and a private firm, M/S Rex Poly-extrusion Pvt. Ltd., in the year 2006 paved way to promote SSD systems on heavy soils (waterlogged saline Vertisols) in Maharashtra and Karnataka through Government departments, cooperative societies and individual farmers. It resulted in private investments in terms of public-private partnership for planning, design and implementation of large-scale drainage projects for waterlogged saline Vertisols in the states of Maharashtra and Karnataka (Kaledhonkar *et al.*, 2009). Rathod *et al*. (2020) evaluated different drain spacings and depths for waterlogged Vertisols of Sangli district of Maharashtra, and found that 30-50 m drain spacing and 1.2 m depth as suitable for waterlogged saline Vertisols.

Gujarat despite being a leader in cooperative system and for agricultural growth, large-scale adoption of SSD for reclamation and management of waterlogged saline soils did not take place. Till the year 2016, the area under SSD system in Gujarat was only 1,300 ha (Bundela *et al.*, 2016) as compared to total waterlogged area of 2,65,000 ha in the state (Anon., 2009). Large part of Ukai-kakrapar command area was under pigeon pea/cotton cultivation before the availability of canal water, but subsequently farmers shifted towards sugarcane cultivation. The injudicious use of canal water for sugarcane crop coupled with absence of drainage system, resulted in severe problems of waterlogging and secondary salinization.

During the year 2012, a commercial SSD installation was done on waterlogged saline Vertisols at village Mulad of Surat district (Gujarat) under the Ukai Kakrapar canal command area. Though subsurface drainage has been found as a technically feasible and cost-effective in reclamation of waterlogged and saline land, performance evaluation of large-scale SSD systems on heavy textured soils are needed to build up confidence in minds of planners and farmers as SSD is generally adopted on large scale through community participation. The main objective of this study was to evaluate the performance of the existing SSD system for its ability to reduce soil salinity and to improve drainage water quality, crop yield and to judge the economic feasibility for greater adoption of SSD systems in the state of Gujarat.

MATERIALS AND METHODS

Study Area

The study area is located in Mulad village (Surat district of Gujarat) having total geographic area of 923.60 ha, and falls under Ukai Kakrapar canal command area with geographical coordinates as 21º 24′ 13.42″ N latitudes and 72º 54′ 18.34″ E longitudes (Fig. 1). It has tropical climate and receives majority of the rainfall from June till late September. The area has flat topography with gentle uniform slope of 0.25% towards the north-east side. Sugarcane and rice are the main crops since commencement of canal irrigation in the region. In the study area, problems of both high groundwater table and prolonged surface water stagnation in monsoon were prevalent. The depth to watertable from ground surface ranged from 0.5 m to 2 m. During peak rainy days, heavy surface waterlogging was observed and ponding of water on ground surface remained for 25 to 30 days, which adversely affected crop growth. Since the past one decade, these soils have been suffering by twin problems of waterlogging and salinity due to interplay of number of factors like cultivation of high water demand crops (sugarcane), mono-cropping, and injudicious use of irrigation water without adequate provision of drainage. As a result, sugarcane yield varied from 32 to 44 $t.ha^{-1}$, and was uneconomical.

Drainage investigations were carried out in 45 ha area in the year 2011 to assess the status of area in terms of soil salinity, waterlogging and crop productivity before SSD installation, and also to work out design parameters of SSD system as design of SSD system is location-specific. Further, pre-drainage data on soil salinity, groundwater quality, depth to water table, crop yield, crop productivity, etc. were necessary for comparison with respective post–SSD data, to quantify the improvements in drainage area in different aspects as a part of evaluation process. The post-SSD data were collected after six years (2012-2018) of successful operation of the system.

Soil and Water Sampling and Analysis

Soil samples for three depths (0-0.3, 0.3-0.6 and 0.6-0.9 m) were collected using Edelman clay auger. The total study area was divided into seven blocks, representing homogenous units comprising field survey numbers of land belonging to thirteen farmers. Representative soil samples from different blocks were collected in the month of May 2011 from 45 ha area during pre-SSD condition. Similarly, the post-SSD soil sampling was done from the same site on per ha basis (total 45 soil sampling locations) in the month of May 2018, and the average data of soil analysis were arranged block-wise. This was done to get adequate representation to each block. Pre-SSD samples were analysed at Soil and Water Testing Laboratory of Rajarambapu Patil Sahakari Sakhar Karkhana Ltd., Rajaramnagar, district Sangli (Maharashtra), while post-SSD soil samples were analysed in the laboratory of ICAR-Central Soil Salinity Research Institute, Regional Research Station, Bharuch, using standard methodologies (Richards, 1954) for properties like electrical conductivity of saturation extract (ECe), soil saturation paste pH (pHs), and sodium adsorption ratio (SAR). Groundwater samples during pre- and post-SSD condition were

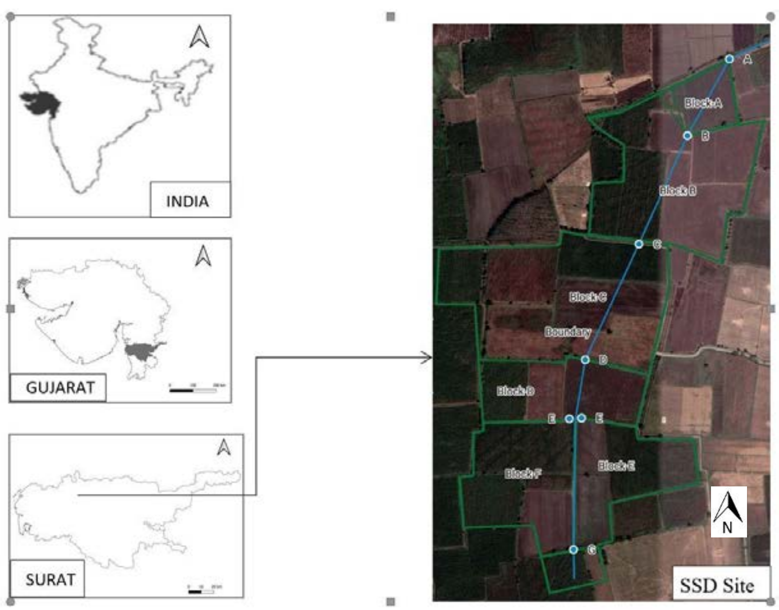

Fig. 1: Location map of Mulad SSD project, Gujarat

collected from seven sumps and were analysed for pH, EC, soluble cations and anions, SAR following standard procedure (Richards, 1954). The pH was estimated using an Analab digital pH meter (Model: Analab pHCal), with pH range of 0 to 14 and 0.01 pH resolution. This instrument was calibrated with 7.0 and 9.2 pH standard buffer solution with temperature range (0-100° C). The EC was estimated using a conductivity meter (Model: Systronics digital conductivity meter 304) with conductivity range of 0 µS to 200 mS, 1.0 cell constant, conductivity resolution of 0.1 µS and accuracy of ±1% with temperature range of 0-100° C. It was calibrated by 0.01 N KCl aqueous solution having conductivity of 1.412 mS at 25°C. Among soluble cations, Na and K were estimated using flame photometer (Model: Systronics Flame Photometer 128), which was a micro-controller based instruments with calibration of Na and K standards with low to high concentration mode (10 to 100 ppm) without dilution (inbuilt curve fitting software) having full scale sensitivity of 1.0 and 2.0 ppm, resolution of 0.01 and 0.02 ppm for sodium and potassium, respectively, and with accuracy range of ±1 to 2% (Low to high concentration mode). Among soluble anions, SO_4^{2-} was estimated with the help of a colorimeter (PG Instruments Ltd. made UV-VIS Spectrophotometer Model: T60V) at wave length of 420 nm with a blue filter. This instrument devising of 325 nm-1100 nm wave length range with wave length accuracy of ±2 nm (with automatic wavelength correction); having ±3% T (0-100% T) photometric accuracy and -0.3-3 Abs photometric range.

Saturated hydraulic conductivity of soils from five representative locations in the study area was estimated using Rossetta Lite v. 10 model (Schaap *et al*., 2001). This model used ANN technique based on per cent sand, silt and clay which were determined using International Pipette method (Piper, 1966) as input parameters. The mathematic expression of model is given below:

$$K(S_e) = K_0 S_e^L \left\{1 - \left[1 - S_e^{n/(n-1)}\right]^{1-1/n}\right\}^2 \quad \ldots(1)$$

Where,

S_e = Effective saturation,

K_0 = Fitted matching point at saturation, cm.d^{-1},

L = Empirical pore tortuosity parameter, and

n = Curve shape parameter.

The model results provided average values of seven hydraulic parameters viz. θ_S, θ_r, α, n, K_S, K_0 and L of different textural classes. The value of saturated hydraulic conductivity was estimated for actual textured condition.

The pre-drainage average sugarcane yield in the area varied from 32 t.ha^{-1} to 44 t.ha^{-1}. Water productivity of sugarcane crop was calculated by considering yield of sugarcane per unit quantity of irrigation water applied. For south Gujarat region, the required depth of irrigation water using flood irrigation for sugarcane crop was reported as 1.2 m (Savani *et al*., 2012), and the same value was used for calculation of water productivity in this study. In similar way, post drainage water productivity of sugarcane was calculated.

Design Parameters of SSD

Appropriate drain depth and spacing as per the soil hydraulic conditions were required for effective functioning of drainage system. In the present study, drain spacing was computed using the Hooghoudt equation (Hooghoudt, 1940) for the steady state flow condition. The Hooghoudt equation is written as:

$$L^2 = \frac{4\,K_s\,h\,(h + 2\,d)}{q} \quad \ldots(2)$$

Where,

L = Drain spacing, m,

K_s = Saturated hydraulic conductivity, m.d^{-1},

d = Depth of impervious layer from bottom of drain, m,

h = Hydraulic head above the drains, m, and

q = Drainage coefficient or drain discharge rate per unit surface area, m.d^{-1}.

The average of estimated saturated hydraulic conductivity i.e. 0.18 m.d^{-1} (Table 1) was taken for design of subsurface drainage system, and the impervious layer was at 6.8 m below the bottom of the drain. The hydraulic head above the drains and drainage coefficient were taken as 0.2 m and 2.0 mm d^{-1}, respectively. Sugarcane is a crop with high water requirement and hence drainage coefficient of 2 mm.d^{-1} was taken instead of 1.5 mm.d^{-1}. As water table was to be maintained at 1 m from the ground level on an average, design drain depth was adopted as 1.2 m. It was assumed that it would meet agronomic requirement of crop. The calculated drain spacing was 31.5 m, and therefore 30 m drain spacing was adopted in this study.

Table 1. Estimated saturated hydraulic conductivity using different particle sizes

Location	Sand, %	Silt, %	Clay, %	K_s, $m.d^{-1}$
1	16	20	64	0.179
2	18	16	66	0.161
3	12	24	64	0.202
4	20	18	62	0.167
5	22	20	58	0.175
			Average	0.177

Layout of SSD System

The layout diagram of SSD system is given in Fig. 2. The composite SSD layout system was adopted in the study as open drain was available at some distance from the SSD installation. As excess water from different fields was to be carried away to the open drain, laterals were laid in herringbone pattern to take the advantage of the available field slope. Total seven inspection chambers i.e. sumps (from A to G) were installed in series, and the water from lowest sump (sump A) was carried away through polyvinyl chloride (PVC) pipe of 0.25 m diameter and discharged into the open drain situated at a distance of 450 m. The 2.5-3.0 mm thick synthetic non-woven fabric type filter material, having 230 $g.m^{-2}$ weight and 75-150 micron opening size, was used as envelope material for laterals. The laterals were installed with an average slope of 0.05% to 0.1%, while collector was also installed at 0.06% to 0.16% slope.

Sugarcane Crop Yield and Economics

The pre-SSD and post-SSD yield data of sugarcane were collected from the individual farmers. There were thirteen farmers in the study area, and subsequently the yield of each block was calculated by taking average value of the yield from farmers representing that particular block.

Economic analysis of SSD was based on the collection of primary (yield data) and secondary (components for cost of cultivation, sugarcane price) data from different sources like farmers, panchayat office, sugarcane mill, etc. The primary data was collected from 13 farmer respondents of SSD project area through personal interviews following a comprehensive interview schedule with open and close ended questions. The data related to socio-economic status of farmers, farm inputs requirement and the yield of the major crops were also collected. The costs of all input and output parameters of crop production along with cost of SSD installation were combined to derive average representative values for estimation of benefit-cost ratio of SSD technology. In general, the SSD system

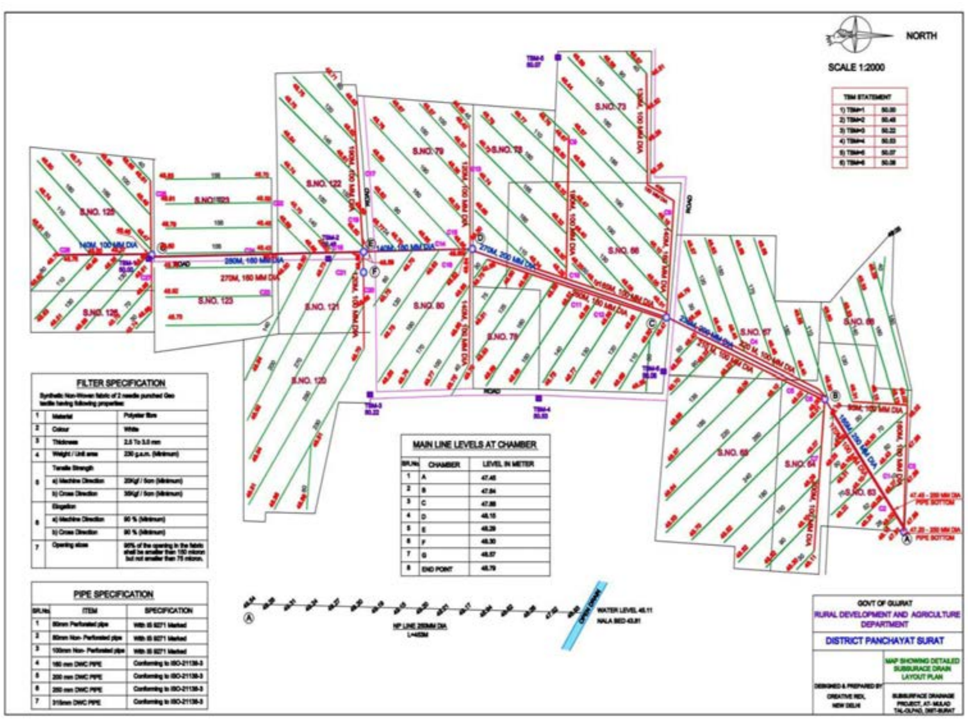

Fig. 2: Layout diagram of SSD system in study area

has an economic life of minimum 30 years (Bundela *et al*., 2017). However, for the safer side in Vertisols, the life of SSD system was considered as 25 years for converting total cost of SSD system into annual cost. The cost of sugarcane cultivation was estimated by taking into account the cost of different field operations like ploughing, harrowing, seed material, labour, irrigation, fertilisers and manure. The cost under all heads remained the same in the pre- and post-SSD situation, except the cost of manures, fertilizer, weedicides and labour.

RESULTS AND DISCUSSION

Performance Evaluation of Drainage System

Soil Salinity

During pre-SSD condition, it was observed that these soils had moderate salinity as EC_e values ranged from 1.2 dS.m^{-1} to 7.3 dS.m^{-1} with relatively higher salinity in surface layer (0-0.3 m) inhibiting optimum crop growth. Block A, C, E and F had EC_e greater than 4 dS.m^{-1} up to 0.9 m soil depth (Fig. 3), and were saline in nature. Remaining 3 blocks were also facing the problems of increasing levels of soil salinity. Soil pH_s ranged from 7.4 to 8.5, showing moderately alkaline nature of soils and SAR ranged from 1.2 to 26.2 (Fig. 3).

The changes in soil properties like EC_e and SAR of different soil layers in different blocks before and after SSD installation are depicted in Figs. 4 and 5, respectively, indicating the impact of the SSD on soil properties. The changes in ECe values in all blocks at 0-0.3, 0.3-0.6 and 0.6-0.9 m soil depths after installation of SSD system are shown in Fig. 4. Soil EC_e which was in the range of 1.2 to 7.3 dS.m^{-1} before installation of SSD decreased to a range of 0.47- 3.9 dS.m^{-1}. Furthermore, EC_e values of all the blocks, except block F, were reduced below 2 dS.m^{-1} which showed that soil became non-saline in the area after operation of the SSD. Block A witnessed more than 60% reduction in soil salinity across all the three soil depths. The highest EC reduction of 75% was observed in the top layer (0-0.3 m) of block C, whereas 67% and 54% reduction in soil ECe was observed in 0.3-0.6 m and 0.6-0.9 m soil layers, respectively. Moreover, some soil layers (0-0.3 m of block B, 0.3-0.6 m of block G, and 0.6-0.9 m of block F) which had low initial soil EC_e did not show any significant changes in EC_e. The reduction in soil salinity after SSD installation and operation was dependent on initial soil salinity and amount of irrigation water used for leaching salts.

There was slight decrease in the pHs value of all blocks, except some layers like in all 3 layers of block E, and 0.3-0.6 m layer of block F. This increase in pH value could be attributed to sharp decline in SAR because of high leaching of salts that can be seen in term of drastic reduction in EC values also.

The change in SAR values of different soil layers in all 7 blocks of the study area are shown in Fig. 5. It was observed that SAR values were less than 10 for all the blocks. The 0.3-0.6 m soil layers of blocks E and F, which had very high SAR values before installation of SSD, were drastically reduced from 26.2 and 18.1 to 5.0 and 4.1, respectively. Though there was increase in SAR values in blocks like E and F (0-0.3 m depth) and blocks like C and D (0.6-0.9 m depth), but the value was still less than 5. It might be due to redistribution of salts during leaching process.

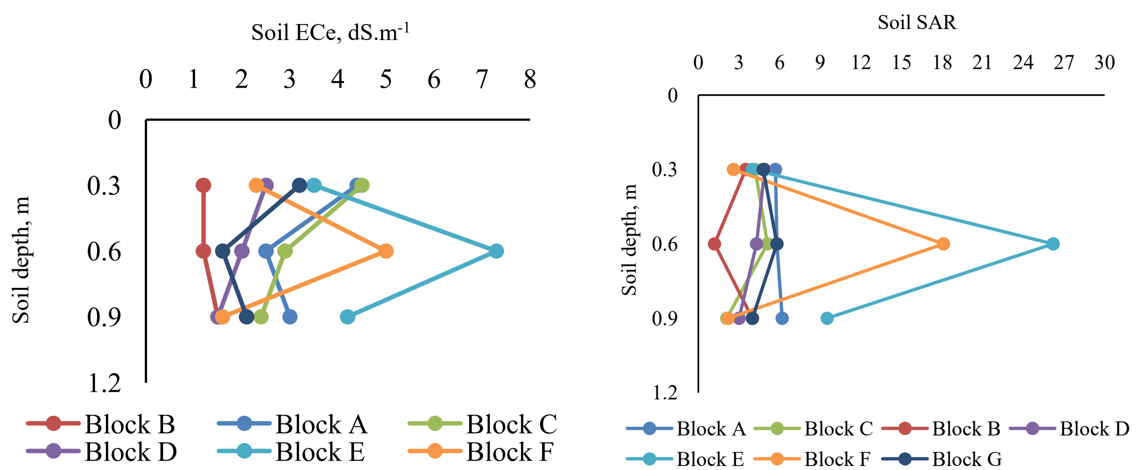

Fig. 3: Block-wise initial soil ECe and SAR values

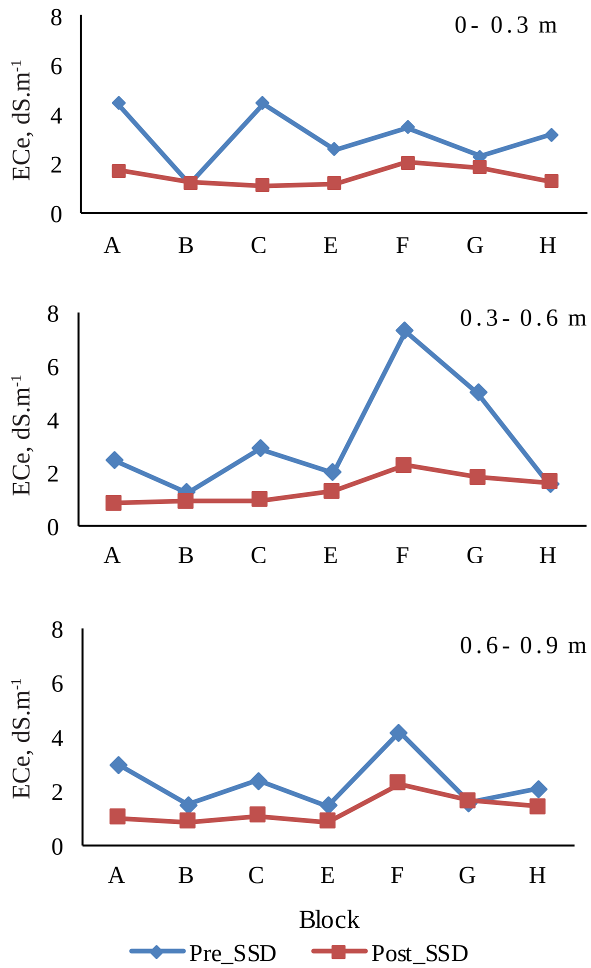

Fig. 4: Block-wise pre- and post-SSD changes in ECe values at different soil depths

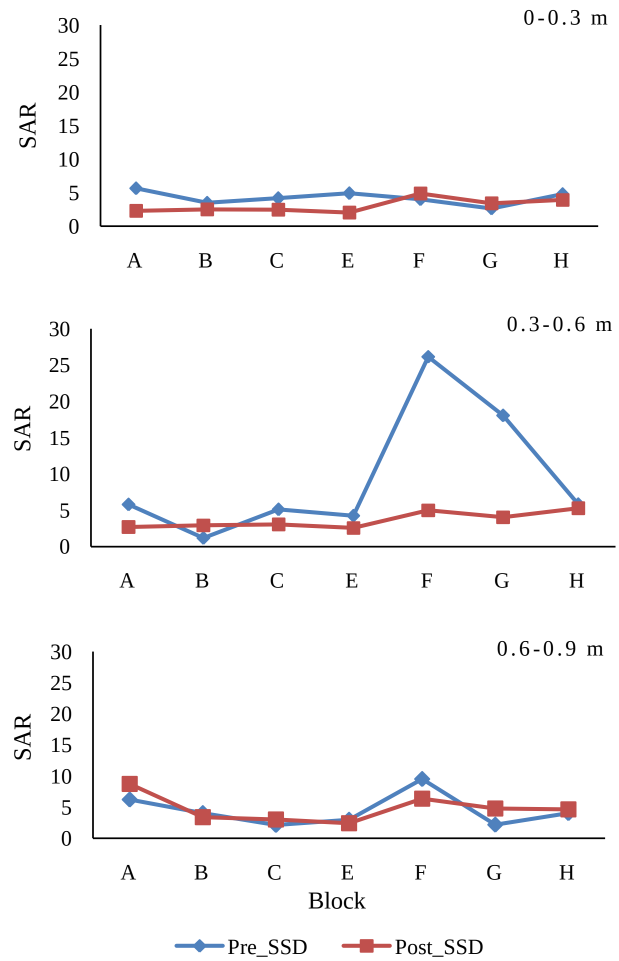

Fig. 5: Block-wise pre- and post-SSD changes in SAR values at different soil depths

The details of overall reduction in ECe, pHs and SAR of various soil layers are given in Table 2. The average soil EC_e was reduced by about 50%, whereas pHs showed marginal reduction up to 10% in all soil layers. There was reduction in average SAR up to 0.6 m soil depth while there was slight increase in SAR for 0.6-0.9 m soil layer. These properties thus indicated improvement in soil condition as compared to initial status of soils.

Groundwater Salinity and Waterlogging

Groundwater in the area was saline in nature with EC values varied from 1.4 to 4.9 $dS.m^{-1}$. The EC values were higher than the permissible limit of 2 $dS.m^{-1}$ for irrigation water in the study area. The pH of groundwater was within the normal range of 7.6 to 8.3 for the entire study area. But, SAR values (5.9 to 31.1) were more than the permissible limit of 10 in five blocks indicating tendency for creation of alkalinity/sodicity problems in soil with the use of groundwater for irrigation. The salinity and sodicity hazards with use of available water were expected to be much serious considering high clay content and smectite as the dominant clay mineral with high swell-shrink potential.

Analysis of water samples collected from all 7 sumps of drainage system revealed that electrical conductivity (EC) of drain water varied from 1.3 to 4.4 $dS.m^{-1}$ (Fig. 6), and was expected to reduce further below 2.0 $dS.m^{-1}$ with time. It was found that EC of water samples of all sumps, except sumps C and D, was reduced to less than 4 $dS.m^{-1}$ after SSD during May, 2018. Similar results were also reported by Raju *et al*. (2016). The EC values of water samples from the sumps, namely C and D, were relatively high because of ponding and subsequently evaporation of water. The post-SSD pH values of water from the sumps were slightly less. The

Table 2. Depth-wise average changes in different soil parameters

Sl. No.	Depth, m	Average ECe, dS.m^{-1}		Change in ECe, %	Average pH,		Change in pH, %	Average SAR,		Change in SAR, %
		Initial	Final		Initial	Final		Initial	Final	
1.	0-0.3	3.07	1.48	(-)51.9	7.99	7.24	(-)9.5	4.23	3.07	(-)27.5
2.	0.3-0.6	3.21	1.39	(-)56.6	7.92	7.41	(-)6.5	9.49	3.66	(-)61.4
3.	0.6-0.9	2.30	1.31	(-)43.2	8.10	7.48	(-)7.7	4.43	4.75	7.2

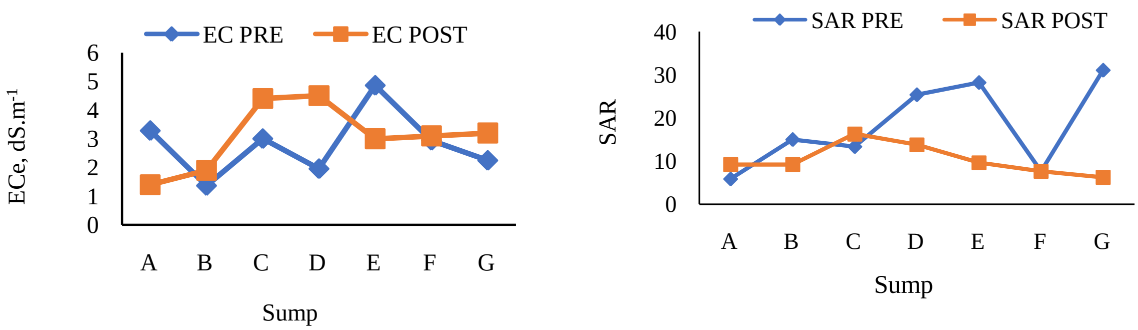

Fig. 6: Pre-SSD and post-SSD changes in EC and SAR of water of different sumps

SAR values were less than 10 for all sumps, except sump C and D. There was high reduction in the SAR values in case of sumps E and G.

The post-SSD analysis of the chemical composition of drainage water (Fig. 7) revealed that sodium was the dominant cation, which constituted about 62% to 78% of total cations followed by magnesium (19% to 30%), calcium (3% to 11%) and potassium (0% to 4%). In case of anions, chloride was dominant anion, which constituted about 44% to 70% of total anions followed by sulphur (11% to 28%), carbonates (6% to 22%) and bicarbonates (4% to 12%). The chemical composition of drainage water gave idea of chemical composition of soil solution, and it was useful in management of soils. The presence of carbonates and bicarbonates indicated that these soils will have tendency towards slight alkalinity development, and use of green manuring after certain time interval could be useful to maintain soil health and crop productivity.

The depth of water table and days required to subside the ponded water during peak rainy season were considered as indicators to judge the improvement in waterlogging conditions during post-SSD period. The waterlogging conditions reduced after installation of the SSD as depth to water table was 0.6 m from ground surface, indicating favourable environment for sugarcane crop. Most root biomass of sugarcane was found close to the surface, and then declined approximately exponentially with depth (Smith *et al.*, 2005). Typically, approximately 50% of the root biomass of sugarcane occurred in top 0.2 m of soils and 85% in the top 0.6 m (Blackburn, 1984). Moreover,

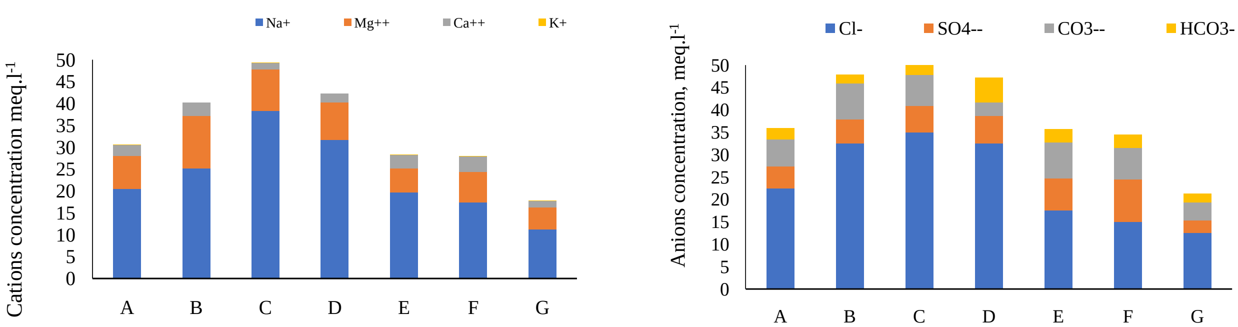

Fig. 7: Cation and anion composition of drain water in selected sumps after SSD

duration of surface ponding was reduced considerably to 6-8 days.

With improvement in drainage water quality with time, it could be easily used for irrigation purpose. Further, drainage water volume can be reduced drastically; if irrigation water use efficiency is improved in drainage area. However, techniques for improving water management including drip irrigation, controlled drainage, etc. are to be adopted after reclamation leaching is completed successfully. These measures would improve irrigation water productivity while reducing drainage volume further.

Improvement in Crop and Water Productivity

Yield and water productivity data of sugarcane before and after implementation of SSD are summarized in Table 3. It was observed that sugarcane yield increased from the range of 32 $t.ha^{-1}$ to 44 $t.ha^{-1}$ to the range of 88 $t.ha^{-1}$ to 107 $t.ha^{-1}$ in different blocks due to SSD installation. The results of crop yield were found in agreement with the findings of Gupta (2015) who observed 100% increase in yield at several places where SSD were installed in India. The water productivity of sugarcane crop ranged from 2.67 to 3.67 $kg.m^{-3}$, and 7.33 to 8.92 $kg.m^{-3}$ during pre- and post-SSD conditions, respectively. A significant increase in crop yield could be attributed to the direct positive effect of the SSD system in lowering the water table, and thereby improving root aeration, reducing soil salinity, creating favourable conditions for better availability of nutrients to plants as well as improving physical conditions of soil.

Economic Analysis

The combined expenditure on cost of cultivation of sugarcane and SSD cost was worked out as ₹ 78,270/- per ha and ₹ 91,076/- per ha in pre-and post- SSD scenarios, respectively, indicating 16.4% increase in average cost of crop cultivation after SSD installation. This increase in cost of cultivation might be due to increase in cost of manure, fertilizers, weedicide and labour with time. The corresponding increase in annual gross income (Table 4) was from ₹ 78,580/- per ha to ₹ 1,94,580/- per ha during post-SSD period, indicating 147.6% increase. The net income increased enormously from ₹ 310/- per ha to ₹ 1,03,504/- per ha due to SSD. The increase in gross and net income occurred largely due to increase in crop yield with intervention of SSD technology. The benefit-cost ratio in drainage project area increased from 1.00 during pre-SSD to 2.14 post-SSD, indicating 114% increase. The results of B: C ratio were in agreement with the findings of Raju *et al*. (2017), who observed

Table 3. Block-wise pre- and post-SSD yield and water productivity of sugarcane

Block	Sugarcane yield, $t.ha^{-1}$		Water productivity, $kg.m^{-3}$	
	Pre-SSD	Post-SSD	Pre-SSD	Post-SSD
A	40	88	3.33	7.33
B	38	91	3.17	7.58
C	32	98	2.67	8.17
D	41	96	3.42	8.00
E	39	103	3.25	8.58
F	44	98	3.67	8.17
G	41	107	3.42	8.92

Table 4. Economics of sugarcane cultivation during pre- and post-SSD

Sl. No.	Particular	Pre-SSD	Post- SSD
1.	Average yield, $t.ha^{-1}$	39.29	97.29
2	Gross income, ₹.ha^{-1}	78580	194580
3.	Cost of cultivation, ₹.ha^{-1}	78270	87698
4.	SSD implementation cost, ₹.$ha^{-1}.year^{-1}$	-	3378
5.	Net income, ₹.ha^{-1}	310	103504
6.	B:C (Benefit: Cost) ratio	1.00	2.14

up to 134% increase in B-C ratio for sugarcane crop in Maharashtra.

CONCLUSIONS

The inherent soil properties like very low hydraulic conductivity and narrow workable soil moisture range have always been considered as hurdles in getting potentially higher crop outcomes from highly fertile Vertisols. Injudicious use of irrigation water is creating problems of waterlogging and salinity. In present performance evaluation study, SSD system installed at Mulad village with 30 m drain spacing and average 1.2 m drain depth was found effective in ameliorating the waterlogged saline Vertisols in the area. The system resulted in reduction of soil salinity up to 0.9 m depth from initial levels of 1.2 -7.3 $dS.m^{-1}$ to 0.47 - 3.90 $dS.m^{-1}$ during the year 2018, and soils of the entire project area had become non-saline. Moreover, the waterlogging situation in the area was reduced with lowering of water table beyond crop root zone, and considerable reduction in duration of water ponding during peak rainy season. The technology was also economically viable as farmers' income increased appreciably, with benefit-cost ratio increasing from 1.00 to 2.14. The results suggest that large-scale implementation of SSD projects for reclamation of waterlogged saline Vertisols in canal irrigated areas of Gujarat could be undertaken through establishment of appropriate nodal agency. Nonetheless, for large-scale projects, proper removal and disposal of high volume of generated drainage water from SSD system also needs due consideration in environment-friendly way.

REFERENCES

Anon. 1988. Handbook for Drainage of Irrigated Areas in India. Irrigation Management and Training Project: Technical Report No. 5. LBII/WAPCOS, Room 213, Ansal Chambers, Bhikaji Cama Place, New Delhi, pp: 12.3, 12.5.

Anon. 2009. Assessment of Waterlogging and Salt and/or Alkaline Affected Soils in the Commands of All Major and Medium Irrigation Projects in the Country using Satellite Remote Sensing. Indian Space Research Organisation, pp: 21.

Blackburn F. 1984. Sugarcane. Longman, New York, pp: 414.ISBN: 0- 582-46028-X.

Bundela D S; Kaledhonkar M J; Gupta S K; Lal M; Kamra S K; Sharma D K; Sharma P C; Chaudhari S K. 2016. Cost estimation of subsurface drainage systems for reclamation of waterlogged saline lands. J. Soil Salinity Water Qual., 8, 131-143.

Bundela D S; Kaledhonkar M J; Gupta S K; Kamra S K; Sharma D K; Sharma P C; Chaudhari S K. 2017. Guidelines and Costs of Sub-surface Drainage Technology for Large Scale Reclamation of Waterlogged Saline Soils. Technical Folder, ICAR-Central Soil Salinity Research Institute, Karnal, pp:1-8.

Gupta S K. 2015. Reclamation and management of waterlogged saline soils. Agric. Res. J., 52, 104-115.

Hooghoudt S B. 1940. General consideration of the problem of field drainage by parallel drains, ditches, watercourses, and channels. In: Series Contribution to the Knowledge of Some Physical Parameters of the Soil (titles translated from Dutch), Bodemkundig Institute, Groningen, The Netherlands, Publ. No.7.

Kaledhonkar M J; Gupta S K; Singh G. 2009. An overview of research, development, opportunities and challenges for subsurface drainage in India. In Proc.: 60th International Executive Council Meeting and 5th Asian Regional Conference, New Delhi, India, 1-12.

Kamra S K; Sharma D K. 2016. Critical evaluation of performance and organizational framework of subsurface drainage projects in Haryana and Maharashtra. Water Energy Int., 64-72.

Piper C S. 1966. Soil and Plant Analysis. Hans Publishing House, Bombay, India, 47-79.

Raju R; Thimmappa K; Kumar P; Kumar S; Tripathi R S. 2016. Impact analysis of reclamation of waterlogged saline soils through subsurface drainage technology in Haryana. J. Soil Salinity Water Qual., 8 (2), 194-201.

Raju R; Thimmappa K; Pathan A L; Siddayya. 2017. Saline soil reclamation through subsurface drainage in Karnataka - An economic impact analysis. Farm Sci., 30, 74-78.

Rao K V G K; Singh O P; Gupta R K; Kamra S K; Pandey R S; Kumbhare P S; Abrol I P. 1986. Drainage Investigations for Salinity Control in Haryana. CSSRI, Karnal, India, Bull. No. 10, pp: 95.

Rao K V R; Kishore R; Singh R. 2009. Mole drainage to enhance soybean production in waterlogged Vertisols. J. Agric. Eng., 46, 54-58.

Rathod S D; Dahiwalkar S D; Gorantiwar S D. 2020. Evaluating effect of subsurface drain spacing and depth on hydrological properties of waterlogged Vertisols in Sangli, Maharashtra. J. Agric. Eng., 57(1), 73-83.

Richards L A. 1954. Diagnosis and Improvement of Saline and Alkali Soils. U. S. Department of Agriculture Handbook, Washington D. C., USA, Vol. 60, pp: 160.

Ritzema H P; Satyanarayana T V; Raman S; Boonstra J. 2008. Subsurface drainage to combat waterlogging and salinity in irrigated lands in India: Lessons learned in farmers' fields. Agric. Water Manage., 95, 179-189.

Ritzema H P. 2016. Drain for Gain: Managing salinity in irrigated lands - A review. Agric. Water Manage., 176, 18-28.

Sanghera G S; Jamwal N S. 2019. Perspective for genetic amelioration of sugarcane towards water logged conditions. Int. J. Pure Appl. Biosci., 7 (3), 484-502.

Savani N G; Patel R B; Solia B M; Naik V R; Patel K Bioscan; Patel J M; Patil R G. 2012. Water Management Technologies - A Compilation. SWMRU, GAU, Navsari (Gujrat), SWMP Pub. 24, pp: 61.

Schaap M G; Leij F J; Van Genuchten M T. 2001. A computer program for estimating soil hydraulic parameters with hierarchical pedotransfer functions. J. Hydrol., 251,163-176.

Sharma P C; Kaledhonkar M J; Timmappa K; Chaudhari S K. 2016. Reclamation of Waterlogged Saline Soils through Subsurface Drainage Technology. ICAR-Central Soil Salinity Research Institute, Karnal, ICAR-CSSRI/Karnal/Technology Folder/ 2016/ 02,1-4.

Singh A. 2019. An Overview of drainage and salinization problems of irrigated lands. Irrig. Drain., 68, 551-558.

Smith D M; Inman-Bambera N G; Thorburn P J. 2005. Growth and function of the sugarcane root system. Field Crops Res., 92, 169-183.

Tiwari P; Goel A. 2015. An overview of impact of subsurface drainage project studies on salinity management in developing countries. Appl. Water Sci., 7 (2), 569-580.

Valipour M. 2014. Drainage, waterlogging, and salinity. Arch. Agro. Soil Sci., 60, 1625-1640.

Vibhute S D; Sarangi A; Singh D K. 2016. Development of crop water demand based water delivery schedule for a canal command. J. Agric. Eng., 53(2), 12-23.

http://www.isae.in / journal_jae.aspx

Journal of Agricultural Engineering

Vol. 57 (3): July-September, 2020

Suppressing Evaporation from Surface Water Reservoirs: A Review

S. Deepika[1*], M. Osman[2], Manoranjan Kumar[3] and H. Sandeep[4]

[1]Research Fellow (Soil and Water Conservation Engineering),[2]Principal Scientist (Agronomy), [3]Principal Scientist (Soil and Water Conservation Engineering), [4]Research Fellow (Water Resources Engineering), ICAR- Central Research Institute for Dryland Agriculture, Santoshnagar, Hyderabad, Telangana. Corresponding author email address: patideepika@gmail.com

Article Info

Manuscript received:
July, 2019
Revised manuscript accepted:
June, 2020

Keywords: Evaporation control techniques, mechanical shields, wind break, floating solar panels

ABSTRACT

The availability of water for agriculture is declining due to competing demands from other sectors, mainly industry and human need. Water conservation and harvesting is the only solution to overcome the vagaries of monsoon in the Indian sub-continent. The precious blue water needs to be converted into green water without loosing through seepage and evaporation. Seepage is beneficial as it recharges groundwater. Evaporation although improves micro-climate, needs to be controlled. The review highlights various physical, chemical, biological or the combination of methods undertaken to control the evaporation in India. Monolayer like cetyl and stearyl alcohol alone, or in combination of both, reported to control evaporation up to 30 % and 57 %, respectively. Biological measures using agricultural waste are cost-effective and reported to reduce evaporation up to 60 % with palm fronds. Mechanical measures like floating type solar panels, though expensive, are useful with multiple benefits. Mechanical shields like suspended shade cloth, thermocol, styrofoam and floating wax studied by various researchers reportedly control evaporation ranging between 25 % and 70 per cent. Bubble plume technique indicated varied reduction in evaporation with depth of water storage structure from 15- 25 per cent. From the extensive review, it could be concluded that floating/fixed type solar panels, depending on the type of water body, are the most effective and may be subsidised to increase it' adoption.

World food requirement is expected to rise by 35 % as the 7.8 billion population is projected to increase to 9 billions by 2050, which alternatively will require more water to meet the food demand of the growing population (Benke and Tomkins, 2018). India accounts 18 % of world population but only 4 % of world water resources. Therefore, water harvesting is one of the avenues to meet the demand for water, but control of seepage and evaporation are the major bottlenecks. Moreover, with increase in temperature under projected climate change scenarios, the evaporation / evapotranspiration demand is projected to increase. Many studies on temperature trend concluded that on an average the temperature has increased by 0.7^{o} C to 0.9^{o} C per decade up to 1975, while after 1975 the rate got doubled to 1.5 ^{o} C to 1.8^{o} C per decade (Arora, 2005; Cowtan and Way, 2014; Reiter and Weidinger, 2016; Radhakrishnan *et al*., 2017; Kumar *et al*., 2018). There are numerous studies that show 50 - 75 % of total precipitation goes back to atmosphere through evaporation, which is loss of blue water and can be converted to green water through transpiration (Sovocool *et al*., 2014; Zhao and Gao, 2019). Weekly estimations of Central Water Commission (CWC), India, show that India is harvesting 6 % of annual rainfall (253 billion cubic metre) from which 150-300 cm.km^{-2}.annum^{-1} is lost due to evaporation. A huge fraction of harvested water is lost from storage structures through evaporation that needs to be controlled (Shaw, 1988).

The primary source of energy for evaporation is solar radiation. The process of diffusion of water molecules forming water vapour that rises up and forms clouds, thus, evaporation is the process of converting liquid to vapour. Though this is a part of hydrological process, it is termed as wastage when the precious harvested water is not made use for productive purposes like life-saving irrigation at critical stage of crop growth, drinking water, etc. The major factors affecting the evaporation are temperature, vapour pressure, wind velocity, humidity and surface area; and thus interventions need to modify them suitably to reduce evaporation. Moreover, quality of water also influences rate of evaporation as pure water will evaporate easily than saline water.

Evaporation issue can be dealt at two stages, which is prior to execution and for the existing structures. Measures can be advised at the time of planning like water surface area or depth of the pond as rate of evaporation increases with exposed surface area. These measures can be grouped as physical, mechanical, biological and chemical methods. Numerous region-specific experiments based on Dalton's model were conducted to quantify the amount of water evaporated from the water bodies due to wind, temperature, radiation, mass transfer, pan coefficient and energy budget methods (Hamblin *et al.*, 2002; McJannet *et al.*, 2012; Hassan, 2013; Li and Zhao, 2018). Estimation of evaporation is made possible in combination of remote sensing and energy balance to monitor instantaneous and accurate loss of water to overcome the uncertainties. Impact on the rate of evaporation per unit surface area from the pond is much higher than that from the reservoir due to variability in radiation, vapour pressure as reported in many studies (Harbeck, 1962; Gokbulak and Ozhan, 2006; Althoff *et al.*, 2019). The primary focus of the present review is to highlight the factors affecting the evaporation of water from water bodies and suitable measures to control them.

Methods Used for Suppressing Evaporation

Plethora of models shown in Table 1, developed during early 19th century were evolved by following the simple prototype like mechanical or chemical barrier to evaporation. Also, various researchers have reviewed publications dealing with evaporation reduction techniques at global level (Magin and Randall, 1962; Frenkiel, 1965; Craig *et al.*, 2007; Youssef and Khodzinskaya, 2019). The different evaporation suppression techniques are summarized in Fig. 1. Wind velocity more than 1 m.s^{-1} will affect the rate of evaporation depending on the storage structure capacity.

Table 1. Techniques to control evaporation by various methods

Sl.No.	Type of measure	Model
1.	Physical measure	Wind breakers, mechanical covers, solar shades, thatch material, shade net, foamed rubber
2.	Biological measure	Azolla cover, algae and creepers
3.	Chemical measure	Application of mono molecular layer, cetyl alcohol, stearyl alcohol, neem oil, silicon oil.

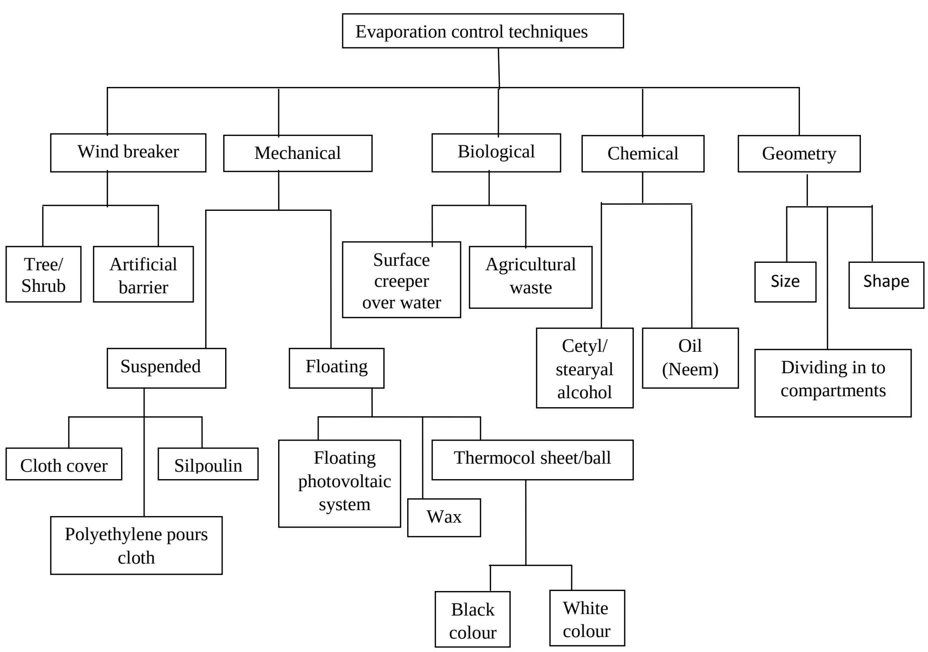

Fig. 1: Different methods of evaporation suppression

Evaporation retardants like chemical application can be adopted where wind velocities ranging between 1 $m.s^{-1}$ and 3 $m.s^{-1}$ and requires barriers. Mechanical shields like solar panels are feasible for the regions with wind speed more than 5 $m.s^{-1}$.

Wind breaks/shelter belts

Evaporation of water from storage is due to wind speed and humidity gradient which can be regulated by wind breaks to obstruct air flow and humidify the dry air flowing towards water storage and thus, reducing the rate of evaporation. Impact of wind breaks is variable and it is affected by height, density and number of tree rows as well as selection and composition of tree or shrub species. Figure 2 shows the quiet and wake zones of wind break. Ganguly and Kaul (1969) reported region-specific list of vegetation, which is set out in Table 2, for different regions of the country. Central Water Commission, India, recommended the spacing of perennials used for wind breaks having different types of canopy as shown in Table 3 (CWC, 2006). Numerous studies reported effectiveness of shelter belts in control of evaporation through reduction in wind speed by 40-50 % by changing plant spacing, orientation and width of shelter belt (Wang *et al.,* 2001; Cleugh *et al.,* 2002; Brandle *et al.,* 2004; Monfared *et al.,* 2019).

Skidmore and Hagen (1970) measured evaporation using atmometer and reported reduction in evaporation at various distances on leeward side of wind breaks, which ranged from 92 % to 40 % starting from the barrier to a distance of 12 times of tree height. Similar work has been reported by other researchers (Lomas and Schlesinger, 1971; Heisler and Dewalle, 1988; Condie and Webster, 1995; Messing *et al.,* 1998). Further, Bardsley and Vetrova (2019) reported statistical approach for sites where eddy correlation time series are available instead of linear models like Penman-Monteith equation for designing the wind breaks relative to net radiation flux.

Mechanical shields

Harvested water can be protected against evaporation losses using shade cover, floating material, etc., and the same materials are being used in different parts of the world (Table 4, Fig. 3). However, still research is being piloted to evaluate the region-specific best intervention for controlling evaporation. Polystyrene foam and plastic water bottles could control evaporation up to 50 % (Takahashi *et al.,* 2012; Simon *et al.,* 2014; Dhirajlal, 2017). Similarly, porous shade cover has also proven to be effective in evaporation reduction (Craig *et al.,* 2005; Martinez-Alvarez *et al.,* 2006; Martinez-Alvarez *et al.,* 2010). Craig *et al.* (2005) worked in Australia with suspended shade caps and reported 87 % reduction in evaporation from water reservoir having 3 m depth, whereas Martinez-Alvarez *et al.* (2010) reported 85 % reduction from 5 m deep reservoir located in south-eastern Spain. Crow (1973) conducted experiment with partially-covered (48 %) painted and unpainted styro-foam and reported 35 % and 49 % reduction in evaporation, respectively. Chaudhari and Chaudhari (2015) reported 32 % reduction in evaporation with floating thermocol. Yao *et al.* (2010) had reviewed the suspended and floating covers available for evaporation reduction like Aqua cap/Aqua Armour floating modules and reported reduction in evaporation up to 88 % (Burston, 2002; Coop, 2011).

Renewable source of energy is also being extensively used in agriculture sector like solar panel for power generation, drying of agricultural produce, etc. Farm ponds can be covered to suppress evaporation with either floating or fixed solar panels, and the renewable power generated can be used to operate electric pump. Marco Rosa-Clot *et al.* (2017) and Taboada *et al.* (2017) worked in South America and Australia, respectively,

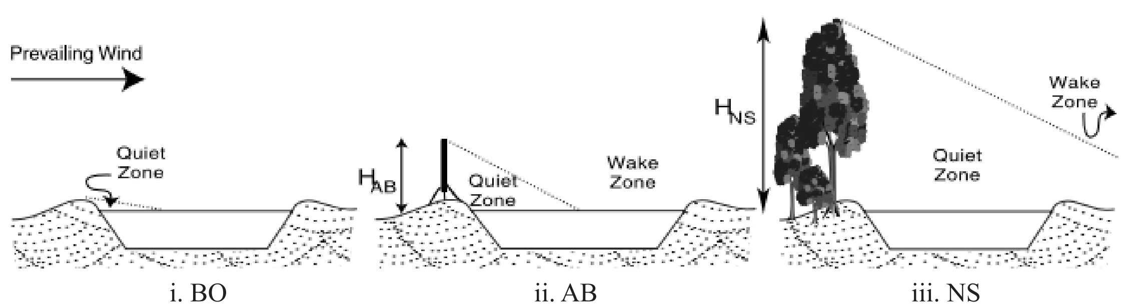

Fig. 2: Windbreak system i) bank only (BO), ii) artificial barrier (AB), and iii) natural shelter (NS)

Source: Hipsey and Sivapalan, 2003

Table 2. Wind breaks suitable for different climatic regions of India

Region	Trees and Shrubs	Small tree	Grass
Northern Region	Babool (*Acacia nilotica*), Kala siris (*Albizialebbeck*), Shisham (*Dalbergia sissoo*), Jamun (*Syzygiucumini*), Farash or Jhau (*Tamarixaphylla*)	Bouli (*A. jacquemontii*), Vilayatikeekar (*Parkinsonia aculeata*)	Munj (*Saccharum bengnalenis*)
Central Region	Babool (*Acacia nilotica*), Khair (*A. Catechu*), Grit kumari (*Agave sislana*), Salai (*Boswellia serrata*), Siamea (*Cassia siamea*), Sitsal (*Dalbergialatifolia*), Anjan (*Hardwickiabinata*), Bakain (*Melia azadirachta*), Ratanjyoti (*Jatropha curcas*), Karanj (*Pongamiapinnata*)	Madre (*Gliricidamaculata*), Ipil-ipil (*Leucaena leucocephola*), Jangal jalebi (*Pithecellobium dulce*), Basna (*Sesbania grandiflora*), Arandi (*Ricinus communis*)	
Southern Region	Babool (*Acacia nilotica*), Wattle (*A. auriculiformis*), Blackwattle (*A. decurrens*), Grit kumari (*Agave sp.*), Kolamavu (*Anacardium occidentale*), Magei (*Albizialebbeck*), Mungli (*Bambusasp*), Panei (*Borassusflabellifer*), Chauku (*Casuarina equisitifolia*), Mulumoduyu (*Erythrina sp.*), Eucalyptus (*Eucalyptus sp.*), Neempalm (*Jatropha curcas*), Chittikatti (*Sesbania sesban*), Jayanti (*S. bispinosa*), Lashtia (*Telphrosia candida*)	Silveroak (*Grevillea robusta*)	
	Kantala (*Agave sislana*), Kaju (*Anacardium occidentale*), Kathal (*Artoarphusheterophyllus*), Gabanal (*Arundo donax*), Tal (*Borassusflabellifer*), Jangulisaru (*Casuarina equisetifolia*), Narial (*Cocos-nucifera*), Shisham (*Dalbergia sissoo*), Jhingal (*Lanneacaromandelica*), Lashtia (*Tephrosia candida*), Nirgandi (*Vitex negundo*)	Kela (*Musa paradisiaca*), Jamun (*Syzygiumcumini*)	Bans (*Bambusasp*), Ulu (*Imperatacylindrica*),
Eastern Region	Sonejhur (*Acacia auricuiformes*), Kaju (*Anacardium occidentale*), Tar (*Borassusflabellifer*), Janglisaru (*Casuarina equisitifolia*), Narial (*Cocos nucifera*), Gulmohar (*Delonixelata*), Politamandas (*Erythrina indica*), Sehund (*Buphurbiatirucalli*), Gad gubar (*Bicusspp*), Sivanimba (*Indiqoferaaspalathoides*), Natilata (*Ipomoea biloba*), Karanj (*Pongamiapinnata*), Vilayatibabool (*Prosopis juliflora*), Farash (*Tamarixaphyila*), Paras pipal (*Thespsiapopulnea*)		Rawanmoonch (*Inifexlittorcus*)
Arid-Region	Babool (*Acacia nilotica*), Reonja (*A.lucophloea*), Gogughtumba (*A.planifrons*), Kummet (*A. Senegal*), Israeli babool (*A. tortilis*), Phog (*Calligonurnpolygonoides*), Kair (*Capparis decidua*), Arni (*Clerodendrumphlomoides*), Eucalyptus (*Eucalyptus camaldulensis*), Thor (*Euphoribiacaducifolia*), Farash (*Tamarixaphyilla*), Jharber (*Zizyphusnummularia*)	Hingot (*Balanites aegyptiaca*),	Munj (*Saccharum munja*), Sewam (*Lasiurus sindicus*), Murat (*Panicum turgidum*),

Note: T = Tree, ST = Small Tree, S = Shrub, G = Grass
Source:Ganguly and Kaul (1969)

Table 3. Recommended spacing of trees planted as wind breaks

Sl. No.	Vegetative barrier	Spacing
1.	Shrub	0.6 to 1.0 m
2.	Medium height broad leaved tree	1.5 to 2.0 m
3.	Medium to tall evergreen tree	2.1 to 2.4 m
4.	Tall broad leaved trees with conical crown	2.4 to 3.0 m

Source: CWC (2006)

with floating photovoltaic systems and reported 90 % reduction in evaporation with additional saving of farm land. Decrease in water level in small water harvesting ponds could be a problem that can be overcome by adopting anchored (bottom/side) or piled (at bottom) solar panel system (Mohit and Sarvesh, 2019). Piled solar panel system with vertical axis will cost more, but can be compensated thorough efficient utilization of generated power. Research should be taken up for enabling dual axis tracking even under floating system by tracking the sun to generate additional power.

Biological measures

Increasing the efficiency of harvested rainwater by minimizing the losses is the need of the hour. Biological measures show reasonably good results with minimal investment. The results of studies that focused on evaluation of cost-effective evaporation suppressants utilizing locally available biological materials are shown in Table 5 and Fig. 4. Pre-disposed palm leaves that are capable of withstanding high heat load were used for covering the exposed area in Saudi Arabia showed that control of evaporation was directly proportional to area concealed (Al-Juruf *et al.*, 1988; Al Hassoun, 2011). Similarly, Alam and Al-Shaikh (2013) reported that the double-layered cover with palm fronds could reduce the evaporation by 58 % and 47 % with single layer in comparison to open pan evaporation.

In north-eastern India, which experiences heavy rainfall during monsoon and water scarcity during post-monsoon, *Jalkund* (a small reservoir of 30 - 60 m^3 volume) was introduced to meet the demand by arresting seepage and evaporation losses of harvested water by lining the *kund* and using evaporation control techniques. Shah *et al.* (2007) experimented and reported that locally available bamboo thatch covered with grass (50 - 80 mm thick) and neem oil application

Table 4. Mechanical shields for evaporation suppression

Sl.No.	Model	Observation	Source
1.	Floating Photovoltaic system	Dual purpose structure for production of energy and evaporation control due to coverage.	Taboada *et al. (*2017); Marco Rosa-Clot *et al. (*2017)
2.	Polystyrene foam (Thermocol); Bamboo; Drinking water bottles; Duckweed.	Evaporation reduction was 38, 25, 33 and 9% with Polystyrene foam, bamboo, drinking water bottles and duckweed respectively.	Daigo and Phaovattana (1999); Takahashi *et al.* (2012); Chaudhari and Chaudhari (2015); Dhirajlal (2017)
3.	Double black polyethylene porous cloth	Impermeable to solar radiation, wind and permeable to rain water	Martinez-Alvarez *et al. (*2010)
4.	Suspended Shadecloth cover	Evaporation reduction reported up to 80 % relative to uncovered water storage reservoir	Burston and Akbarzade (1995); Hunter *et al.(*2007); Yao *et al.* (2010); Maestre-Valero *et al.* (2011); Gallego-Elvira *et al.* (2011); Aminzadeh *et al.* (2018).
5.	Styrofoam	Partially covered pond reduced evaporation ranging from 35 to 49 % under unpainted and white painted conditions	Crow (1973); Assouline *et al.* (2010); Assouline *et al.* (2011).
6.	Floating wax	Reported that the efficiencies ranged from 23-79% in evaporation reduction tested under different temperatures	Cooley and Mayer (1973); NAS (1974)
7.	Parasol type float (Polypropylene)	Designed a protective float with more than 0.5 m height to avoid overlap long term durability	Segal and Burstin (2010)
8.	Floating spheres and disks	With 91% surface cover evaporation reduction reported 80 and 70% with disks and spheres, respectively	Lehmann *et al. (*2019)

Suspended permeable (shade cloth) covers
(*Source:* Hunter *et al.*, 2007)

Shade balls
(*Source:* Dhirajlal, 2017)

Aquacaps
(*Source:* Burston, 2002)

Covered with empty bottles
(*Source:* Simon *et al.*, 2014)

Stingray technology

Floaters design

Single axis based floating solar PV plate in Suvereto, Italy

Floating type solar panels for evaporation control
(*Source:* Mohit and Sarvesh, 2019)

Fig. 3: Mechanical barriers to control evaporation from pond

Table 5. Biological measures for evaporation suppression

Sl.No.	Model	Country (Location)	Observation	Source
1.	Duckweed (small and gaint), Azolla, Waterlilly, Water lotus and Water Hyacinth	Thailand	Evaporation reduction ranged from 9 to 15 % except with water lotus and water hyacinth resulted in loss due to evapotranspiration	Daigo and Phaovattana (1999)
2.	Maize cob	Rajasthan, India	Reported 15 % evaporation reduction	Dhirajlal (2017)
3.	Palm leaves	Saudi Arabia	Fully covered and partially covered water surface reported 63 and 26 % reduction in evaporation, respectively	AlHassoun *et al.* (2011)
4.	Palm fronds	Saudi Arabia	Single layered and double layered cover showed 47 and 58 % respectively in comparison to open pan	Alam and AlShaikh (2013)
5.	Bamboo thatch and neem oil spreading	North East India	Thatch made of bamboo and grass with neem oil as surface applicant on water	Shah *et al.* (2007); Das *et al.* (2017); Singh and Athokpam (2018)

Azolla spread over Esanai lake of Perambaluru district, Tamil Nadu	Rings and azollain place, 31 days after planting at RMIT, Melbourn	Pan covered with palm fronds - Saudi Arabia

Fig. 4: Biological barriers to control evaporation at different locations

at a rate of 10 ml.m^{-2} reduced evaporation by 80 % and 43 %, respectively, in comparison to control (uncovered). Similar studies are reported by Das *et al.* (2017) in north-eastern India and by Singh and Athokpam (2018) in Manipur. Although agricultural waste is the cheapest source for reducing evaporation in experiments conducted at Plasticulture Farm of College of Technology and Engineering, Udaipur, Rajasthan, maize cob could reduce evaporation by 15 % only compared to control (uncovered) (Dhirajlal, 2017).

Similarly, few studies were conducted with azolla and surface creepers. Azolla is experimentally proven for providing habitat for living organisms and aquatic life and the harvested water can be used for irrigation purpose while azolla is also used as fertilizer and feed for livestock. Few studies reported that azolla used for evaporation control is not effective as the transpiration rate increased (Burston and Akbarzade, 1995). However, completely covered water body with plastic cover or shade-net may result in decrease in dissolved oxygen content. Hence, it can be opted only where the poultry/livestock is the secondary source of income in addition to agriculture.

Chemical method

Certain polar (vegetable oil) and non-polar (cetyl alcohol) substances can also be used as surface layer to control evaporation. Chemicals which attract molecules as diffusion barriers formed by long-chain fatty alcohol like, cetyl alcohol (hexadecanol), stearyl alcohol (octadecanol) and palmitic acid (hexadecanoic acid) having melting point of 49°C, 58°C and 63°C, respectively, are available in powder form (Archer and La Mer 1955). The chemical when applied over water surface form an interface barrier by preventing the escape of water vapour few of such studies are reported in Table 6. The application of monolayer like cetyl and stearyl alcohol ranging from 0.3 kg.ha^{-1}.day^{-1} to 0.5 kg.ha^{-1}.day^{-1} resists evaporation by 16 - 30 %, respectively (McJannet, 2008a; Saggai *et al.*, 2018). This method of evaporation control will not interfere with other operations like boating, fishing, etc. (Panjabi *et al.*, 2016). Reports show that it requires re-application

Table 6. Chemical applicators and combination of chemical and mechanical obstruction for evaporation suppression

Sl. No.	Country (Location)	Chemical treatment	Observation	Source
1.	Aurangabad, India	Cetyl and stearyl alcohol	Cetyl and stearyl alcohol applied individually could reduce evaporation 27 % with each and 30 % evaporation reduction observed when both applied in combination	Kahalekar and Kumawat (2013)
2.	Aji reservoir, Rajkot, Gujarat, India	Mixture of cetyl and stearyl alcohol	19.3 % evaporation reduction with of cetyl and stearyl mixture.	Panjabi *et al.* (2016)
3.	Brazil	Mixture of cetyl and stearyl alcohol	Cetyl and stearyl alcohol mixture in 1:9 and 2:8 proportions retarded 57 and 46 %, respectively	Gugliotti *et al.* (2005)
4.	Australia	Cetyl and stearyl alcohol	Application of 0.35 kg/ha/day retarded evaporation up 30 %	McJannet, (2008a); Saggai and Bachi (2018)

within three days as the wind and wave action can break down the layer of chemical (Boon and Dowing, 1957; Chang *et al.,* 1962; Reiser, 1969; Drummond *et al.,* 1992; Barnes, 2008). Instead of applying the chemical intuitively after every three days, Brink *et al.* (2011) developed an automated model to analyse the application demand, thickness of application and dosage corresponding to the on-site environmental conditions like the evaporation demand, wind direction, water temperature and rainfall (Hancock *et al.,* 2011). Further, to overcome the impact of wind on efficiency of chemical applicator the combination of chemical and mechanical barriers could resist the wind velocity and increased the re-application period (Manges and Crow, 1965; Gallego-Elvira *et al.,* 2010). Mozafari *et al*. (2019) conducted experiment on effect of wind speed on evaporation suppression over monolayer at Tehran, Iran, and found that by increasing the wind speed from 0 $m.s^{-1}$to 9 $m.s^{-1}$ decreased the efficiency of monolayer from 60 % to 13 per cent. Region-specific effective combination of windbreak and monolayers as an evapo-retardant needs further research.

Combination of cetyl and stearyl alcohol is proven to be more stable evaporation retardant than application of single at a time (McArthur and Durham, 1957; Gugliotti *et al.,* 2005; Yan *et al.,* 2009; Kahalekar and Kumawat, 2013; Panjabi *et al.,* 2016). Gugliotti *et al.,* (2005) experimented with the water collected in Petri dishes from the reservoirs of Guarapiranga and Billings at Sao Paulo, Brazil, by applying a mixed film of cetyl and stearyl alcohol in 1:9 and 2:8 proportion and reported 57 % and 46 % reduction in evaporation, respectively.

Pond Geometry

Studies indicated that evaporation is positively correlated with wind direction, maximum and minimum temperatures, wind speed and sunshine hours, whereas it is negatively correlated with relative humidity (Dhirajlal, 2017). More water is evaporated when more water surface area is exposed, therefore, without altering the storage capacity, depth of the pond can be increased. McJannet *et al.,* (2008) studied effect of pond surface area on heat storage and developed an equation for heat modification by adjusting storage area.

Along with the effect of temperature and wind, surface area exposed to air plays an imperative role on amount of water getting evaporated (Harbeck, 1962; Bradley, 1968; Condie and Webster, 1997). Studies related to shape and depth of pond conducted by Daigo and Phaovattana (1999) reported that round-shaped ponds with steep slopes better controlled evaporation in comparison to rectangular-shaped ponds. Evaporation of freshwater is dependent on the depth of storage structure and wind velocity, especially in semi-arid regions (Larry *et al.,* 2007). Various models have been worked out as the evaporation is inversely proportional to depth of the storage structure. Depth affects the energy storage of the water body due to different thermal characteristics as the transmission of solar radiation decreases (or slows the rate of transmission) with the increase in the depth of water, resulting in decrease in evaporation with increase in depth of storage structure (deBruin, 1978; Condie and Webster, 1997; Jensen, 2010).

Condie and Webster (1995) and Dalton *et al.* (2001) studied surface area reduction for small storage structures by increasing depth of storage. The excavated pond could be of different shape like square, rectangular, trapezoidal or circular cross section with recommended side slope as mentioned in Table 7. Generally, recommended farm pond shape is rectangular with permissible side slopes according to the type of soil (Kumar and Singh, 2010; Reddy *et al.,* 2012).

Comparative Studies

Assouline *et al.,* (2011) reported that using suspended covers for evaporation control was 23 % less effective due to formation of vapour pressure in comparison to partial floating cover, while similar studies performed in USA reported 58 % reduction in evaporation (Bean and Florey, 1968; Onen, 2019). Alvarez *et al.* (2006) controlled evaporation by shading materials like single layer aluminized sheet and single and double layered coloured polyethylene mesh. The results indicated reduction in evaporation loss ranging from 50 % to 80 % in aluminized screen and coloured polyethylene mesh. Takahashi *et al.* (2012) conducted an experiment with different proportions of surface coverage using polystyrene foam in Adami Tulu Agricultural Research Centre, Central Ethiopia, and reported 80 % coverage

Table 7. Recommended side slope for farm pond

Sl. No.	Soil type	Slope (horizontal: vertical)
1.	Clay	1:1 to 2:1
2.	Clay loam	1.5:1 to 2:1
3.	Sandy loam	2:1 to 2.5:1
4.	Sandy	3:1

Source: Critchley et al. (2011)

of surface area to be effective in comparison to 0, 40, 60, 100 and 200 per cent (double layer). At Plasticulture Farm of College of Technology and Engineering, Udaipur, use of plastic film, plastic balls, polystyrene and maize cob cover showed evaporation reduction up to 85, 65, 55 and 15 %, respectively, during summer (Dhirajlal, 2017). In another study black, white and a mix of both colour balls were analysed, which revealed that evaporation was less with white coloured disks/ balls, followed by equal mix of both white and black coloured balls (Rezazadeh *et al.,* 2020). Table 8 summarises the outcome of comparative studies carried out by various researchers across the world.

Other Methods

Bubble plumes curtail evaporation from water bodies as it churns the water surface with the cool water from the bottom of reservoir without contaminating or disturbing ecology of aquatic living organisms. Destratification is an evaporation suppression technology used since the late 19th century, which induces the artificial bubble plume to disturb the stratified water layer (formed during summer). Thus, plume brings the lowermost cooler water to the upper surface by thermal mixing, and consequently, modifying the temperature gradient (Koberg and Ford, 1965; Hughes *et al.,* 1975) (Fig. 5), resulting in reduction in evaporation (Van Dijk and Van Vuuren, 2009; Helfer *et al.,* 2011; Helfer *et al.,* 2012) (Table 9). Koberg and Ford (1965) and Brown (1988) reported evaporation reduction ranging from 15 - 25 % in lakes with depth more than 15 m and 40 m, respectively. Further, Helfer *et al.,* (2018) reported that the shallow impoundments could not effectively reduce the surface temperatures in comparison to deeper ones.

Fig. 5: Bubble plume breaking the surface and spreading outward

Evaporation suppression technique has to consider its physical and chemical changes besides the cost incurred in technique adoption. Cost analysis needs to consider the cost of construction of the cover, annual maintenance, evaporation loss from the uncovered water body, efficiency of evaporation suppression method and alternate water cost (Aminzadeh *et al.,* 2018).

Critiques of Past Studies

This study conducted at ICAR-CRIDA reviewed various techniques of evaporation control for small storage structures andfarm pond (10 x 10 m^2 to 30 x 30 m^{2}cross-section) at different parts of the world to understand their various pros and cons. It is evident that there is no single cost-effective solution to this complex issue.

Table 8. Outcome of different studies conducted for control of evaporation

Sl.No.	Model	Country (Location)	Observation	Source
1.	Polystyrene foam; Bamboo; Drinking water bottles; Duckweed	Central Ethiopia and Thailand	Evaporation reduction was 38, 25, 33 and 9 % with polystyrene foam, bamboo, drinking water bottles and Duckweed, respectively	Daigo and Phaovattana (1999); Takahashi *et al.* (2012)
2.	Suspended and floating cover	Bet Dagan, Israel	Floating cover proven to be more effective than suspended.	Assouline *et al.* (2011)
3.	Single layered aluminized net, white and coloured polyethylene meshes	University of Cartagena, Southern Spain	Evaporation control ranged from 50 % to 80 % reduction for aluminized screen and coloured polyethylene mesh	Alvarez *et al.* (2006)
4.	Floating material like maize cob, thermocol, plastic ball and plastic film	Udaipur, Rajasthan	Order of evaporation suppression reported as plastic film followed by plastic ball, polystyrene and maize cob	Dhirajlal (2017)
5.	White and Black colour floating balls	Switzerland, Iran		Mady *et al.* (2018); Rezazadeh *et al.* (2020)

Table 9. Studies on evaporation control by other methods

Sl.No.	Model	Observation	Location	Reference
1.	Compartment	Partitioning of pond into small ponds proved to be more effective in controlling evaporation loss by 13 % compared to standard pond	Thailand	Daigo and Phaovattana (1999)
2.	Bubble plume	Artificial destratification, induces the bubble plume to agitate the water by bringing the cool water from the deeper layers to surface, thus reducing the surface water temperature	South Africa, Australia	Koberg and Ford (1965); Hughes *et al.* (1975); Van Dijk and Van Vuuren (2009); Helfer *et al.* (2011); Helfer *et al.* (2012); Helfer *et al.* (2018)

Wind breaks may be advantageous where sufficient area is available for planting suitable plant species on the banks and field boundaries. Wind break is proven to be more effective for small reservoirs (area less than 3600 m^2) and compared to large dams as the wind breakeris effective up to 5 times the height of the plant, which is termed as quiet zone (Helfer, 2009; Monfared *et al*., 2019). Nevertheless, evapotranspiration of the species, stability of the pond structure, and the density of trees/bushes as required in a particular area calls for detailed studies.

Among mechanical barriers, floating solar-panel system with dual benefit is the recent technique for controlling the evaporation losses, and utilizing the renewable energy as an alternative source of energy. The initial installation cost of this advanced system is high, but the system has longer life, saves power consumption charges, and has minimal recurring cost unlike other methods. In future, research has to be taken up at field level on the efficacy of the various methods of installing solar panels like floating, bank anchored, bottom anchored or moored on piles in view of varying water level, depth and shape of storage structure (Mohit and Sarvesh, 2019).

Biological measures using agriculture waste is the cheapest method, but has a negative impact on the quality of water, as well as supports growth of pests and mosquitoes. There are pros and cons of growing azolla and depends upon the objective of water storage structure, and can be a part of integrated farming system where it can supplement nutrient rich feed for poultry and livestock.

Way Forward

Research is required to develop low-cost, durable floating-type mechanical, biological cover and monolayer chemicals considering their feasibility and availability. There is a need to identify plant species which should yield wax, be eco-friendly and effective in control of evaporation.

If budget is not a constraint and the reservoir is perennial, floating solar-panels need to be promoted for evaporation control and power generation. Generated power can be used for operating pressurized irrigation system.

Cross-section of a pond can be manipulated by decreasing the surface area and increasing the depth up to permissible limit of the soil. Region-specific permissible depth and side slopes need to be established.

New techniques like bubble plume and floating/fixed solar-panels need more research with varying water levels as well shape of pond in different agro-climatic settings on pilot scale.

CONCLUSIONS

Water resources are important resources for any kind of livelihood. Its conservation thus assumes high significance. Evaporation is one of the major causes of water loss from storage, and thus its control is of paramount importance. Wind is a major factor contributing to evaporation loss as it accelerates the vapour pressure deficit from the water surface. Several evaporation suppressant techniques are reported in the literature that require region-specific studies to tackle the local environment like high temperature, wind, amount of rainfall, locally available material to make them feasible and cost-effective. Wind break to control wind speed and water loss through evaporation can be an effective biological measures, but occupy considerable space. Covering the water surface with barriers either mechanical or biological reported evaporation control up to 70 % and 60 %, respectively. Chemicals (cetyl and stearyl alcohol) used in combination recorded evaporation reduction up to

57 % and up to 85 % with combination of mechanical and chemical barrier used as evaporation retardant. Chemical evapo-retardent methods require low initial capital investment, but operational and maintenance expenses are high and they are not farmer-friendly. Biological method, though cost effective, cannot be recommended uniformly over regions, and also occupies large tract of land. Mechanical methods, though easy to construct in relatively little land, are costly prepositions and economically may not be suitable. The chemical method may further aggregate the issue of environment. Thus, there is a need to devise mechanisms which are economically and functionally viable.

REFERENCES

Alam S; AlShaikh A A. 2013. Use of palm fronds as shaded cover for evaporation reduction to improve water storage efficiency. J. King Saud Univ.– Eng. Sci., 25, 55-58.

Al-Juruf R S; Ahmed F A; Alam I A. 1988. Development of heat insulating material using date palm leaves. J. Therm. Insul., 11, 158-159.

Al Hassoun S A; Al Shaikh A A; Al Rehaili A M; Misbahuddin M. 2011. Effectiveness of using palm fronds in reducing water evaporation. Can. J. Civil Eng., 38(10), 1170-1174.

Althoff D; Rodrigues L N; David da Silva D. 2019. Evaluating evaporation methods for estimating small reservoir water surface evaporation in the Brabilian Savannah. Water, 11(9), 1-17.

Alvarez V M; Baille A; Martinez J M M; Gonzalez-Real M M. 2006. Efficiency of shading materials in reducing evaporation from free water surfaces. Agric. Water Manage., 84, 229-239.

Aminzadeh M; Lehmann P; Dani Or. 2018. Evaporation suppression and energy balance of water reservoirs covered with self-assembling floating elements. Hydrol. Earth Syst. Sci., 22, 4015-4032.

Archer R J; La Mer V K. 1955. The rate of evaporation of water through fatty acid monolayers. J. Physic. Chem., 59(3), 200-208.

Arora M; Goel N K; Singh P. 2005. Evaluation of temperature trends over India. Hydrol. Sci. J., 50(1), 37-41.

Assouline S; Narkis K; Or D. 2010. Evaporation from partially covered water surfaces. Water Resour. Res., 46(10), 1-12, W10539.

Assouline S; Narkis K; Or D. 2011. Evaporation suppression from water reservoirs: Efficiency considerations of partial covers. Water Resour. Res., 47(7), 1-8, W07506.

Bardsley E; Vetrova V. 2019. Estimating evaporation for low wind speeds at an eddy correlation site: Potential for windbreak evaluation. J. Hydrol. (NZ), 58(1), 57-63.

Barnes G T. 2008. The potential for monolayers to reduce the evaporation of water from large water storages, Agric. Water Manage., 95, 339-353.

Bean B R; Florey Q L. 1968. A field study of the effectiveness of fatty alcohol mixtures as evaporation reducing monomolecular films. J. Water Resour. Res., 4, 206-208.

Benke K; **Tomkins B.** 2018. Future food-production systems: vertical farming and controlledenvironment agriculture, sustainability. Sci. Pract. Policy, 13(1), 13-26.

Boon A G; Downing A L. 1957. Observations on the use of cetyl alcohol for conservation of water. Inst. Water Eng. J., 11, 443-448.

Bradley E F. 1968. A micro meteorological study of velocity profiles and surface drag in the region modified by a change in surface roughness. Q. J. R. Meteorol. Soc., 94, 361-379.

Brandle J R; Hodges L; Zhou X H. 2004. Windbreaks in North American agricultural systems. Agro. For. Syst., 61, 65-78.

Brink G N; Symes T W; Hancock N H. 2011. Development of a smart monolayer application system for reducing evaporation from farm dams: Introductory paper. Aust. J. Multidiscip. Eng., 8(2), 121-130.

Brown J. 1988. The potential for reducing open water evaporation losses: A review. In: Proc. Hydrology and Water Resources Symposium, 1-3 February, Canberra, Australia, 108-115.

Burston I A; Akbarzadeh A. 1995. Fresh water storage – Evaporation research. Report to the Cotton Research and Development Corporation, Sainty and Associates, NSW, Sainty and Associates, Australia, pp: 68.

Burston I A. 2002. Conservation of water from open storages by minimizing evaporation. Unpublished Ph.D. Thesis, RMIT University, Melbourne, Australia.

Chang S; McClanahan M; Kabler P. 1962. Effect of bacterial decomposition of hexadecanol and octadecanol in monolayer films on the suppression of evaporation loss of water. In: La Mer VK (Ed.), Retardation of Evaporation by Monolayers. Transport Processes, Academic Press, New York, 119-131.

Chaudhari N; Chaudhari N D. 2015. Use of thermocol sheet as floating cover to reduce evaporation loss in farm pond. In: Hydro-2015 International Conference on Hydraulics, 17-19 December, Water Resources and River Engineering, IIT, Roorkee, India, 1-9.

Cleugh H A; Prinsley R; Bird R; Brooks S J; Carberry P; Crawford M; Jackson T; Meinke H; Mylius S; Nuberg I; Sudmeyer R; Wright A. 2002. The Australian national windbreaks program: Overview and summary of results. Aust. J. Exp. Agri., 42, 649-664.

Condie S A; Webster I T. 1995. Evaporation mitigation from on-farm water storages. CSIRO Centre for Environmental Mechanics, CSIRO, Canberra, Australia, Technical Report No. 90, pp: 68.

Condie S A; Webster I T. 1997. The influence of wind stress, temperature and humidity gradients on evaporation from reservoirs. Water Resour. Res., 33, 2813-2822.

Cooley K R; Myers L E. 1973. Evaporation reduction with reflective covers. J. Irrig. Drain. Div., 99(3), 353-363.

Coop P A. 2011. Detection of evaporation reducing monolayers on open water surfaces. Unpublished Ph.D. Thesis, University of New England, Australia.

Cowtan K; Way R G. 2014. Coverage bias in the had CRUT4 temperature series and its impact on recent temperature trends, Q. J. R. Meteorol. Soc., 140, 1935-1944.

Craig I; Aravinthan V; Baillie C P; Beswick A; Barnes G; Bradbury R; Connell L; Cooper P; Fellows C; Fitzmaurice L; Foley J P; Hancock N; Lamb D; Morrison P; Mossad R; Misra R K; Pittaway P; Prime E; Rees S; Schmidt E; Solomon D; Symes T; Turnbull D. 2007. Evaporation, seepage and water quality management in storage dams: A review of research methods. Environ. Health, 7(3), 84-97.

Craig I; Green A; Scobie M; Schmidt E. 2005. Controlling Evaporation Loss from Water Storages. National Centre for Engineering in Agriculture, University of Southern Queensland, Australia, Publication No. 1000580/1, pp: 207.

Critchley W; Siegert K; Champman C; M Finkel. 1991. A Manual for the Design and Construction of Water Harvesting Schemes for Plant Production. Food and Agriculture Organization, Rome, Italy, Pub. No. AGL/MISC/17/91, pp: 148.

Crow F R. 1973. Increasing Water Supplies by Suppression of Reservoir Evaporation. Research Project Final Technical Completion Report Agreement No.: 14-31-0001-3036., Oklahoma Water Resources Research Institute, Oklahoma State University, Stillwater, Oklahoma, United States, pp: 37.

CWC. 2006. Evaporation Control in Reservoirs. Report, Central Water Commission (CWC), Government of India, New Delhi, India, pp: 96.

Daigo K; Phaovattana V. 1999. Evaporation and percolation control in small farm ponds in Thailand. The Japan Agric. Res. Q., 33(1), 47-56.

Dalton P; Raine S; Broadfoot K. 2001. Best Management practices for maximising whole farm irrigation efficiency in the Australian cotton industry. Final Report for CRDC Project No. NEC2C, National Centre for Engineering in Agriculture, USQ, Toowoomba, Queensland, Australia, Publication No. 179707/2, pp: 104.

Das A; Singh R K; Ramkrushna G I; Layek J; Tripathi A K; Ngachan S V; Choudhury B U; Patel D P; Rajkhowa D J; Chakroborty D; Ghosh P K. 2017. Roof water harvesting in hills- Innovations for farm diversification and livelihood improvement. Current Sci., 113(2), 1-5.

deBruin H A R. 1978. A simple model for shallow lake evaporation. J. Appl. Meterol., 17, 1132-1134.

Dhirajlal P A. 2017. Study on effectiveness of floating material for controlling evaporation from small water bodies. Unpublished M. Tech. Thesis, Maharana Pratap University of Agriculture & Technology (MPUAT), Udaipur, Rajasthan, India.

Drummond C J; Elliott P; Furlong D N; Barnes G T. 1992. Water permeation through two component monolayers of polymerized surfactants and octadecanol. J. Colloid Interface Sci., 151(1), 189-94.

Frenkiel J. 1965. Physical and chemical principles and review of experiments. United Nations Educational, Scientific and Cultural Organization (UNESCO), France, pp:79.

Gallego B; Alvarez V; Pittaway P; Symes T; Hancock N. 2010. The combined use of shade-cloth covers and monolayers to prevent evaporation in irrigation reservoirs. In: International Conference on Agricultural Engineering (AgEng 2010), 06-08 Sept., Clermont-Ferrand, France, pp: 9. .

Gallego-Elvira B; Baille A; Martin-Gorriz B; Maestre-Valero J F; Martinez-Alvarez V. 2011. Energy balance and evaporation with loss of an irrigation reservoir equipped a suspended cover in a semi-arid climate (south-eastern Spain). Hydrol. Process., 25, 1694-1703.

Ganguly J K; Kaul R N. 1969. Wind Erosion Control. ICAR, New Delhi. Tech. Bull. (Agric.) 20, 1-53.

Gokbulak F; Ozhan S. 2006. Water loss through evaporation from water surfaces of lakes and reservoirs in Turkey. E-Water, Official Publication of the European Water Association (EWA), pp: 6.

Gugliotti M; Baptista M S; Politi M J. 2005. Reduction of evaporation of natural water samples by monomolecular films. J. Braz. Chem. Soc., 16(6A), 1186-1190.

Hamblin P F; Verburg P; Roebber P; Bootsma H A; Hecky R E. 2002. Observations, evaporation and preliminary modelling of over-lake meteorology on large African lakes. Adv. in Global Change Res., Springer, 12, 121-125.

Hancock N H; Pittaway P A; Symes T W. 2011. Assessment of the performance of evaporation suppressant films: Analysis and limitations of simple trialling methods. Aust. J. Multidiscip. Eng., 8(2), 157-167.

Harbeck G E. 1962. A practical field technique for measuring reservoir evaporation utilizing mass-transfer theory. Geological Survey Professional Paper 272-E, United States Government Printing Office, Washington, USA, 101-105.

Hassan M. 2013. Evaporation estimation for Lake Nasser based on remote sensing technology. Ain Shams Eng. J., 4, 593-604.

Heisler G M; Dewalle D R. 1988. Effects of windbreak structure on wind flow. Agric. Ecosyst. Environ., 22–23, 41-69.

Helfer F; Zhang H; Lemckert C J. 2009. Evaporation reduction by windbreaks: Overview, Modelling and Efficiency. Urban Water Security Research Alliance Technical Report No. 16, pp: 18.

Helfer F; Zhang H; Lemckert C. 2011. Modelling of lake mixing induced by air-bubble plumes and the effects on evaporation. J.Hydrol., 406, 182-198.

Helfer F; Zhang H; Lemckert C. 2012. Influence of bubble plumes on evaporation from non-stratified waters. J.Hydrol., 438-439, 84-96.

Helfer F; Andutta P F; Louzada A J; Zhang H; Lemckert C. 2018. Artificial destratification for reducing reservoir water evaporation: Is it effective? Lakes and Reservoirs, Wiley Online library, 23(4), 1-18.

Hipsey M R; Sivapalan M. 2003. Parameterizing the effect of a wind shelter on evaporation from small water bodies. Water Resour. Res., 39(12), 1-9.

Hughes T C; Richardson E A; Franckiewicz J A. 1975. Water Salvage Potentials in Utah. Volume II: In: Volume II: Evaporation Suppression by Reservoir Destratification, Report by Utah Water Research Laboratory College of Engineering, Utah State University, United States, pp: 387.

Hunter K; Finn N; Barnes S. 2007. The benefits of shade cloth covers for potable water storages. In: Proc. 70th Annual Water Industry Engineers and Operators' Conference, Bendigo Exhibition Centre, Australia, 4 to 6 September, 86-92. http://www.csiro.au/resources/Shadeclothcovers.html.

Jensen M E. 2010. Estimating evaporation from water surfaces. CSU/ARS Evapotranspiration Workshop, Fort Collins, CO, 1-27.

Kahalekar U J; Kumawat H S. 2013. Evaporation suppression from water surfaces using chemical films. Int. J. Civil Eng. Technol., 4(3), 185-196.

Koberg G E; Ford M E. 1965. Elimination of thermal stratification in reservoirs and resulting benefits. Geol. Surv. Water Supply Paper, 1809-M, pp: 28.

Kumar A; Singh R. 2010. Plastic lining for water storage structures. Directorate of Water Management, Chandersekharpur, Bhubaneswar, India, Technical Bulletin No. 50, pp: 34.

Kumar R; Farooq Z; Jhajharia D; Singh V P. 2018.

Trends in temperature for the Himalayan environment of Leh (Jammu and Kashmir), India. In: Climate Change Impacts, Water Science and Technology Library 82, Springer Nature Singapore Pvt. Ltd., pp: 13.

Larry P; Karen W; John B; Victor H B. 2007. Design information for evaporation ponds in Wyoming. Wyoming Water Research Centre, University of Wyoming, Colourado, USA, Report No. WWRC-85-21. http://library.wrds.uwyo.edu/wrp/85-21/85-21.html

Lehmann P; Aminzadeh M; Or D. 2019. Evaporation suppression from water bodies using floating covers: Laboratory studies of cover type, wind, and radiation effects. Water Resour. Res., 55(6), 4839-4853.

Li F; Zhao Y. 2018. Estimation of open water evaporation using land-based meteorological data. Theor. Appl.Climatol., 134, 397-409.

Lomas J; Schlesinger E. 1971. The influence of a windbreak on evaporation. Agric. Meteorol., 8, 107-115.

Mady B; Lehmann P; Or D. 2018. Evaporation suppression from water reservoirs using floating covers – preliminary results from field experiments. Geophys. Res. Abstr., 20, EGU2018-11778.

Maestre-Valero J F; Alvarez V M; Elvira B G; Pittaway P. 2011. Effects of suspended shade cloth cover on water quality of an agricultural reservoir for irrigation. Agric. Water Manage., 100, 70-75.

Magin G B; Randall L E. 1962. Review of literature on evaporation suppression. Geol. Survey Professional Paper 272- C,United States Government Printing Office, Washington, USA, 53-69.

Manges H; Crow F R. 1965. Evaporation suppression by Chemical and mechanical treatments. Proceedings of the Oklahoma Academy of Science, 46, 251-254.

Marco Rosa-Clot; Tina G M; Nizetic S. 2017. Floating photovoltaic plants and wastewater basins: An Australian project floating photovoltaic plants and waste. Energy Procedia, 134, 664-674.

Martinez-Alvarez V; Baille A; Molina Martínez J M; González-Real M M. 2006. Effect of black polyethylene shade covers on the evaporation rate of agricultural reservoirs. Spanish J. Agric. Res., 4(4), 280-288.

Martinez-Alvarez V; Maestre-Valero J F; Martín-Gorriz B; Gallego-Elvira; B. 2010. Experimental assessment of shade-cloth covers on agricultural reservoirs for irrigation in south-eastern Spain. Spanish J. Agric. Res., 8(S2), S122-S133.

McArthur I K H; Durham K. 1957. Fatty Alcohols for Water Conservation. In: Proc. International Congress on Surface Activity, London, Preprint 1, AL, 208-215.

McJannet D; Cook F; Burn S. 2008. Evaporation reduction by manipulation of surface area to volume ratios: Overview, analysis and effectiveness. CSIRO: Water for a Healthy Country National Research Flagship, Urban Water Security Research Alliance, The Urban Water Security Research Alliance ,Quuensland, Technical Report No. 8, pp: 21.

McJannet D; Cook F; Knight J; Burn S. 2008a. Evaporation reduction by monolayers: Overview, Modelling and Effectiveness. Urban Water Security Research Alliance, The Urban Water Security Research Alliance, Queensland, Technical Report 6, pp: 32.

McJannet D L; Webster I T; Cook F J. 2012. An area-dependent wind function for estimating open water evaporation using land-based meteorological data. Environ. Model. Software, 31, 76-83.

Messing I; Afors M; Radkvist K; Lewan E. 1998. Influence of shelterbelt type on potential evaporation in an arid environment. Arid Soil Res. Rehabil., 12, 123-138.

Mohit A; Sarvesh D. 2019. Floating solar photovoltaic (FSPV): A third pillar to solar PV sector. TERI Discussion Paper: Output of the ETC India Project, The Energy and Resources Institute (TERI), New Delhi, India, pp: 64.

Monfared S A H; Rezapour M; Zhian T. 2019. Using windbreakers for decreasing lake and reservoir evaporation: A case study from Iran. Polish J. Environ. Stud., 28(4), 2289-2298.

Mozafari A; Mansouri B; Chini S F. 2019. Effect of wind flow and solar radiation on functionality of water evaporation suppression monolayers. Water Resour. Manage., 33, 3513-3522.

NAS. 1974. More Water for Arid Lands, Promising Technologies and Research Opportunities. National Academy Sciences, Washington, USA, pp: 153.

Onen I I. 2019. Reducing evaporation losses in surface water using local available materials in semi-arid region (A case study of Maiduguri metropolis). Int. J. Eng. Sci. Comput., 9(10), 23872-23880.

Panjabi K; Rudra R; Goel P. 2016. Evaporation retardation by monomolecular layers: An experimental study at the Aji Reservoir (India). Open J. Civil Eng., 6, 346-357.

Radhakrishnan K; Sivaraman I; Jena S K; Sarkar S; Adhikari S. 2017. A climate trend analysis of temperature and rainfall in India. Climate Change Environ. Sustainability, 5(2), 146-153.

Reddy K S; Kumar M; Rao K V; Maruthi V; Reddy B M K; Umesh B; Babu R G; Reddy K S; Vijayalakshmi; Venkateswarlu B. 2012. Farm Ponds: A Climate Resilient Technology for Rainfed Agriculture: Planning, Design and Construction. Central Research Institute for Dryland Agriculture, Santoshnagar, Saidabad, Hyderabad- 500059, Andhra Pradesh, India, pp: 60.

Reiser C O. 1969. A system for controlling water evaporation. Ind. Eng. Chem. Res., 8, 63-69.

Reiter A; Weidinger R. 2016. Trends in Temperature and Precipitation. In: Mauser W; Prasch M (Eds.), Regional Assessment of Global Change Impacts, Springer, Chapter 13, 117-123.

Rezazadeh A; Akbarzadeh P; Aminzadeh M. 2020. Modelling and experimental investigation of evaporation suppression using floating covers in the presence of surface flows. Amirkabir J. Mech. Eng., 53(1), 1-3.

Saggai S; Boutoutaou D; Elkheir Bachi O. 2018. Effects of monolayers made from different emulsions on surface water evaporation in a typical Algerian oasis. Lebanese Sci. J., 19(3), 445-454.

Segal L; Burstein L. 2010. Retardation of water evaporation by a protective float. Water Resour. Manage., 24,129-137.

Shah R; Ghosh P K; Mishra V K; Bujarbaruah K M. 2007. Low-cost micro-rainwater harvesting technology (*Jalkund*) for new livelihood of rural hill farmers. Current Sci., 92(9), 1258-1265.

Shaw E M. 1988. Hydrology in Practice. Van Nostrand Reinhold International, London, United Kingdom, pp: 535.

Simon K; Shanbhag R; Slocum A H. 2014. Reducing evaporative water losses from irrigation ponds through the reuse of polyethylene terephthalate bottles. J. Irrig. Drain. Eng., 142(2), 1-12.

Singh K S; Athokpam H. 2018. Jalkund: Low cost rainwater harvesting structure for sustainable livelihood of the Chandonpokpi village, Chandel district, Manipur, India. Int. J. Pure Appl. Biosci., 6(5), 1326-1334.

Skidmore E L; Hagen L J. 1970. Evaporation in sheltered areas as influenced by windbreak porosity. Agric. Meteorol., 7, 363-374.

Sovocool K; Morgan M; Drinkwine M; Sims D; Toussaint G. 2014. Testing an innovative evaporative suppressant for reducing losses from lakes. J. Am. Water Works Assoc., 106, 41-50.

Taboada M E; Caceres L; Graber T A; Galleguillos H R; Cabeza L F; Rojas R. 2017. Solar water heating system and photovoltaic floating cover to reduce evaporation: Experimental results and modeling. Renewable Energy, 105, 601-615.

Takahashi S; Suzuki S; Watanabe F; Goto A; Kubo A. 2012. The prevention methods of leak and for consecutive water reservoir. Desert Res. Japan Soc. Desert, 22(1), 287-290.

Van Dijk M; Van Vuuren S J. 2009. Destratification induced by bubble plumes as a means to reduce evaporation from open impoundments. Water SA, 35(2),158-167.

Wang H; Takle A; Shen J. 2001. Shelterbelts and windbreaks: mathematical modelling and computer simulations of turbulent flows. Annu. Rev. Fluid Mech., 33, 549-586.

Yan W; Bingwen W; Qingzhu J; Wei Z. 2009**.** Study on retardation of water evaporation by single and mixed monolayers at air/water interface. In: Proc. International Conference on Environmental Science and Information Application Technology, Wuhan, 179-182.

Yao X; Zhang H; Lemckert C; Brook A; Schouten P. 2010. Evaporation reduction by suspended and floating covers: Overview, Modelling and Efficiency. Urban Water Security Research Alliance, The Urban Water Security Research Alliance, Queensland, Technical Report No. 28, pp: 16.

Youssef Y W; Khodzinskaya A. 2019. A review of evaporation reduction methods from water surfaces. In: E3S Web of Conferences, 97, 05044. https://doi.org/10.1051/e3sconf/20199705044

Zhao G; Gao H. 2019. Estimating reservoir evaporation losses for the United States: Fusing remote sensing and modeling approaches. Remote Sens. Environ., 226, 109-124.

http://www.isae.in / journal_jae.aspx

Journal of Agricultural Engineering

Vol. 57 (3): July-September, 2020

Biochar Pelletisation and Physio-mechanical Properties of Pellets

Syed Imran[1], B. Sanjeeva Reddy[2*], D. Ashish[3] and G. Venkatesh[4]

[1]Scientist (FMP), ICAR – Central Institute of Agricultural Engineering, Nabi Bagh, Bhopal - 462 038; [2]Principal Scientist (FMP), [3]Scientist (FMP),[4]Senior Scientist (Agro-forestry), ICAR – Central Research Institute for Dryland Agriculture, Santosh Nagar, Saidabad, Hyderabad - 500 059. *Corresponding author e-mail address: Bs.Reddy@icar.gov.in

Article Info

Manuscript received: October, 2018
Revised manuscript accepted: August, 2020

***Keywords*:** Biochar pellet, drum pelletiser, binder, mechanical properties

ABSTRACT

Application of powder biochar to soil is a major concern due to losses as high as 30 % at various stages as well as safety of applicator from dust pollution. A drum-type machine capable of using easily available binder materials as maize flour, rice starch, carboxymethyl cellulose sodium (CMC) and commercial starch with thermal treatment were evaluated. Results showed that on average commercial starch 66.4 % and rice starch binder yielded 62.77 % pellets in the desirable size range. The pellets were non-hygroscopic in nature, biochar field capacity was 93 % (d.b.), and pellets values varied from 57.8 % to 78 % (d.b.) depending on type of binder. Pellet using rice starch binder had highest bulk density of 390.2 kg.m^{-3}. Pellet using rice starch binder also had 99.12 % and 97 % attrition resistance as compared to CMC (98.02 %) and inter-granular (91.78 %) in presence of similar size harder foreign material. Commercial and rice starch binder added pellets also showed promising value of crushing strength of 2.5 kg.cm^{-2} and 2.4 kg.cm^{-2}, respectively.

Biochar is a black, carbon-rich powder produced from biomass through pyrolysis process, and can be used in agriculture as a soil amendment. The production of biochar and its processing had been the main focus of many researchers all over the world in recent times due to its advantages in terms of use as an energy source in industries, as a carrier medium to enhance fertilizer-use efficiency when used for soil, and as a means for reducing greenhouse gases in the atmosphere by sequestration of carbon in soil (Fulton and Port, 2016; Antanas *et al*., 2016; Bowden - Green and Briens, 2016a; Hu *et al*., 2015).

In India, 234.5 Mt of crop residues surplus potential was estimated, of which most of the materials are burnt on farms to clear the field for next crop (Hilaidhari *et al*., 2014). Any type of crop residue is considered as potential renewable source for biochar production and thermal applications to derive energy for industrial uses. However, low calorific value and biochar yield dependence on quality of biomass and processing methodology up to some extent are major limitations (Tripathi *et al.*, 2016). When biomass is utilized for production of biochar and used to reduce the greenhouse gas emission to atmosphere, it helps the farmers to address the issue of climate change by providing a means to permanent carbon sequestration. Although farming practices adopting various technologies as conservation tillage, organic farming have been adopted as a means to mitigate climate change; these practices release soil carbon much faster into the atmosphere compared to the biochar application (Alexandre and Francesco, 2019).

Application of biochar to soil as amendment helps to increase water retention and microbial growth within the soil, while the chemical characteristics help reduce nutrient leaching and heavy metal tainting of crops. The major problem encountered in field application of biochar is non-availability of appropriate equipment, due to its fine powder particle size between 1 micron to 100 microns, which can easily become airborne. Handling of biochar powder is also difficult due to its particle sizes. Application of powder biochar at 5.6 t.ha^{-1} target rate with an existing full-size lime spreader encountered considerable losses despite of low wind velocity; estimated at 25 % while handling, at 2 % during transportation and all together for a total of 30 %, including losses during incorporation in soil (Major *et al.*, 2010). A slew of measures and application conditions were prescribed for powder biochar application. These include broadcasting using lime, fertilizer or manure spreaders, followed by mixing with tillage implements (Brewer, 2012). Creating furrow and directing biochar to the base of the furrows using mould board plough, sub-soiler and chisel plough with special attachments (Bishop *et al*., 2012); use of slurry injecting equipment (Sohi *et al*., 2010) and top dressing of biochar by trench and fill methods (Williams and Arnott, 2010). However, fulfilment of these conditions is difficult in Indian conditions where mechanization is at low pace, especially in application of farmyard manure, vermin compost, lime powder and other soil amendment materials.

It has been reported that pelletisation and densification can improve feedstock uniformity and enhance the handling and conveyance efficiency when compared with powder materials (Tumuluru *et al*., 2011). Recently, to reduce phosphorus (P) release and enhance the effectiveness of P fertilizer in soil, new technologies of phosphate fertilizer have been developed, such as coating with polymers, pelletisation or granulation with biochar and treating the biochar to produce biochar-based fertilizers. Wet granulation technique is the proven process of agglomerating fine powder materials into larger agglomerates or granules/ pellets using liquid binding agents as per the desired applications. The pelletisation techniques include simple agitation of powder material with binder, compression and extrusion at low pressure with binder and high-pressure extrusion without binder and layering of powder and suspension. In recent decade, advanced techniques developed, such as melt agglomeration, freeze pelletisation and fluid bed pelletisation. Wherever high pressure is involved that requires costly equipment with high energy expenditure. The advanced techniques besides cost consideration also required skilled man power (Hirjau *et al*., 2011; Sirisha *et al*., 2014). The availability and usability of such technologies are presently beyond the reach of India farming community.

Pelletising biochar leads to engineered biochar reducing dustiness and health risks due to inhaling while handling and field applications. Biochar pelletisation reduces dust pollution and also gives the product uniform shape and size, thus allowing more uniform distribution in soil using mechanical equipment. The technique of pelletisation has been popular for powder materials such as coal powder, fertilizer manufacturing industries. However, limited studies were reported using biochar (Hu *et al*., 2015). In view of growing demand and importance of biochar application in Indian agriculture, the present investigation on biochar pelletisation and determination of physio-mechanical properties of pellet was undertaken.

MATERIALS AND METHODS

Granulation process is commonly being employed in many industrial applications where powder material is involved to reduce dust problem, improve handling and minimize caking of materials during storage and transportation. The present investigation was taken up at ICAR – Central Research Institute for Dryland Agriculture (CRIDA), Hyderabad, during the period 2016 - 2017. The drum granulation process is simple, and pelletisation could be carried with a low-cost machine in batch process (Walker, 2007). An axially mounted rotating drum was used to agitate powder materials along with precisely quantified liquid binding agents. Due to continuous tumbling action, the granules started enlarging layer by layer due to coalescence mechanism (Kapur and Fuerstenau, 1969). When precise liquid binding agents' application equipment is not available; starch material mixed with boiling water was added to powder biochar and stirred for about 5 min to obtain proper consistency of mixture to use in a drum granulator. Hence, this process methodology was taken up in the present investigation for biochar pelletisation.

Selection of Operational Parameters

A number of process parameters affect the extent of pellet size formation and yield of different size grades by a drum granulation machine. The parameters related to pelleting machine are drum diameter, rotational speed and angle of inclination of rotating drum that affect the mean residence time of the biochar and binder mix within the drum. Among these parameters that could be easily manipulated are the drum diameter and rotational speed of pelletising equipment. With low rotational speeds of drum, the material to be pelletised slides on the bottom portion of wall of the drum with little agitation, and increasing drum speed to the half of critical speed (defined as the speed at which the dry material is carried around the drum by centrifugal force), the powder materials begins to roll, cascading occurs and the probability of agglomeration increases (Walker, 2007). At higher rotational speed of the drum beyond critical speed, the material being subjected to higher centrifugal force and thrown towards the drum wall rotates along with drum. The critical speed mostly depends on particle size of powder material, nature of binder and added moisture content for effective pellets formation.

When the dry powder is put into the drum for rolling, it has been suggested that the optimum drum speed is half the critical speed. The critical speed also corresponds to the speed at which the Froude number is equal to unity. Froude number is the dimensionless ratio of the inertial force to the gravitational force, and expressed as denoted by the formula (Walker, 2007):

$$Fr = n^2 D/g \qquad \ldots(1)$$

Where,

Fr = Froude number,

n = Rotational speed of drum, rpm,

D = Diameter of drum, m, and

g = Gravitational force, $m.s^{-2}$.

When the value of Fr is equal to 1, the optimum rotational speed of the drum then equals, and

$$n = 42.4 \times D^{-0.5} \qquad \ldots(2)$$

In practice, good pelletisation can be achieved in drum containing no internal flights at speeds $n_{Fr} = 0.3 - 0.5$. For the present study, a drum of 0.25 m diameter (D) was considered for development of a batch pelletising machine.

Now, critical rotational speed, $n = 42.4 \times (0.25)^{-0.5} = 84.8$ rpm. …(3)

Optimal rotational speed, $(n_{Fr}) = 84.8 \times 0.5 \sim 43$ rpm. …(4)

Development of Drum Granulation Machine

To avoid rusting and frequent spoilage of pelletising equipment working with moist binding materials, a fibre plastic cylinder was fabricated for batch process pelletisation of biochar. The fibre plastic drum to roll the material was of 340 mm in length and 250 mm in diameter. A 1.5 mm thick metal plate was fitted with rivet fasteners for fixing the drive attached to the end of the drum, and a removable lid with viewing window was provided. A metal bush of 50 mm in diameter with 25 mm bore was welded at the central position of the bottom metal plate to facilitate direct fitment of the drum with the motor shaft. A lid for the rotary drum was fabricated for feeding biochar through an open end, which had 150 mm opening at its central location. A 1.49 kW AC geared motor synchronized with a VACON make NXL0006-2 variable frequency drive was used for rotating the drum at defined rotary speed as deduced from the Eq. 4, and experimental runs carried with varied biochar and binder proportions (Fig. 1). Technical specifications of the drum pelletiser are presented in Table 1.

Biochar Preparation

Prosopisjuliflora tree small stems and twigs were used to prepare char using a biochar unit developed at ICAR-CRIDA, Hyderabad (Venkatesh *et al.*, 2013). The line diagram of biochar preparation unit and its dimensional details are given in Fig. 2. The biochar unit is vertical cylindrical in structure with both ends closed, with 20 % bottom area perforated in a set pattern, and the top portion having a vent to place the cut-biomass. The unit was fabricated using a 3 mm thick GI sheet. The capacity of unit was 200 liters on water volume basis.

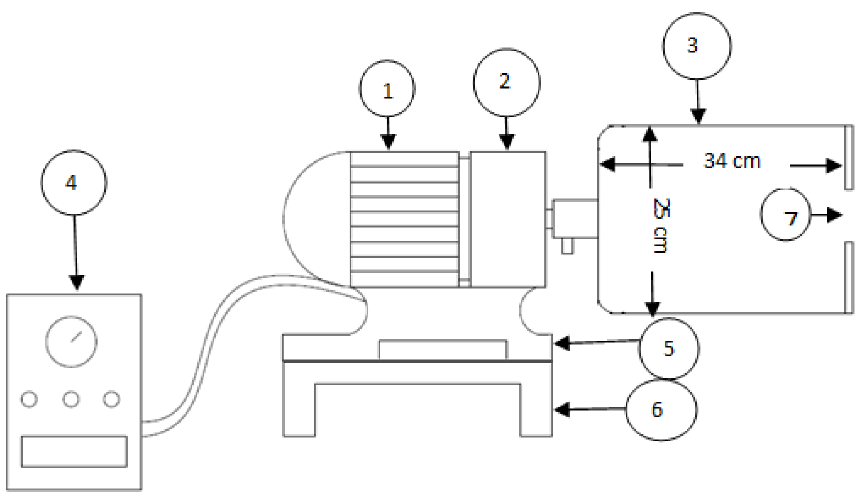

1. Electric motor
2. Gear box
3. Rotary drum
4. Motor speed control unit
5. Motor base
6. L angle support frame
7. Process view window

Fig. 1: Biochar batch pelletiser machine

Table 1. Technical specifications of drum pelletiser machine

Sl.No.	Component	Specification
1.	Drum size (Length x Dia x Drum sheet thickness), mm	340 x 250 x 2
2.	Drum material	Fibre plastic
3.	Drive type	Directly coupled
4.	Power source	AC, Variable frequency motor
5.	Motar capacity, kW	1.49
6.	Operating speed range, rpm	10-110
7.	Speed lest count, rpm	01
8.	Practical speed for pelletising, rpm	60
9.	Inputcapacity per batch,g	1000
10.	Pellet yield per batch, g	930

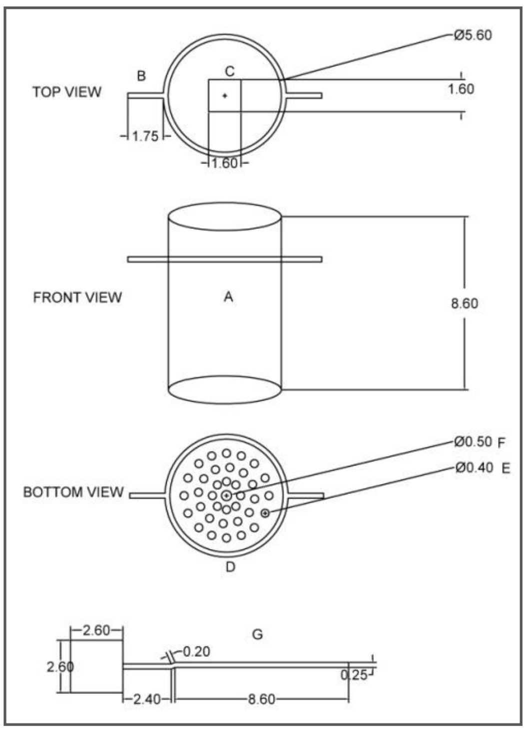

A. Body of biochar unit, B. Handles, C. Vent on top lid, D. Unit bottom portion, E. Holes in concentric circles, F. Central hole, G. Closing device for vent on top lid

(*To obtain dimension of biochar unit in mm, multiply given values in Fig. by 100*)

Fig. 2: Biochar process unit for crop residue

Selection of Binder Materials

The key to successful granulation is a proper solid-to-liquid relationship, both to be proportioned as feedstock to the drum, as also the extent of wetting of the solids by the liquid binder (Bowden – Green and Briens, 2016a). The solid and liquid materials in the drum tend to granulate mainly by two phenomena: (a) by the natural surface tension of the liquid that draws wetted solid particles into contact, and (b) the mechanical forced contact of wetted particles during rotation of the drum. When one or more of the materials being granulated is water soluble, it is the total volume of liquid or solution phase rather than the moisture content that controls the granulation behaviour in the drum (Rajagopalan and Murthy, 1988).

Hofstee and Huisman (1990) and Luiz *et al*. (2017) had reported that the size of fertilizer particles and their proportion in a manufactured fertilizer has great influence on metering mechanism application rates with various types of field equipment. Fertilizer having particle sizes in the range of 1 - 4.75 mm was reported to be better from the application point of view. An upper limit of diameter of most of the fertilizers commercially used in agriculture is in the range of 4 - 4.75 mm, and larger size fertilizer granules may cause uneven spatial distribution of nutrients (Rutland and Polo, 2005). Hence, in the present study biochar pellet sizes in the range of 1 - 4.75 mm as that of common commercial fertilizer granule sizes, was considered.

The results on pelletisation of biochar using cellulose/ lignin-based binders indicates that binder concentrations at about 10 % (weight by weight on binder and biochar proportion) gave reasonably good compressive strength and reasonable pellets yields (Hu *et al.,* 2015; Bowden – Green and Briens, 2016b). Accordingly, binder concentrations in the range of 5- 15 % were used in this study in order to determine the best proportions for the selected binder materials in terms of proper pellet size range (1 - 4.75 mm) yields to mix properly in soil as suggested by Antille *et al.* (2015).

The optimised treatment combinations for the selected 4 binder materials are presented in Table 2. Five trial runs were undertaken, each with three commonly available binder materials and one commercial cellulose, with different binder quantities for a fixed quantity of biochar for arriving at optimized treatments.

Physio-mechanical Property Evaluation

The physio-mechanical properties of pellets (Fig. 3) play a major role in design of storage hopper of field application machinery, and moisture retention related properties in the soil matrix for crop growth. The pertinent properties were thus determined following the test procedures as detailed below.

Particle size distribution

Dry sieving procedure was used to separate the pellets which were in sizes lower and more than the size range of 1 - 4.75 mm, to measure particle size distribution, specifically to determine the percentage of biochar pellets that are of common commercial fertilizer granule sizes. From each treatment, 500g of dried pellet samples were drawn and subjected to sieve analysis using sieves of 1 mm and 4.75 mm. The segregated quantity of biochar pellets less than 1 mm, more than 4.75 mm, and in between 1-4.75 mm were weighed separately.

Table 2. Optimized treatments for pellets preparation using biochar and binders

Sl. No.	Treatment
1.	Water 400 ml at boiling point + add maize flour 50g slowly and stir continuously + remove sample from stove and add 500g biochar and vigorously stir the components
2.	Water 400 ml at boiling point + add rice starch 62g slowly and stir continuously + remove sample from stove and add 500g biochar and vigorously stir the components
3.	Water 400 ml at boiling point + add carboxymethyl cellulose sodium (CMC) 25g slowly and stir continuously + remove sample from stove and add 500g biochar and vigorously stir the components
4.	Water 400 ml at boiling point + add commercial starch 50g slowly and stir continuously + remove sample from stove and add 500g biochar and vigorously stir the components

Fig. 3: Biochar pellets prepared using different binding materials

Biochar pellet yield from a given treatment was calculated as:

Biochar pellet yield (%) =

$$\frac{\text{Mass of biochar pellets in the specified size range, g}}{\text{Total mass of biochar pellets produced, g}} \times 100 \quad \ldots(5)$$

Moisture retention related properties

Moisture content

Moisture contents of raw biochar used, pellet mix, and pelleted biochar were determined by hot air oven method. Samples from the four freshly added binding materials before rolling into pellets, after rolling into pellets, and from dried pellet samples were drawn. These samples were weighed using an electrical balance (capacity: 1000g, least count: 0.001g), and then oven-dried using a cabinet type tray hot air drier (SISCO Make, Model: 3636) at 105 °C for about 24 h. Oven-dried samples were re-weighed, and per cent moisture content determined on dry weight basis (d.b.).

Water capacity and hygroscopicity

Available water capacity (AWC) is required for plant growth, which is the difference between the field capacity (FC) and wilting point (WP) of any soil amendment.

Field capacity and wilting points were measured by subjecting the samples to 0.3 bar and 15 bar pressures, respectively, dried and weighed. The pressure plate apparatus used in the study was of Soil Moisture Equipment Co. make, California, USA.

Hygroscopicity of raw biochar and pelleted biochar was determined by measuring the change in moisture content of the samples after exposure to air at 60 % and 80 % humidity in a controlled temperature chamber having fan and pad system. Biochar powder and pellets weighing 7g were spread in a thin layer on trays, and placed in a humidity chamber with separate samples for 48 h at each humidity setting. The temperature and humidity of the air within the chamber were maintained at constant levels during the period. After 48 hr, moisture contents of the samples were determined by oven drying method.

Bulk density, true density and porosity

Bulk density is the ratio of the mass of pelleted biochar samples to its total volume. Biochar pellet sample was filled in a cylindrical jar having diameter of 62 mm and 92 mm in depth. The weight and volume occupied by the dried pellets prepared with four binding materials were recorded.

The pelleted biochar material being a disintegrable substance, the toluene displacement method was used to determine the true density, which is defined as the ratio of mass of the pelleted biochar to the true volume of displaced liquid (Mohsenin, 1980). True density was determined by taking 5g of weighed pelleted biochar and filling in a glass cylinder containing 50 ml of toluene. The difference in liquid volume by displacement in the graduated volumetric cylinder.

Porosity was deduced from the true and bulk density values. Similarly, particle density of pellet was measured using a Picnometer of 200 ml capacity.

Mechanical properties

Terminal velocity

Terminal velocity is an important parameter and considered in calculating the air suction needed in the metering devices of pneumatic-type mechanical applicator. Terminal velocity of biochar pellet was measured experimentally by using a laboratory terminal velocity apparatus. The setup consisted of a transparent glass tube to view the status of an object under investigation in an adjustable flowing air stream, and a small hopper to release the pellets in a controlled manner at the lower portion of the tube. A wire mesh was provided in the transparent tube just above the air entrance point. For each test, about 100 g of sample was used, and air blown from the bottom of the wire mess in the upward direction through a regulating device for varying air flow to suspend the material in the air stream for 30s. The air flow rate was varied till the air stream lifted most of the material. The air flow rate was used to calculate velocity using the equation described by Kachru *et al.* (1994).

Angle of repose

Angle of repose of pellets was determined using an open-ended plywood box having dimensions of 255×25.5×260 mm provided with a removable front panel. The box was filled with pellet samples, followed by quickly removing the panel so that pellets could flow and assume a natural slope. The angle of repose was calculated from the measurement of depth of the free surface of the sample at centre, and the base diameter of the heap formed, using the following formula

(Meghwal and Goswami, 2011):

$$\omega = \tan^{-1}\left(2h/d\right) \quad \ldots(6)$$

Where,

ω = Angle of repose, degree,

h = Height of heap, mm, and

r = Radius of heap, mm.

Static co-efficient of friction

The static coefficient of friction of biochar pellets was determined on four different materials, namely, plywood, mild steel sheet, aluminium sheet, and galvanized iron sheet for pellets prepared with the four binding materials following the procedure described by Kumar *et al.* (2016).

A tilting platform of 350×120 mm was fabricated and used for experimentation. A top and bottomless thin-walled mild steel cylinder (49.4×90 mm) was filled with pelleted biochar, and placed on the adjustable tilting surface. The cylinder was slightly raised so as not to touch the surface. The tilting platform with the cylinder resting on it was gradually inclined with a screw lever device until the cylinder just started to slide down. The angle of tilt platform surface was read from a graduated scale.

Static co-efficient of friction was determined as:

$$\mu = \tan\theta \quad \ldots(7)$$

Where,

μ = Co-efficient of friction, and

θ = Angle of inclination, degree.

Attrition resistance

Pellets within the size range of 1-4.75 mm were tested for strength using an attrition resistance testing device (Tumbler device) developed under the study. The tests involved agitation of the pellets with or without additional solids of steel medium to provide enhanced agitation, and comparison of size changes through sieving. For attrition resistance measurements of biochar pellet, a 20g sample along with 10 number of 5 mm diameter steel beads were placed in a tumbler device (diameter: 60 mm, length: 90 mm) with internal flights. The tumbler was rotated at 30 rpm for 510 rotations. The pellets were then sieved with a 1 mm sieve and reweighed.

The resistance to attrition was calculated as:

$$\text{Attrition resistance (\%)} = \frac{\text{Pellet mass after test , g}}{\text{Pellet mass before test , g}} \times 100 \quad \ldots(8)$$

Crushing strength

A force gauge was developed to determine the crushing strength of individual pellet, and test procedure standardized under this study.

The minimum force required for crushing granule was measured by applying diametric compression to an individual granule of a specified range, and noting the pressure required for fracturing each pellet. A hand-held portable force gauge (Make: CEP Services Pvt. Ltd, Singapore, Model: S-170, Foot diameter: 6.35 mm, Maximum load: 5.5 kg) was used for measurement of crushing strength. Two uniform size pellets (3 mm and 5 mm) formed with each binding material were taken. Individual sample was kept on a horizontal metal platform, and the movable lower face of the instrument plunger rod was placed vertical above the test pellet. The instrument was held firmly with palm, and force was uniformly applied at the top of the plunger with the right-hand thumb finger until the pellet buckled/ cracked. As long as the pellet remained intact, the plunger moved down pushing a frictionless marker ring under force on the sleeve, and instantly retracted upwards once the pellet developed crack / crumbled. The marker ring displayed the reading (in $kg.cm^{-2}$). The crushing strength of pellet was read on the plunger sleeve with the help of a lens.

Statistical Analysis

Each experimental trial was measured with four replicated samples. The data sets were analysed using completely randomized block design. A statistical software package 'Dry Soft' developed by the ICAR-CRIDA, Hyderabad, was used for the factors considered and the levels of variables.

RESULTS AND DISCUSSION

The agglomeration process of biochar with thermally treated binders in a batch-type drum pelletising machine was studied. The important physio-mechanical properties of biochar pellets which play major role in handling, application processes using mechanical equipment, stability in storage and crop growth were also studied. The physical properties of raw biochar and that of pellets prepared using binding materials were measured by standard procedures.

Drum Pelletising Machine Process Parameters

Ten combinations of quantity of water, binder materials and biochar samples in limited quantity were prepared, and the mixture consistencies were checked by rolling into small balls with both palms. Whenever the biochar – binder combination was not too sticky and could be moulded into small balls, such mixtures were transferred into the drum pelletiser and rolled keeping a watch on the pelletising process and time required to agglomerate into near uniform size pellets. While processing, the drum rotational speeds were varied from 40 - 90 rpm, and process times from 5 - 25 min.

The pelletising machine could deliver sufficient quantity of pellets (in size range of 1-4.75 mm) at rotational speed of 60 rpm and operational time range of 10 – 12 min. The pellets were spherical in shape with asperities on the outer surfaces. After stipulated operational time period of each batch, the pellets formed were taken out by opening the lid of the drum. The input capacity of the drum pelletiser was 1000 g of fresh mixture per batch, and 930 g of pellet yield was obtained. The observed rotational speed of the pelletiser (60 rpm) was higher than the theoretical speed, because the samples used in this study were binder- water pre-mixed ones rather than dry powder as assumed for theoretical considerations. The theoretical rotational speed served as a lower boundary condition to initiate the experiment.

Particle Size Distribution of Pellets

Sieve analysis of dried biochar pellets samples indicated that the quantity of desired size granules (1 - 4.75 mm) varied from 50.34 % to 66.41 % (weight basis) for various binding materials (Table 3). The highest quantity of desired sized pellet yields achieved for various binding materials was of commercial starch (66.41 %), followed by rice starch (62.77 %), maize flour (56.45 %); while the least was CMC (50.34 %). Statistical analysis showed that the binder material significantly influenced the pellet yield. Pellet yields of desired size from biochar powder with the four binding materials were higher compared to other reported studies using hydroxypropyl methylcellulose (HPMC) binder as 43.0 % (Bowden - Green and Briens, 2016a) and organic fertilizer granules of limestone powder and anaerobic digestion liquor as 46.0 % (Mangwandi *et al.*, 2013).

Moisture Content Related Properties

Moisture content

Pellets samples were randomly drawn to determine the moisture content of fresh biochar pellets as well as the dried pellets for determination of the physio-mechanical properties. The results are presented in Table 4.

Biochar moisture content was 6.5 % (d.b.), and was almost dry. Moisture contents of fresh biochar pellets produced using four binder materials ranged from 59.03 % to 63.79 % (d.b.), and that of dried pellets from 2.25 % to 3.67 % (d.b.). The range of moisture content of fresh biochar pellet was narrow with variation of 4.76 % using about 400 ml of water for 500g of biochar powder and different quantities of various binding materials. The narrow range of moisture content of dried pellets indicated that the samples were dried properly and variation in determined properties occurred only due to the effect of binding materials and their effects on rolled pellets.

Majority of the available recommendations of researchers were for powder biochar material due to lack of studies on granulation technology with biochar and performance of pelleted material in its homogeneous distribution or interaction with the soil matrix. In recent past, the choice of application of granulated biochar, instead of the more common powder form, was motivated by the greater efforts made by researchers to make available biochar pellets using various binder materials (Antanas *et al.*, 2016; Desta *et al.*, 2017; Joung and Sang, 2018). Better understanding of the mechanisms of incorporation of coarse biochar pellets that affect even in the short term, hydrological

Table 3. Effects of binder treatment on yield of various size range biochar pellets (% weight)

Sl. No.	Binding material	Over size, > 4.75 mm	Desired size, 1-4.75 mm	Under size, < 1 mm
1.	Maize flour	34.20	56.45	9.35
2.	Rice starch	31.63	62.77	5.60
3.	CMC	40.72	50.34	8.94
4.	Commercial starch	28.70	66.41	4.89
	Size: 1 – 4.75 mm	F -test = 26.57**	SEm = 1.96	LSD (0.01) = 6.37

Table 4. Moisture content of fresh and dried pellets of different treatments

Treatment	Moisture content, % (d.b.)	Moisture content, % (d.b.)
Powder biochar	06.50	-
	Fresh pellet	Dried pellet
Maize flour binder	60.24	2.85
	60.86	2.69
Rice starch binder	59.03	2.25
	59.13	2.62
CMC binder	62.83	3.42
	62.76	3.45
Commercial starch	63.79	3.67
	63.25	3.66

behaviour alone and in combination of soil matrix also supported the shift to use of granulated biochar. The hydrological properties (as available water capacity, hygroscopicity) were, therefore, studied.

Biochar is not merely another type of compost or manure, but is more efficient in enhancing soil quality than any other organic soil amendment (Lehmann and Joseph, 2009). Biochar produced from agricultural residues feed stocks can provide a small amount of nutrients, whose contribution to crop productivity is likely to be for short term. However, properties like stability in soils, high water-holding capacity, and high nutrient (soil organic matter) retention has significant potential to increase irrigation and fertilizer use-efficiencies. Previous studies in these aspects (Gaskin *et al*., 2007; Sohi *et al*., 2009) showed the benefits of biochar to crop yield through higher moisture retention as a key factor. This might be of advantage in sandy loam and coarse texture soils that generally have lower moisture holding capacity.

Field capacity and hygroscopicity

The results of hydrological properties are presented in Table 5. The field capacity and wilting point of pelleted material was 1.5 and 0.92 times, respectively, the weight of raw biochar. Significant variation was, however, not observed among pallets prepared using different binding agents. The pelleted biochar materials of all treatments showed lower moisture holding capacity when compared with powder biochar in raw form. This might have occurred as the raw biochar particles were very small in size and possessed larger surface area with moisture particles spreading the entire surface. The same might not have occurred in pelleted biochar as some of the inter-granular space was lost due to compression during rolling of the biochar into pellets.

Hygroscopicity of biochar material and pellets was low; and there was not much difference among the pellets prepared using different binder materials, and under two relative humidity conditions. Hygroscopicity of pellets ranged from 1.5 % to 2.6 % (d.b.), which clearly indicated that they were non-hygroscopic in nature. Even after 48 h of exposure to air at a humidity of 80 %, the moisture content of the powder reached 2.6 % (d.b.). This was in conformity to the observation reported by Bowden – Green and Briens (2016a). The pelleted materials with negligible hygroscopicity could be expected to be more stable without formation of lumps during storage in farms unlike some commercial fertilizers.

Bulk density, true density, porosity and terminal velocity

The observed bulk density, true density and porosity values for different binder added biochar pellets ranged from 276.1 kg.m^{-3} to 390.2 kg.m^{-3}, 819.7 kg.m^{-3} to 905 kg.m^{-3}, and 0.53 - 0.69 %, respectively. The nature of binders significantly influenced the bulk density of pellets. The CMC binder-added pellets exhibited lowest bulk density of 276.1 kg.m^{-3}, highest true density of 905 kg.m^{-3} and highest porosity of 0.69 % (Table 6). Bulk density of pellets was about 2.0 - 2.5 times lower than the granular commercial fertilizers such as prilled ammonium nitrate, diammonium phosphate, granular urea and granular triple superphosphate (Fulton and Port, 2016). They were half of organic granular fertilizers prepared from dairy cattle and poultry manures with pressurized pelletising machine

Table 5. Hydrological properties of biochar pellets (1-4.75 mm size)

Binding material	Field capacity, % (d.b.)	Hygroscopicity moisture, % (d.b.)	
		At 60% RH	At 80% RH
Biochar raw powder	93.0	1.5	2.1
Pellets prepared with different binders			
Maize flour	61.7	1.6	2.6
Rice starch	60.0	1.7	2.4
CMC	78.0	1.6	2.2
Commercial starch	57.8	1.8	2.4
F-test	95.17**	Binder (B) = NS	LSD (P=0.01) = NS
SEm	1.33	RH = 25.87**	0.398
LSD(P=0.01)	4.919	BXRH = NS	NS

Table 6. Bulk density, true density, porosity and terminal velocity of biochar pellets (1-4.75 mm size)

Binding material	Bulk density, $kg.m^{-3}$	True density, $kg.m^{-3}$	Porosity, %	Terminal velocity, $m.s^{-1}$
Maize flour	353.4	882.4	0.59	2.14
Rice starch	390.2	833.3	0.55	1.90
CMC	276.1	905.0	0.69	2.06
Commercial starch	341.4	819.7	0.53	2.22
F - test	127.06**			
SEm	6.515			
LSD (P=0.01)	21.17			

as reported by Mangwandi *et al.* (2013). Bulk density is also important in design of hopper of field application machines to avoid a greater number of stoppages for fillings, since the application rates recommended was high in case of sole pellets. However, the pellets possessed fair flowable characteristics in terms of hygroscopicity and angle of repose, and can be metered at higher flow rates without their particles bridging during conveyance.

The terminal velocity of pellets varied from 1.9 $m.s^{-1}$ to 2.22 $m.s^{-1}$, but not much variation was observed among the treatments (Table 6). Terminal velocities of biochar pellets were lower than grain materials (about 7.5 $m.s^{-1}$ for wheat; 7.78 $m.s^{-1}$ for barley, and 7.78 $m.s^{-1}$ for lentil) and organic based granular fertilizers. These properties are important in design of components of air assisted application and conveyance equipment for field applications.

Angle of repose, coefficient friction and pellet strength

The measured angles of repose were about 40^0 for various pellets (Table 7). There was not much difference in the angle of repose of various binding materials rolled pellets, and the differences were statistically not significant. As for the Carr classification of flowability (ASTM – D6393, 2014), the pellets were in the category of "fair to passable flow" with angle of repose ranging between $38^0 – 45^0$. So, the pellets were amenable to mechanical equipment used in storage, handling, metering and placement in soils. Keeping the angle of repose of pellets in mind, the side wall face of the application machine hopper should be kept at an inclination angle of 42^0 to the horizontal to ensure free movement of pellets from upper storage portion to the lower portion of a hopper.

The coefficient of friction of various agricultural

Table 7. Angle of repose and coefficient of friction of biochar pellets (1-4.75 mm size)

Binding material	Angle of repose, Deg	Influence of surfaces on coefficient of static friction			
		Al Sheet	MS Sheet	GI Sheet	Plywood
Maize flour	40.46	0.642	0.554	0.690	0.724
Rice starch	41.11	0.639	0.518	0.649	0.670
CMC	40.21	0.681	0.610	0.582	0.848
Commercial starch	40.13	0.649	0.592	0.670	0.722
F – test				SEm	LSD (0.01)
	NS	Binder (B) = 81.76**		0.006	0.016
		Surface (S) = 54.04**		0.006	0.016
		B X S = 11.01**		0.012	0.032

(Al: Aluminium, MS: Mild steel, GI: Galvanized iron)

inputs such as seed, fertilizer as well as any soil amendments on various metal surfaces is important in selecting appropriate materials required to ensure easy gravitational flow. Coefficients of friction data of various sheet metal surfaces indicated that the pellet binders, metal sheet surfaces individually and their interactions significantly influenced in contrast to the angle of repose (Table 7). Coefficients of friction ranged from 0.52 to 0.85. Plywood offered the highest coefficient of friction (0.67 to 0.85) for pellets with four types of binding materials; followed by galvanized iron sheet, and the least was on mild steel sheet (0.52 to 0.61). Among the treatments, rice starch binder material added pellets recorded lower friction in the range of 0.52 to 0.67. Higher degree of friction experienced between a material and another surface such as spinning disc in a grain or fertilizer spreader causes longer contact time, resulting in a larger departure angle, that might give uneven spreading. The coefficients of friction of biochar pellets on aluminium, mild steel and GI sheet was close to some commercial granular fertilizers as reported by Fulton and Port (2016). The lower the coefficient of static friction for a given material, higher was the mobility, hence requiring smaller hopper opening and lower hopper side wall slopes.

Attrition resistance

Attrition resistance is the resistance to fragment into formation of dust and fines and fracturing of any granular material. In granular materials such as seed, fertilizer, organic granular soil amendment, fracturing happens because of the occurrence of granule-to-granule and granule-to-equipment component contacts during storage, handling and transport from production to end-use. Attrition resistance was determined by measuring the percent dust and fines created by subjecting a biochar pellets to attrition action.

Materials having higher attrition losses while in field application would create fine particles that could then become airborne. In the present study, maximum attrition loss was less than 10 % (Fig. 4). Figure 4 further showed that the type of binder material used and presence of similar size harder materials significantly influenced the attrition resistance (Table 8). Rice starch binder added pellets showed higher resistance of 97.21 % with beads and 99.21 % without beads, followed by commercial starch (97.37 % and 99.16 %). The observations indicated that the damage due to inter-granular pellet-to-pellet was lower than external material (steel bead) interaction of similar size. Granular materials that exhibit a higher mass loss during the tests are considered to be more prone to attrition or low resistant. The factors inherent to pellets that also influence granule strength primarily was granule porosity, and lower the porosity the granules strength would be higher (Bowden - Green and Briens, 2016a). Minimal attrition is desirable in most cases to reduce product loss as dust, to avoid a hazardous work environment, and to mitigate other dust related issues.

In the drum granulation process pellets consolidation occurs through particles collisions with other particles and the walls of the drum and it reduces the porosity thereby increasing the granule strength. The agitation from the drum rotation provided stronger forces and more opportunities for granule collisions thereby increasing consolidation and granule strength. Granule behaviour during a rolling is controlled by inter-particle friction, concentration and liquidity of binder material used. As granules consolidate, inter-particle friction

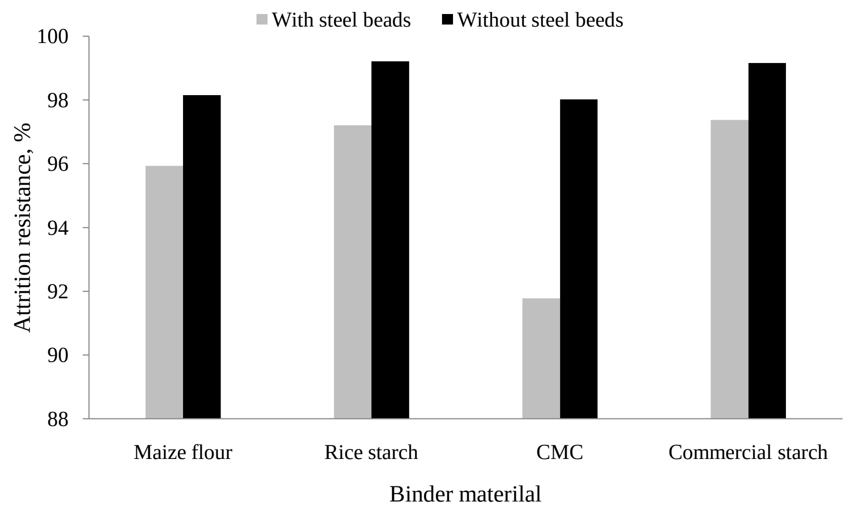

Fig. 4: Attrition resistance of biochar pellets

Table 8. Statistical analysis for attrition and crushing strength of pellets

Statistical test	Attrition resistance, %			Crushing strength, $kg.cm^{-2}$		
F-test	Factors	SEm	LSD(P=0.01)	Factors	SEm	LSD(P=0.01)
	Binder(B)=9.05**	0.740	2.181	Binder(B)=31.94**	0.151	0.444
	Medium(M)=34.05**	0.523	1.542	Pellet Size(Ds)=17.77*	0.107	0.314
	B XM=4.14*	1.047	LSD(P=0.05) =2.231	B XD=NS	0.213	NS

and viscous resistance increase as the number of inter-particle contacts increases. Increasing the viscosity of the binder solution reduces the rate of consolidation while pellets rolling (Litster and Ennis, 2004).

Crushing strength

One more damage that is expected to occur in use of pelleted biochar material is crushing of pellets during handling, storage and even during field application using mechanical equipment like scooper, spreader, band application machine like fertilizer application drills and planters. As depicted in the Fig. 5, the crushing strength was significantly influenced by binding material as well as pellet size to some extent (Table 8). However, the binding material and pellet size interaction was not significant. The crushing strength of pellet made with commercial starch was highest (2.50 $kg.cm^{-2}$), followed by rice starch binder medium. The CMC added pellets had low crushing strength in the range of 1.25 $kg.cm^{-2}$ to 1.58 $kg.cm^{-2}$, hence it could be expected that the pellets may easily be damaged while storage, transport and other handling processes.

The maximum crushing strength recorded was 2.5 $kg.cm^{-2}$ for pellet of 3 mm diameter using commercial starch binder. This was less than crushing strength of biochar granule of HPMC binder solution (1.5–4.0 $kg.cm^{-2}$) as reported by Bowden - Green and Briens (2016b).The results of the present study were, however, within acceptable limit for handling and storage as per the Fertilizer Encyclopaedias (Gowariker *et al.*, 2009). Pellets in the size range of 2.36 mm to 2.80 mm diameter with a crushing strength of less than1.5 $kg.cm^{-2}$ tend to fracture easily and transform into dust during handling. Particles with a crushing strength in the range of 1.5 $kg.cm^{-2}$ to 2.5 $kg.cm^{-2}$ would need special handling precautions. Biochar pellets of 5 mm size prepared with commercial starch and rice starch showed promising results with crushing strength of 2.50 $kg.cm^{-2}$ and 2.44 $kg.cm^{-2}$, respectively.

It was observed that the strength of 5 mm biochar pellet was more by 18.85 % to 28.34 % than that of 3 mm diameter for all binding materials. Similar observations were reported by Gowariker *et al.* (2009). At higher limit of pellet diameter, except CMC binder,

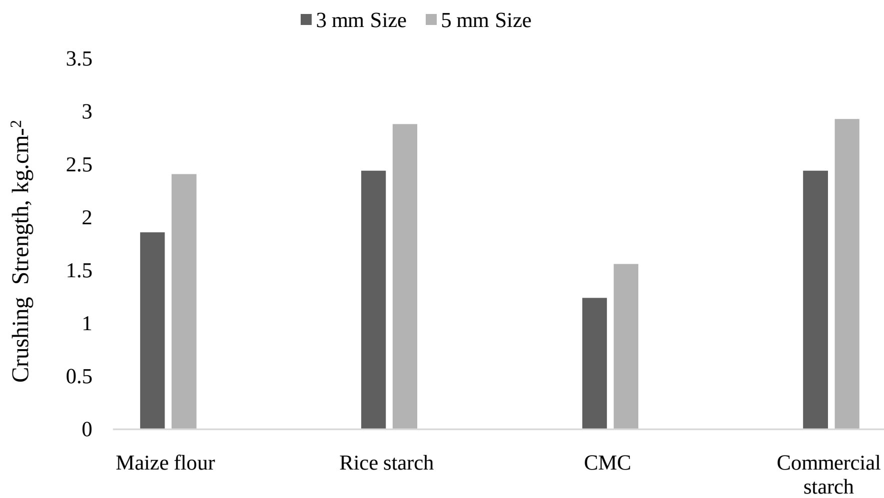

Fig. 5: Crushing strength of pellets using various binding materials and sizes

other 3 binding materials showed crushing strength in the promising range. In general, crushing strength increased significantly with particle size and binder, but for all practical purposes pellets of equal size should be considered for comparing the results.

The application quality of dry granular fertilizer or any other granular soil amendment depends on several variables. In general, the performance of a distributor or applicator can be contributed to 1/3 material characteristics alone (Antille *et al.*, 2015). Important mechanical properties like angle of repose, coefficient of friction and crushing strength values were numerically comparable with that of spherical or near spherical fertilizer of granular urea, DAP and prilled ammonium nitrate (Fulton and Port, 2016). Hence, it is expected that the biochar pellets have proper ability in terms of metering, deposition and uniform distribution. However, this needs to be corroborated under actual field conditions.

CONCLUSIONS

A drum-type pelletiser with three commonly available binders' maize flour, rice starch, commercial starch and ananalytical binder (CMC) material was used for pelletisation of biochar. The results indicated that the nature of binder had strong influence on pellets yield in the desirable size range of 1-4.75 mm, and the pellets possessed desired angle of repose, coefficient of friction, attrition resistance and crushing strength. The technology needs to be upscaled to produce pellets on farm-scale, field tested and enhance the uses by enriching them with different types of nutrients, custom made organic fertilizers.

REFERENCES

Alexandre T; Francesco C. 2019. Potentials, limitations, co-benefits and trade-offs of biochar applications to soils for climate change mitigation. Land, 8, 179, 1-34.

Antanas P; Jotautiene E; Juozas P; Palsauskas M. 2016. Investigation of physical-mechanical properties of experimental organic granular fertilizers. Eng. Rural Dev., 25, 1115 -1120.

Antille D L; Gallar L; Miller PCH; Godwin R J. 2015. An investigation into the fertilizer particle dynamics of the disc. Appl. Eng. Agric., 31(1), 49-60.

ASTM. 2014. Standard Test Method for Bulk Solids Characterization by Carr Indices. ASTM-D6393, ASTM International, Book of Standards, 04.09, pp:8.

Bishop P; Hedley M; Knox C; Rikhihana P; Jones J. 2012. Practical aspects on the production of biochar and its delivery to soil. In: Proc. Biochar Workshop 2012, New Zealand Biochar Research Centre, Massey University, 32, 2308-2316.

Brewer C E. 2012. Biochar characterization and engineering. Unpublished Graduate Thesis, Iowa State University, USA. Accessed at https://lib.dr.iastate.edu/etd/12284.

Bowden-Green B; Briens L. 2016a. An investigation of drum granulation of biochar powder. Powder Technol., 288, 249 - 254.

Bowden-Green B; Briens L. 2016b. Granulation of biochar for soil amendment. Electronic Thesis and

Dissertation Repository, The University of Western Ontario, Canada. Accessed at https://ir.lib.uwo.ca/etd/3475.

Desta W; Pay D; Bernd M; Fisseha I; Heluf G. 2017. Effect of biochar derived from faecal matter on yield and nutrient content of lettuce (*Lactuca sativa*) in two contrasting soils. Environ. Sys. Res., 6, 2, 1-12.

Fulton John; Port Kaylee. 2016. Physical properties of granular fertilizers and impact on spreading. Fact sheet. FABE-550.1, The Ohio State University. Accessed at http://ohioline.osu.factsheet/fabe - 550.1.

Gaskin J W; Speir A; Morris L M; Ogden L; Harris H; Lee D; Das K C. 2007. Potential for pyrolysis char to affect soil moisture and nutrient status of loamy sand soil. In: Proc. Georgia Water Resources Conference, 27-29March, 2007, University of Georgia, USA. Accessed at http://www. gwri.gatech.edu/conferences/previous-gwrc-conferences/gwrc-2007.

Gowariker V; Krishnamurthy V; Gowariker S; Dhanorkar M; Paranjape K. 2009. The Fertilizer Encyclopaedia. John Wiley and Sons Inc., Hoboken, New Jersey, pp: 861.

Hirjau M; Nicoara A C; Hirjau V; Lupuleasa D. 2011. Pelletization techniques used in pharmaceutical fields. Pract. Pharm., 4(4), 206-211.

Joung D S; Sang W P. 2018. Optimization of blended biochar pellet by the use of nutrient releasing model. Appl. Sci., 8, 2274. Doi: 10.3390/app8112274.

Hilaidhari M; Das D; Baruah D C. 2014. Bioenergy potential from crop residue biomass in India. Renewable Energy Rev., 32, 504-512.

Hofstee J W; Huisman W. 1990. Handling and spreading of fertilizer part I: Physical properties of fertilizers in relation to particle motion. J. Agric. Eng. Res., 47(4), 213-234.

Hu Q; Jingai S; Haiping S; Dingding Y; Wang Y; Chen H. 2015. Effects of binders on the properties of bio-char pellets. Appl. Energy, 157, 508-516.

Kapur P C; Fuerstenau D W. 1969. A coalescence model for granulation: Industrial process design and development. Indian Chem. Eng., 8, 56-62.

Kachru R P; Gupta R K; Alam A. 1994. Physio-chemical Constituents and Engineering Properties of Food Crops. Scientific Publishers, New Delhi, India, pp:188.

Kumar J; Prabhakar P K; Srivastav P P; Bhowmick P K. 2016. Moisture dependent physical properties of chironji nut. J. Agric. Eng., 53(2), 45-53.

Lehmann J; Joseph S. 2009. Biochar for Environmental Management: Science and Technology. Earths can Publishers, London, U.K., pp: 405.

Litster J; Ennis B. 2004. The Science and Engineering of Granulation Processes. Kluwer Academic Publishers, Dordrecht, Netherlands, pp: 247.

Luiz C G; Renan N D; Carlos H R; Natali M S; Pedro H W N. 2017. Performance of fertilizer metering mechanisms of planters as function of longitudinal inclination. J. Braz. Assoc. Agric. Eng., 37(6), 1155-1162.

Major J M; Rondon M A; Molina D; Riha S J; Lehmann J. 2010. Maize yield and nutrition during 4 years after biochar application to a Colombian Savanna oxisol. Plant Soil, 333 (1-2), 117-128.

Mangwandi C L; Jiang Tao; Albadarin A B; Allen S J; Walker G M. 2013. Alternative method for producing organic fertilizer from anaerobic digestion liquor and limestone powder: High shear wet granulation. Powder Technol., 233, 245-254.

Meghwal M; Goswami T K. 2011. Effect of moisture content on physical properties of black pepper. J. Agric. Eng., 48(2), 8-14.

Mohsenin N N. 1980. Physical Properties of Plant and Animal Materials. 3rd Edition, Gordon and Breach Science Publishers, New York, pp: 742.

Rajagopalan S; Murthy D V S. 1988. A method for granulation of fertilizer. J. Inst. Eng. (India), 68 (2), 46-49.

Rutland D; Polo J. 2005. Fertilizer Dealer Hand Book: Products, Storage and Handling. IFDC -An International Centre for Soil Fertility and Agricultural Development, Muscle Shoals, Alabama, pp: 37.

Sirisha V R K; Suresh K; Vijayasree K; Devanna N; Murthy P N. 2014. Recent advances in pelletisation techniques: A review. Int. J. Pharma. Sci. Rev. Res., 27(1), 217-223.

Sohi S; Lopez-Capel E; Krull E; Bol R. 2009. Biochar, Climate Change and Soil: A Review to Guide Future Research. CSIRO Land and Water Science Report 05/09, Victoria, Australia, pp: 64.

Sohi S; Krull E; Lopez-Capel E; Bol R. 2010. A review of biochar and its use and function in soil. Adv. Agron., 105, 47-82.

Tripathi M; Sahu J N; Ganesan P. 2016. Effect of process parameters on production of biochar from biomass waste through pyrolysis process: A review. Renewable Sustainable Energy Rev., 55, 467-481.

Tumuluru Jaya Shankar; Wrigt Christopher T; Hess J Richard; Kenney Kevin L. 2011. A review of biomass densification systems to develop uniform feedstock commodities for bioenergy application. Biofuels Bioprod. Bioref., 5, 683-707.

Venkatesh G; Venkateswarlu B; Gopinath K A; Srinivas Rao C H; Korwar G R; Sanjeeva Reddy B. 2013. Low cost portable kiln for biochar production. NICRA Technical Broachure, ICAR -Central Research Institute for Dryland Agriculture, Hyderabad, pp: 6.

Walker G M. 2007. Drum Granulation Process. In: Hand Book of Powder Technology, Book chapter 4, Elsevier, Netherlands, 219-254.

Williams M M; Arnott J C. 2010. A comparison of variable economic costs associated with two proposed biochar application methods. Ann. Environ. Sci., 4, 23-30.

INFORMATION FOR AUTHORS

The Journal of Agricultural Engineering contains only original research papers, and submission of a manuscript will be considered to imply that no similar manuscript has been or is being submitted elsewhere. Soft copy of the manuscript in MS Word, along with a request letter, should be submitted to the Chief Editor through website of ISAE, IndianJournals.com, or through e-mail (jae.chiefeditor@gmail.com). The manuscript is to be written in English language, typed in double space on A-4 size. The e-mail address and mobile number of the corresponding author must be indicated for further correspondence.

The subject matter reflects the full range and interdisciplinary nature of research in engineering and allied disciplines for agriculture. Manuscripts describing engineering innovations for field crops, horticulture, livestock, fisheries, and those reporting research seeking to understand and model the physical processes underlying agricultural systems are welcome.

The following three types of manuscripts are invited for publication. Research manuscripts are the normal type of papers published and make up the main content of the Journal. They should not normally exceed 15 Journal pages. Research notes enable important findings to be speedily communicated, and facilitate the reporting of work not meriting a full-length paper. They should not exceed five Journal pages. Review papers are intended to be in-depth studies of the state-of-the-art in the chosen subjects. They should not normally exceed fifteen Journal pages.

The manuscript should be arranged as follows:

Softcopy in MS Word (Times New Roman), Font size for various sections are: Font: Times New Roman, Title heading: 14 pt bold upper lower, Author name: 11.5 pt italic bold u/L, Abstract heading: 11pt bold cap, Abstract text: 9 pt normal, Text: 10.5 pt normal, Sub-heading : 9 pt Cap bold centre, Fig/ table caption: 10 pt bold u/l centre, Conclusion and references: same as text, Footnote: 8 pt italics.

- *Title, authors'name(s), affiliations, addresses.* Please necessarily include e-mail address of the corresponding author.
- *Abstract and key words.* The Abstract of not more than 200 words should state the problem investigated, outline the methods used and summarize the main conclusions. A list of maximum seven keywords or phrases must follow the abstract.
- *Main body text.* The main body of the text should be divided under suitable headings, in proper hierarchical order. Some or all of the following headings may be appropriate.
  - *Introduction:* This should explain the problem investigated, review of recent (*not older than 10 years, unless of classical nature*) related studies, and statement on the intention of the present manuscript. The objective(s) of the reported investigation must be stated.
  - *Materials and Methods*: Include theoretical considerations appropriate to explain or develop a theory to shed light on a problem or to correlate experimental results, design of experiment, experimental procedures and details, technical details of instruments/ equipment used, statistical procedures used, as applicable
  - *Results and Discussion*: The results should be presented with reference to appropriate figures and tables. The most appropriate presentations should be chosen and tabulated data should not duplicate that shown graphically. The discussion must include the comparison of findings with the previous research studies done
  - *Conclusions:* Research and Review papers must have this final section, but it is optional in Research Notes. Conclusions emerging from the work should be succinctly summarized. These conclusions must have been discussed in the manuscript and new material must not be introduced at this stage. The contents of the Abstract and Conclusions should not be repetitive.
- *List of symbols*
- *Acknowledgments:* Optional.
- *References:* Citations of references in the text should be in the format of surnames of authors, followed by the year of publication of the appropriate reference, separated by a semi colon. The artifice "Leading author *et al*." should be used in the text for multiple (more than two) authorship papers. Each reference should give the names of all authors (or, if anonymous, the name of the organisation), the year of publication, the title in that order. Some examples of references are given below.

  In the text: "Previous work has shown (Hammer and Langhans, 1972; Federer, 1955) ..."

  In the references 1ist (to journals):
  Sharma P; Sharma S R; Mittal T C. 2020. Effects and application of ionizing radiation on fruits and vegetables: A review. J. Agric. Eng., 57 (2), 97-126.
  Reference list (to books): **Saldivar S O S.** 2015. Snack Foods: Types and Composition. Reference Module in Food Science Encyclopaedia of Food and Health, Elsevier, 13-18.
- *Appendices:* It may be appropriate to place detailed mathematical derivations in appendices, rather in the main body of the text.
- *Figure captions:* These should be listed, together with any 'key' information necessary to aid interpretation.
- *Tables:* Each table must be placed on a separate page after References, and chronologically numbered throughout the text (with Arabic numerals), and referred to as Table 1, Table 2, etc. There must be a caption (Table 1. Estimated saturated hydraulic conductivity using different particle sizes) at the top of each Table.
- *Figures*: Figure 1, Figure 2, etc. Figure captions should be placed beneath each figure (Fig. 1: Effect of germination and roasting on colour of chickpea), and should also be placed in separate page after References. The publisher will suitably organise them after acceptance of the manuscript.

All illustrations, whether line drawings, graphs or photographs, are presented as figures and are given numbers (e.g. Fig. 1) in ascending numerical order as reference is first made to each in the text. All graphs must be submitted in EXCEL software embedded in the Word file, and the respective data made available in a separate spreadsheet included with the softcopy of the manuscript. All figures must be in pleasing colours in good contrast. The style of graphs may be seen in any recent issue of the Journal. Softcopies of the line drawings is acceptable, without title, provided they are in printable quality.

Journal of Agricultural Engineering

ISSN (Print): 0256-6524
ISSN (Online): 0976-2418
www.isae.in

VOL. 57, No. 3, July-September 2020

Contents

Page

Design and Performance Evaluation of Self-propelled Intra-Canopy Boom Spraying System
— *Bhabani Shankar Dash, Arun Kumar, Rajesh U. Modi and Sharad Kumar Namdev* 195

Enhancing Shelf-life of Fresh-cut Carrot and Cauliflower Floret with Combined Ozone and Ultraviolet-C Radiation Treatment
— *S. K. Giri, Sadvatha R. H., M. K. Tripathi and Dilip A. Pawar* 210

Qualitative Analysis of Roasted and Germinated Green Chickpea for Snack Food: Proximate, Functional and Pasting Properties
— *Yogesh Kumar, Vijay Singh Sharanagat, Lochan Singh, Promita Gundev, Saravanan Mani and Prabhat K. Nema* 226

Rheological and Surface Properties of Edible Coating Solution Prepared from Vasa Plant (*Justicia Adhatoda* L.) Leaf Extract
— *Hanumantharaju K. N., Thangavel K. and Ganapathy S.* 236

Performance Evaluation of Subsurface Drainage System under Waterlogged Saline Vertisols for Sugarcane Crop in Ukai Kakrapar Canal Command, Gujarat
— *Anil R. Chinchmalatpure, Sagar D. Vibhute, M. J. Kaledhonkar, Sanjay Vasant Kad, Shrvan Kumar, David Camus, Indivar Prasad, S. K. Kamra and P. C. Sharma* 248

Suppressing Evaporation from Surface Water Reservoirs: A Review
— *S. Deepika, M. Osman, Manoranjan Kumar and H. Sandeep* 259

Biochar Pelletisation and Physio-mechanical Properties of Pellets
— *Syed Imran, B. Sanjeeva Reddy, D. Ashish and G. Venkatesh* 274

Information for Authors 289

INDIAN SOCIETY OF AGRICULTURAL ENGINEERS